Appendix G
Applied Coastal Pipeline Impact Assessment

Final Report

Simulating the Potential Impact of Borrow Site Excavation on Sediment Transport Along the Gulfstream Pipeline, Petit Bois Pass, Alabama

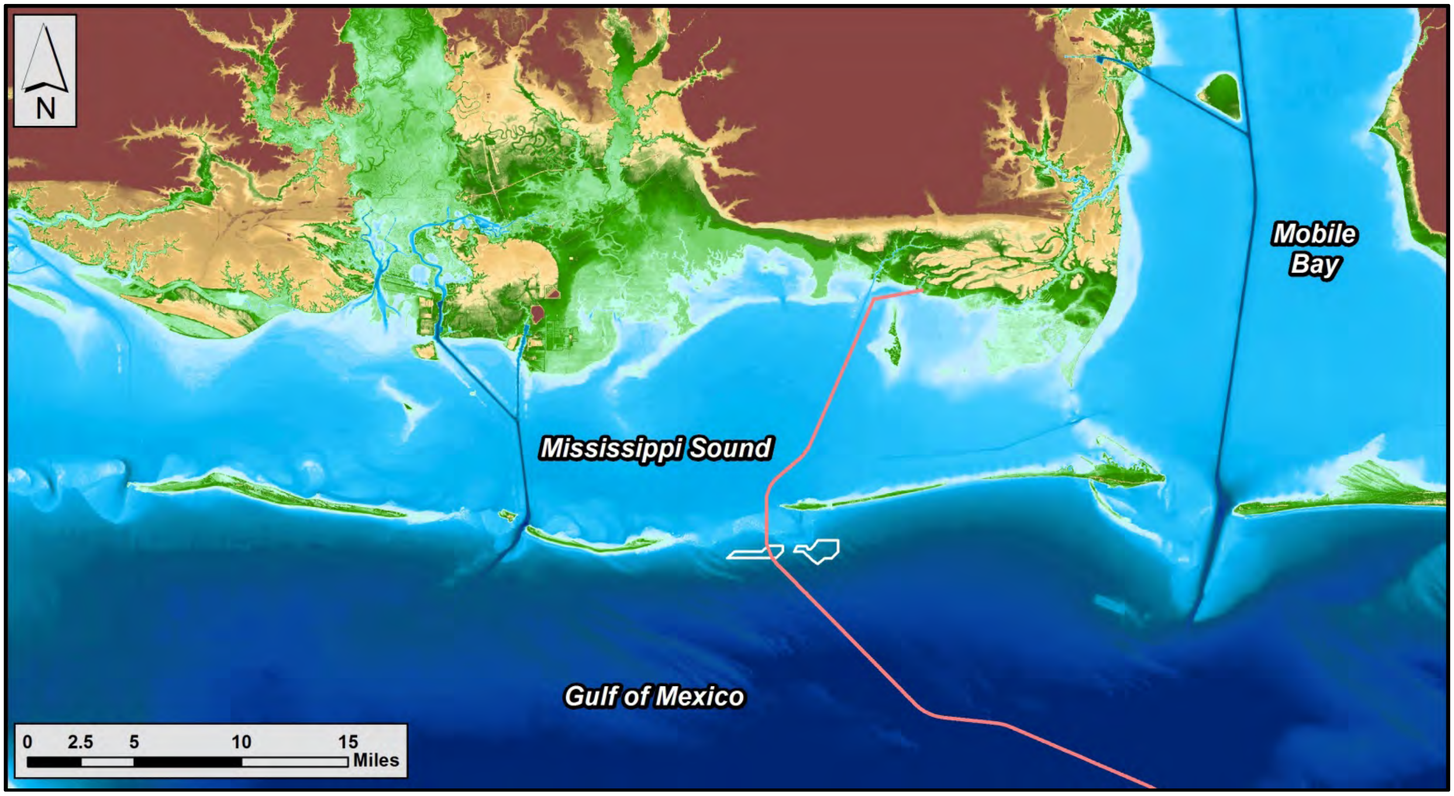

Prepared for:

Mississippi Coastal Improvements Program (MsCIP)
U.S. Army Corps of Engineers District, Mobile
109 St. Joseph Street, P.O. Box 2288
Mobile, Alabama 36628

Prepared by:

Sean W. Kelley and Sarah F. Griffee
Applied Coastal Research and Engineering
766 Falmouth Road, Mashpee, MA 02649
508-539-3737

July 10, 2013

Final Report

TABLE OF CONTENTS

1.0 INTRODUCTION 1

1.1 PROPOSED BORROW SITES 1

1.2 MODELS EMPLOYED IN THIS STUDY 2

1.2.1 CMS 3

1.2.2 ADCIRC 5

2.0 HISTORICAL INLET AND NEARSHORE MORPHOLOGY 6

2.1 DATA SOURCES 6

2.1.1 Vertical Adjustments 9

2.1.2 MLW Reference Elevation 11

2.2 SURFACE MODELING 11

2.2.1 Regional Morphology 11

2.2.1.1 1847-53 Bathymetric Surface 11

2.2.2 Island and Channel Migration 16

2.3 REGIONAL SEDIMENT TRANSPORT DYNAMICS 17

3.0 MODEL DEVELOPMENT 21

3.1 WAVE MODELING 21

3.1.1 Wave Data 21

3.1.2 CMS-Wave Model 23

3.1.3 Annual Wave Input Conditions 24

3.1.4 Storm Wave Input Conditions 25

3.2 HYDRODYNAMIC MODELING 28

3.2.1 ADCIRC Simulation of Tides 28

3.2.2 CMS-Flow 33

3.3 MORPHOLOGICAL MODELING 34

4.0 MODELING RESULTS 37

4.1 WAVE MODELING 37

4.2 MORPHOLOGICAL MODELING 40

4.2.1 Existing Conditions 40

4.2.2 Dredged Borrow Sites 41

5.0 CONCLUSIONS AND RECOMMENDATIONS 47

6.0 REFERENCES 49

1.0 INTRODUCTION

A computer modeling analysis was completed to estimate potential seafloor erosion impacts to the Gulfstream pipeline from dredging at the proposed Petit Bois East and West (PBE and PBW) borrow sites (Figure 1). A suite of computer models was employed in this analysis, including the synoptic-scale hydrodynamic model ADCIRC (ADvanced CIRCulation Model for Ocean and Estuarine Waters) and the local-scale coastal processes modeling package CMS (Coastal Modeling System). The different models relied on various sources of data to specify required inputs such as bathymetry, shorelines, wave spectra, hydrodynamic boundary conditions, and sediment characteristics. Other data sources including tide data and the results of bathymetric change analysis presented below were used to calibrate and corroborate model performance.

Three separate model simulations were run for the same 12-month period, which represent 1) existing bathymetric conditions and 2) the proposed PBE and PBW borrow sites including a 305-meter (1000-ft) buffer area along the BP pipeline. By running the same time period for both pre- and post-dredging bathymetric conditions, a direct comparison of bathymetric change can be made which indicates change that occurs as a result of dredging at the borrow sites.

In addition to the 12-month simulation, a single high-return-period storm was simulated to gauge what additional impacts to the pipeline may result from relatively infrequent large storm events. Littoral transport in the region of the barrier islands of Mississippi Sound is heavily influenced by storm activity (Byrnes et al., 2012) compared with average conditions, so the storm simulation was considered a necessary component of the study.

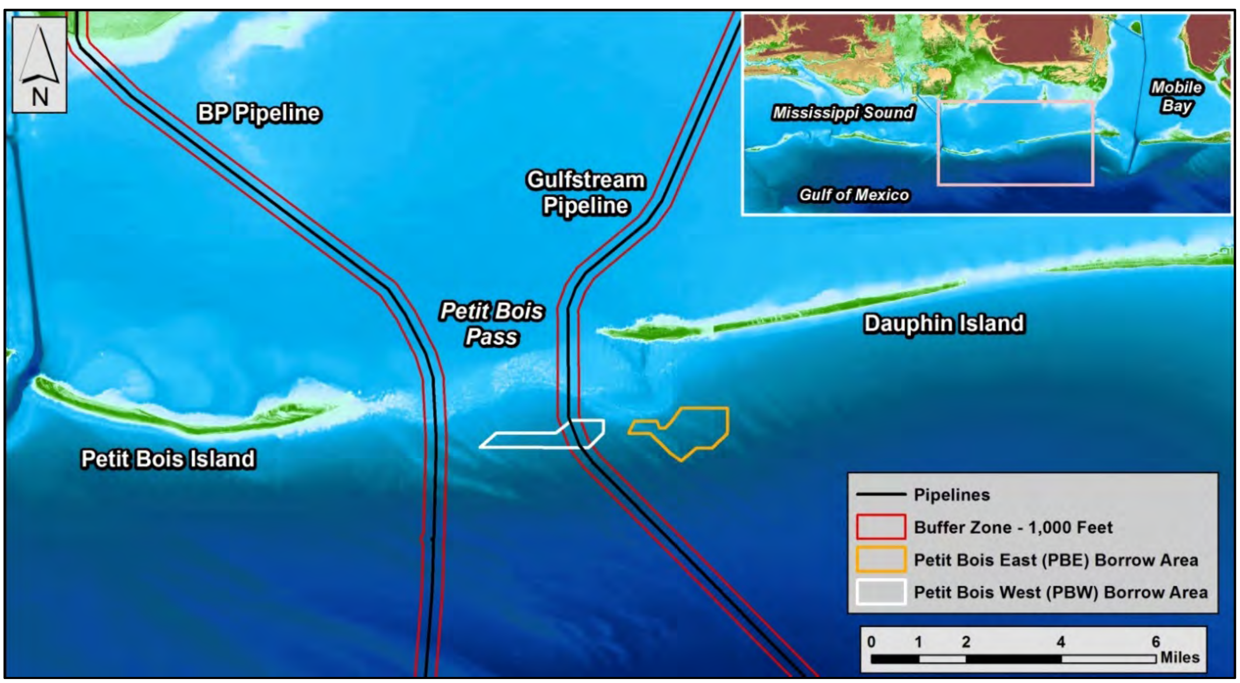

Figure 1. Project area illustrating borrow site locations relative to the Gulfstream pipeline.

1.1 PROPOSED BORROW SITES

As originally conceived, a total of 12.2 million cubic meters (16 million cubic yards) were to be dredged from the Petit Bois borrow sites. This volume includes 3.3 MCM (4.3 MCY) from PBW. In order to accommodate the existing BP natural gas pipeline that traverses a portion of PBW, it was proposed to leave an untouched 1000-foot buffer along either side of the pipeline. This buffer is intended to prevent adverse impacts to the pipe due to the dredging of the remaining portion of the borrow site. The selection of the 1000 ft buffer distance is based on the results of a morphological modeling investigation for borrow sites located offshore Louisiana (Nairn et al., 2004), where 6 meter excavations were simulated. The effect of this modification is to reduce the volume extracted from PBW by 1.4 MCY (1.0 MCM).

Though the bathymetric change analysis shows that there has been very little net change in seafloor elevation at depths of the borrow sites, this does not mean that sediments are never mobilized at these depths. By definition, areas where no net changes in seafloor elevation occur are located beyond the depth of closure (Dean and Dalrymple, 2002). Although sand motion can occur at bottom depths that are greater than the depth of closure (e.g., during storms), the net flux of sediment is not great enough to cause measureable changes in bottom elevation. The depth of closure is about half the depth for incipient sediment motion (Hallermeier, 1978).

The situation is different for excavated borrow sites which lie beyond the depth of closure but are within the zone where sediment can still be mobilized by waves. An excavated hole will tend to trap and collect sediment from adjacent undisturbed bottom areas. Over time, as the hole fills, adjacent bathymetry will lower. The rate at which these changes occur depends on the elevation of the bottom and local wave climate.

The depth of closure (h_c) can be computed using the relationship developed by Birkemeier (1985),

$$h_c = 1.75H_e - 57.9\left(\frac{H_e^2}{gT_e^2}\right)$$

which uses the significant wave height and period that is expected to be exceeded only for 12 hours each year, H_e and T_e. A useful approximation to this is given by $h_c = 1.57H_e$, where H_e is computed as $H_e = \overline{H} + 5.6\sigma_H$, and $\overline{H}$ and $\sigma_H$are the mean wave height and standard deviation for the wave record, respectively. Using a 28-year wave hindcast from offshore Petit Bois Pass (Oceanweather, 2012), H_e is computed to be 12.0 feet (3.7 meters), which results in a depth of closure of 18.8 feet (5.7 meters). Therefore, the depth of incipient sand motion is approximately 37.6 feet (11.4 meters).

These results show that both borrow sites are located outside the depth of closure, since the minimum depth of the undisturbed bottom at either site is 23.6 feet (7.2 meters). This is supported by results of the bathymetric change analysis (see Section 2.0). Change results also indicate that the entire extent of PBW is within the zone of mobile sediment, including the area within the 1000-foot buffer along the pipeline corridor. This indicates that waves will mobilize sand in the buffer area during some portion of each year, and as a result, storm waves have the potential to move sand from the buffer zone and into the adjacent excavated areas, causing erosion of the buffer zone.

Though this depth of closure analysis is useful for determining whether sediment is mobilized along the pipeline buffer, it cannot provide any quantitative assessment of how much material would erode from the pipeline buffer, and whether erosion could impact the pipeline itself.

1.2 MODELS EMPLOYED IN THIS STUDY

For the purposes of quantifying possible impacts to the Gulfstream pipeline due to dredging of the Petit Bois borrow sites, a series of computer models was developed to simulate complex coastal processes that drive sediment transport in the study area. The modeling package used as the core of this analysis is the Coastal Modeling System (CMS), a self-contained suite of models that includes waves, hydrodynamics, and sediment transport. CMS was used to model two-dimensional sediment transport and morphology change by wave and hydrodynamic forces is the area of Petit Bois Pass and the borrow sites. Tidal boundary conditions for the CMS model were developed using the hydrodynamic model ADCIRC, which can simulate synoptic-scale ocean tides and currents.

1.2.1 CMS

CMS software was developed by the US Army Corps of Engineers (USACE), Coastal and Hydraulics Laboratory (Sanchez *et al*., 2012). It includes separate CMS-Wave and CMS-Flow models that can be run independently or together to simulate sediment transport and morphology change that results from a combination of waves and hydrodynamic currents. CMS is an integral part of the Surface Water Modeling System (SMS) software application. SMS is used to create model grids and specify all required model inputs and run-time parameters. Post-processing and visualization of model output also is accomplished using SMS.

The latest release of the model (CIRP, 2012) integrates CMS-Wave and CMS-Flow into the same executable file. Before this version of the program was available, simulations that included waves and hydrodynamics relied on a steering module within SMS to coordinate the running of separate modules. Now with the new “in-line” version of the Flow and Wave models, the CMS executable handles coordination between the two models internally. This simplifies the process required to set up a simulation, and has some useful secondary benefits, like the ability to pause a simulation, which makes it easier to view intermediate results during the course of a simulation run.

1.2.1.1 CMS-Wave

CMS-Wave is a finite difference spectral wave model. The wave action balance equation is the basis for model formulation, similar to other wave models such as STWAVE and SWAN. Model formulation includes wave diffraction terms, though the model must be calibrated to ensure that diffraction is correctly applied in areas where this process is an important contributor to wave propagation (such as behind breakwaters and jetties). Other physical processes that are included in CMS-Wave are wind-wave growth, wave energy dissipation by breaking and white capping, wave shoaling and refraction, and reflection.

As presently implemented in SMS, model grids for CMS-Wave can be either regular Cartesian grids (like with STWAVE) made up of square cells with equal edge dimensions, or irregular Cartesian grids made up of rectangular elements. The irregular mesh capability allows a method of model mesh refinement in areas of interest without requiring the same small cell size be used for the entire grid.

Wave data used for the each CMS-Wave model run can come from most any source of wave data, including buoy measurements or wave hindcasts. Two-dimensional spectral wave data from buoy records are available from sources such as the National Oceanographic Data Center (NODC). Before using such sources of spectral data, they typically must be reformatted. In the case of NODC spectral data, CHL has developed a helper program (ndbc-spectra.exe) that converts the data from the archive format to the proper format that is readable by SMS and CMS-Wave.

In addition to spectral data, parameterized wave data can be used to develop input spectra data required by CSM-Wave. WIS hindcast data provide 20-year-long records of waves at many stations along the coastline of the United States (Tracey, 2002), but only wave parameters (e.g., height, period, and direction) and not complete spectra. These data can be imported into SMS and used to create spectra for a CMS-Wave simulation. Within SMS, the user must select the type of frequency spectrum (e.g., JONSWAP or Bretschneider) and the directional spreading function to use for the calculation of a two-dimensional spectrum.

The ability to nest wave simulations into grids with larger-scale simulations is also a feature of CMS-Wave. This is another method that can be employed to efficiently refine a grid mesh only in areas that are considered most important for the analysis. A grid nested within a larger mesh receives spatially-varying open boundary wave spectra along the full length of the offshore open boundary of the grid, extracted at locations that correspond to the cells of the nested grid.

1.2.1.2 CMS-Flow

Simulations of hydrodynamics and sediment transport in the CMS system are computed using CMS-Flow. This model also has a finite volume formulation and can utilize grids developed for use with CMS-Wave. The latest releases of CMS and SMS allow a particular type of irregular Cartesian grid, called a "telescoping mesh", to make more efficient refinements of the grid in locations of interest within the model domain without forcing small cell sizes in areas where it is not required or desired. Each level of mesh refinement is achieved by dividing a cell edge into two equal segments that become the edges of two new cells with a quarter of the area of the larger cell. As a result, no grid cell edges in a mesh are ever connected to more than two adjacent cells. This allows a very rapid change in mesh cell size over short distances.

Hydrodynamic Model

Hydrodynamic features within CMS-Flow include stable wetting and drying, with the possibility of ponding, wind forcing, spatially varying bottom friction, and multiple methods for designating hydrodynamic boundary conditions. CMS-Flow also can model salinity transport. Boundary conditions can be specified by using a time series of water level elevations from a source such as a NOAA tide gauge or some other source of tide data. Alternately, boundary conditions can be can be extracted from a larger hydrodynamic simulation.

Both explicit and implicit numerical formulations are available within the CMS-Flow code. The implicit formulation has been made available in the most recent public distributions of CMS. The key advantage of the implicit scheme is that simulations are much less restrained by issues related to time step size. Explicit formulations can require very small model time steps (of the order of 1 second) in order to ensure that no instabilities develop during the course of the model run. Small time steps are generally required with model meshes that have a high degree of refinement (small grid size) in areas with large depths that experience strong tidal currents. Common examples of this situation would be model meshes that include navigation channels or naturally deep inlet channels. With the implicit formulation that is now included in CMS-Flow, model time steps can be much larger (of the order of 10 minutes) because its stability is much less sensitive to the selected time step. The main benefit of being able to use large time steps is to reduce model total run times considerably. Simulations that take several days to run using the explicit formulation may be completed in a matter of several hours using the implicit version.

Sediment Transport Model

CMS-Flow also includes a non-equilibrium total-load sediment transport model that computes two-dimensional transport resulting by action of waves and hydrodynamics. Features of the sediment transport model include the ability to include spatially varying sediment grain sizes, hard bottom areas, multiple-sized sediment transport, and sand-permeable structures such as groins and jetties. Updates to the bottom elevation due to the movement of sediment across the model grid are computed at the same time interval as the hydrodynamic time step in the implicit version of CMS-Flow.

1.2.2 ADCIRC

Hydrodynamic boundary conditions used in the runs of the CMS-Flow model were developed using the hydrodynamic model ADCIRC (ADvanced CIRCulation Model for Oceanic, Coastal and Estuarine Waters; Luettich and Westerink, 2004). ADCIRC is a finite element model that can be run using grids specified in either Cartesian coordinates (e.g., state plane systems) or spherical systems (coordinates in Latitude and Longitude). ADCIRC includes several different options for specifying boundary conditions and for applying other model forcing. The simplest types of open boundary conditions that are typically applied to the model are a time series of water elevations (e.g., water levels for tide gauges) and water discharges from rivers and streams. Other boundary conditions that can be applied include atmospheric forcing from barometric pressure fields and wind stresses.

Tidal potential forcing is included in ADCIRC so tides can be generated by forcings applied within the model domain and not only by a water level time series applied to an open boundary. This feature of the model makes it well suited for modeling large ocean basins (>1000 miles across) like the Gulf of Mexico. At this scale, tides generated within the basin from the gravitational interaction of the Earth, Moon, and Sun become a large portion of the total observed tide at points in the basin, compared with the tide at the boundaries of the basin (e.g., the Straits of Florida in the case of the Gulf of Mexico).

ADCIRC is fully integrated into the SMS software package. Different model forcings and run-time parameters used as inputs to a simulation can be specified through menus available in SMS. Tides at open boundaries can be input using an SMS interface that uses tidal constituent databases that have been developed by the USACE. This type of boundary specification is useful when an open boundary extends across a broad ocean expanse (e.g., the Straits of Florida), where tide elevations vary significantly in phase and amplitude along the length of the boundary. Tidal potential forcing parameters that are applied across the model domain during the simulation can also be specified in SMS. With boundary condition forcing and tidal potential forcing, the user selects which individual tidal constituents (e.g., the M2 principle lunar and K1 principle solar constituents) from the constituent database are included in the simulation.

2.0 HISTORICAL INLET AND NEARSHORE MORPHOLOGY

The most direct method for evaluating regional sediment transport pathways for the Petit Bois Pass system is to quantify historical change in inlet and nearshore morphology with a time series of shoreline and bathymetric surveys. This section focuses on evaluating bathymetry data collected between 1847 and 2011. For some coastal areas, survey data are lacking for drawing detailed and confident conclusions regarding beach and nearshore evolution relative to dominant sediment transport pathways and quantities. However, the Mississippi Sound and nearshore was surveyed on five separate occasions over a 164-year period, providing ample data for documenting net beach and inlet shoal evolution, regional sediment transport pathways, and the exchange of sediment between ebb-tidal shoals and adjacent shorelines.

2.1 DATA SOURCES

Seafloor elevation measurements, compiled from historical and modern hydrographic surveys, were used to identify seafloor morphology and historical seafloor change. Five bathymetry data sets were compiled to document seafloor changes between 1847-53 and 2006/11. Historical data sets were compiled from hydrographic surveys completed by the U.S. Coast and Geodetic Survey (USC&GS) in 1847-53, 1917-20, 1961-62, and 1970/87 (Table 1; Figure 2-6). Recent survey data sets were compiled from the National Ocean Survey (NOS), U.S. Geological Survey (USGS), and U.S. Army Corps of Engineers (USACE) Mobile District surveys to create the 2006/11 surface. Regional data extend from Mississippi Sound to the nearshore fronting Dauphin and Petit Bois Islands.

Table 1. Bathymetry Source Data

Date	Data Source	Map Numbers and Comments
1847-53	USC&GS Hydrographic Sheets 1:20,000 USC&GS Coast Chart 1:80,000	First bathymetric survey (Figure 2). H-00191 – 1847; Mississippi Sound north of eastern Dauphin Island H-00261 – 1851; Offshore Dauphin Island H-00328 – 1853; North and south of Petit Bois Island H-00329 – 1852; Mississippi Sound north of western Dauphin Island Ch-189 – 1852; South of Petit Bois Pass and Island
1917-20	USC&GS Hydrographic Sheets 1:40,000 1:80,000	Second bathymetric survey (Figure 3). H-04020 – 1917 to 1918; Mississippi Sound and nearshore H-04171 – 1920; Offshore Petit Bois Island and Dauphin Island
1961-62	USC&GS Hydrographic Sheet 1:20,000	Third bathymetric survey (Figure 4). H-08647 – September 1961 to May 1962; Mississippi Sound, Petit Bois Pass, and nearshore areas
1970/87	USC&GS Hydrographic Sheets 1:20,000	Fourth bathymetric survey (Figure 5). H-09118 – April 21 to June 15, 1970; Horn Island Pass to Petit Bois Pass H-10208 – November 25 to December 9, 1985; Offshore Petit Bois Pass H-10247 – June 18 to November 5, 1987; Offshore western Dauphin Island H-10261 – December 4 to 22, 1987; Offshore Petit Bois Pass and Island
2006/11	USC&GS Hydrographic Sheet 1:10,000 USGS Hydrographic Survey (digital) USACE Hydrographic Surveys (digital)	Fifth bathymetric survey (Figure 6). H-11621 – October 4 to December 15, 2006; Mississippi Sound and offshore western Dauphin Island June 2009; Swath bathymetry; Petit Bois Island and Pass July 20 to 26, 2011; Offshore Petit Bois Pass

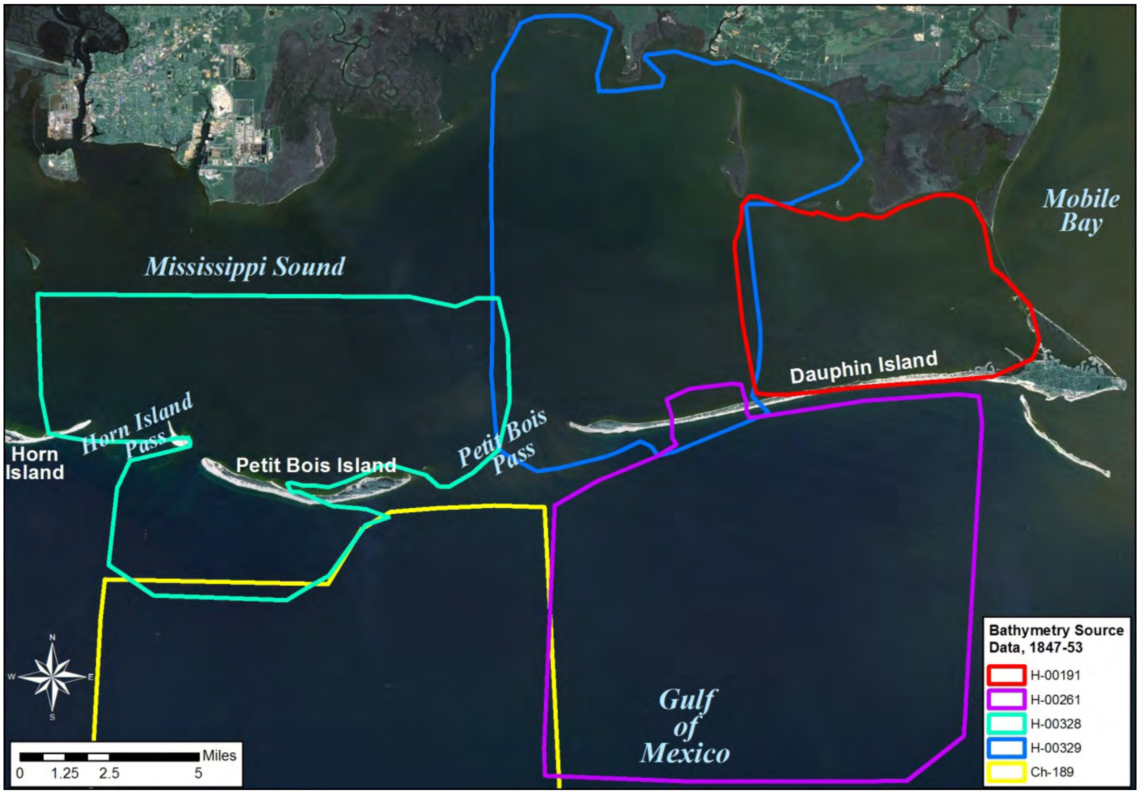

Figure 2. Hydrographic survey coverage, 1847-53.

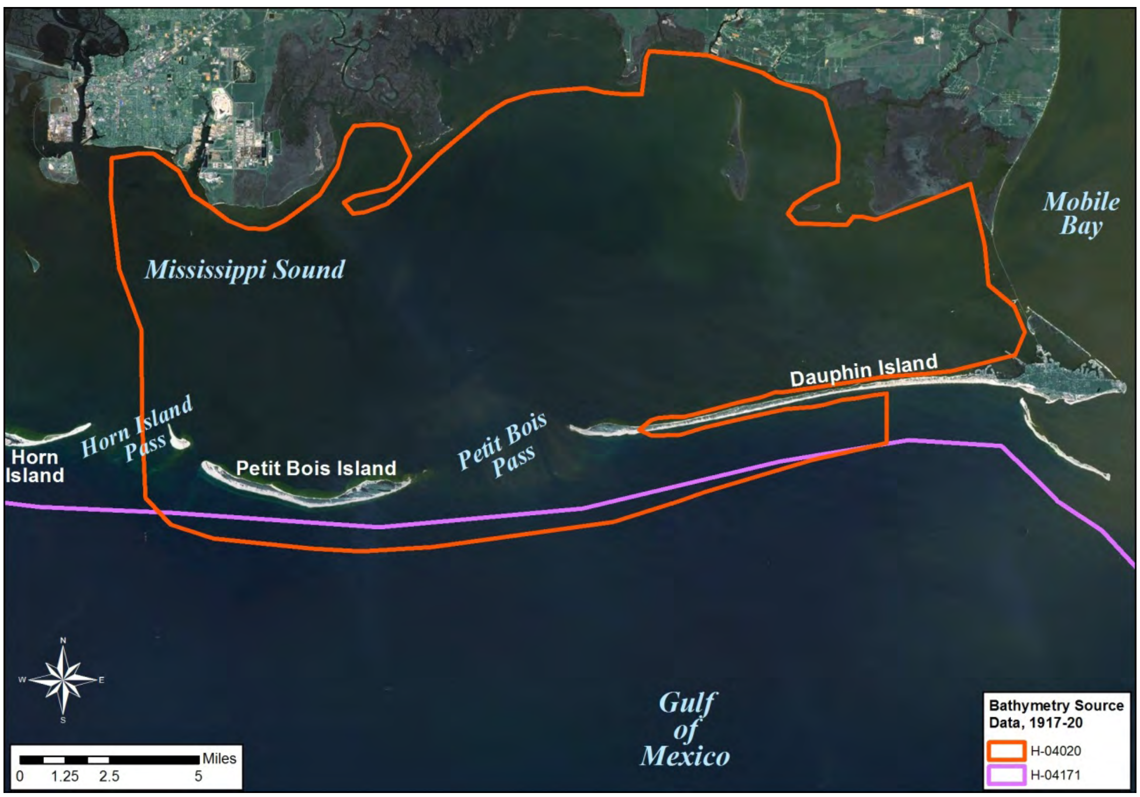

Figure 3. Hydrographic survey coverage, 1917-20.

Figure 4. Hydrographic survey coverage, 1961-62.

Figure 5. Hydrographic survey coverage, 1970/87.

Figure 6. Hydrographic survey coverage, 2006/11.

Historical hydrographic survey data were developed from scanned NOS hydrographic survey sheets that were digitized at Applied Coastal using standardized digitizing and registration procedures (see Baker and Byrnes, 2004). All bathymetry data were combined with concurrent shoreline data to produce bathymetric surfaces that extend offshore from the high-water shoreline. An elevation of 4.0 ft was assigned to the high-water shoreline boundary based on berm crest elevations identified in 2010 LiDAR data from the National Coastal Mapping Program (NCMP).

2.1.1 Vertical Adjustments

Because historical seafloor elevations are temporally inconsistent for all survey sets (i.e., reference tidal datums change with time), adjustments to depth measurements were made to bring all data to a common plane of reference (NOAA, 2003). These adjustments included changes in tidal datums due to relative sea level change and differences in reference vertical tidal datums. Vertical adjustments were made to each data set based on the time of data collection and the original vertical reference datum.

USC&GS hydrographic survey data were obtained online from the NOS hydrographic survey viewer, and all data were compiled relative to the mean low water (MLW) vertical tidal datum, the average of all the low water heights for each tidal day observed at a specific tidal station over the National Tidal Datum Epoch (NTDE; 18.6-year tidal epoch, rounded to a full year cycle, over which tide observations are recorded and reduced to establish mean values for tidal datums; NOAA, 2001). Reference tidal datum epochs are necessary for measurement standardization because of periodic and secular trends in relative sea level. The MLW tidal datum, therefore, varies with changes in sea level over time depending on the 19-year cycle referenced for measurement (Marmer, 1951; Harris, 1981; Hess, 2003; Foxgrover et al., 2004; Meyer et al., 2004). Because relative sea level changes, tidal datums at a specific site become out of date and must be updated to account for long-term vertical adjustments, such as global sea level change, subsidence, and glacial rebound (Hicks, 1981; NOAA, 2003). As such, all bathymetric data were adjusted to a common vertical reference plane (relative to 2011) to account for changing tidal datums accompanying fluctuations in relative sea level for the period of record (Table 2).

Table 2. Vertical adjustments to historical bathymetry data for accurate comparison of surface change between 1847/53 and 2006/11.

Survey Date	Sea Level Rise Adjustment (ft)
1847-53	-1.5
1917-20	-0.9
1961-62	-0.5
1970/87	-0.4/-0.2
2006/11	0.00

Vertical tidal datum adjustments were based on NOAA tidal benchmark #8735180. Although sea-level observations at the USACE Biloxi gauge were longer than changes recorded at the Dauphin Island gauge, USC&GS and USACE bathymetric surveys referenced the Dauphin Island gauge for tidal corrections during surveys. Water level measurements at the USACE Biloxi gauge indicated a sea-level rise trend consistent with that recorded at Dauphin Island (0.00956 feet/year; see Figure 7). Table 2 documents vertical adjustments used to bring historical bathymetric surfaces to the same vertical reference datum used for the 2006/11 bathymetric surveys. The unit of measure for all surfaces is feet, and final values were rounded to tenths of feet before computations were completed.

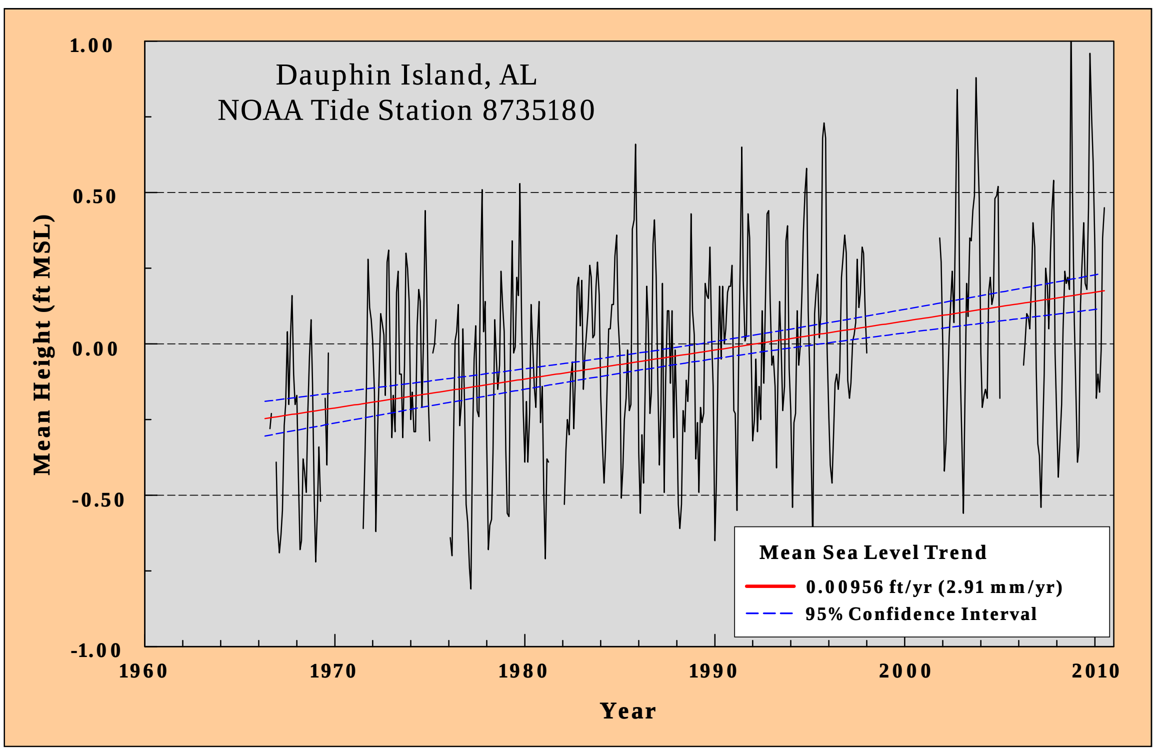

Figure 7. Monthly mean water level measurements and sea-level rise trend at Dauphin Island, AL gauge 8735180, 1966 to 2010.

2.1.2 MLW Reference Elevation

From the shoreline to a distance offshore of about 500 to 800 feet, bathymetry data are absent for most historical surveys. To better estimate beach and nearshore profile shape for change comparisons, the position of the MLW line was determined using documented distances between the position of MLW and the position of the high-water line (HWL) on recent USACE LiDAR surveys. The horizontal position of the MLW line (0.01 ft MLLW) was on average approximately 100 ft seaward of the HWL. To verify the accuracy of this relationship, a MLW line was established about 100 ft seaward of the HWL for a composite LiDAR and bathymetry surface (see Byrnes et al., 2012). Two surfaces were created; one included beach and nearshore elevations from the original surveys, and the other used the HWL, estimated MLW line, and offshore data deeper than 8 ft. Cross-sections were compared for each surface to evaluate beach shape obtained using each method. After completing many similar comparisons, it was determined that the described technique for estimating profile shape between the HWL and offshore bathymetry data provided a good estimate of profile shape in the absence of nearshore survey data.

2.2 SURFACE MODELING

Digitized soundings and shorelines were used to create digital elevation models of the seafloor for the period 1847-53 to 2006/11. The Triangulated Irregular Network (TIN) method was used in this study to form surfaces of continuous connected triangular planes based on irregular points (Petrie, 1991). The elevation of each point in the model is determined by solving equations for its horizontal location on the triangulated surface. Therefore, only points existing in the original data sources are used to create the surface model, as opposed to grid models which interpolate evenly spaced points from original data. TIN model surfaces were used for all calculations of bathymetric volumes and change; however, grid surfaces were generated for graphic display purposes.

2.2.1 Regional Morphology

Nearshore sediment transport processes influence the evolution of shelf sedimentary environments to varying degrees depending on temporal and spatial response scales. Although micro-scale processes, such as turbulence and individual wave orbital velocities, determine the magnitude and direction of individual grain motion, variations in micro-scale processes are considered noise at regional-scale and only contribute to coastal response in an average way. By definition, regional-scale geomorphic change refers to the evolution of depositional environments for large coastal reaches (10 km or greater) over extended time periods (decades or greater) (Larson and Kraus, 1995). An underlying premise for modeling long-term morphologic change is that a state of dynamic equilibrium is approached as a final stage of coastal evolution. However, the interaction between scale of response and forces causing change often results in a net sediment deficit or surplus within a system, creating disequilibrium. This process defines the evolution of coastal depositional systems. Five bathymetric surfaces were established for Petit Bois Pass for the periods 1847-53, 1917-20, 1961-62, 1970-87 and 2006-11 to describe large-scale variations in coastal and nearshore morphology.

2.2.1.1 1847-53 Bathymetric Surface

Bathymetry data for the period 1847-53 were combined with 1847-49 shoreline data to create a continuous surface from the shoreline seaward to about the 70-ft depth contour. The most prominent geomorphic features throughout the study area are shoals associated with the pass between the barrier islands (Figure 8). Inlet shoals reflect the redistribution and conveyance of littoral sand between barrier islands within a relatively narrow zone of sand transport bound by the 30- to 35-ft depth contour in the Gulf and the 10- to 15-ft contour in the Sound. This approximate 1 to 4 mile wide nearshore region (narrower for islands, wider for the pass) encompasses the zone of littoral sand transport through which islands and inlets fronting Mississippi Sound have evolved in response to storm and normal coastal processes. Overall deposition on ebb shoals is skewed to the west. This observation is consistent with net shoreline migration, documenting the influence of net westward sediment transport along the shelf and shoreline in coastal Mississippi and Alabama (Byrnes et al., 2013).

Unlike Mobile Pass and ebb shoal at the eastern boundary of Dauphin Island, the inlet shoals and channel of the Petit Bois Pass system do not extend far offshore, reflecting the geomorphic characteristics of a wave-dominated inlet. Inlet shoals and channel at the pass are oriented to the west, consistent with the dominant direction of net sand transport resulting in westward lateral growth of all the islands in the Mississippi Sound barrier island system. Between the passes, offshore contours appear relatively straight and parallel to shoreline orientation.

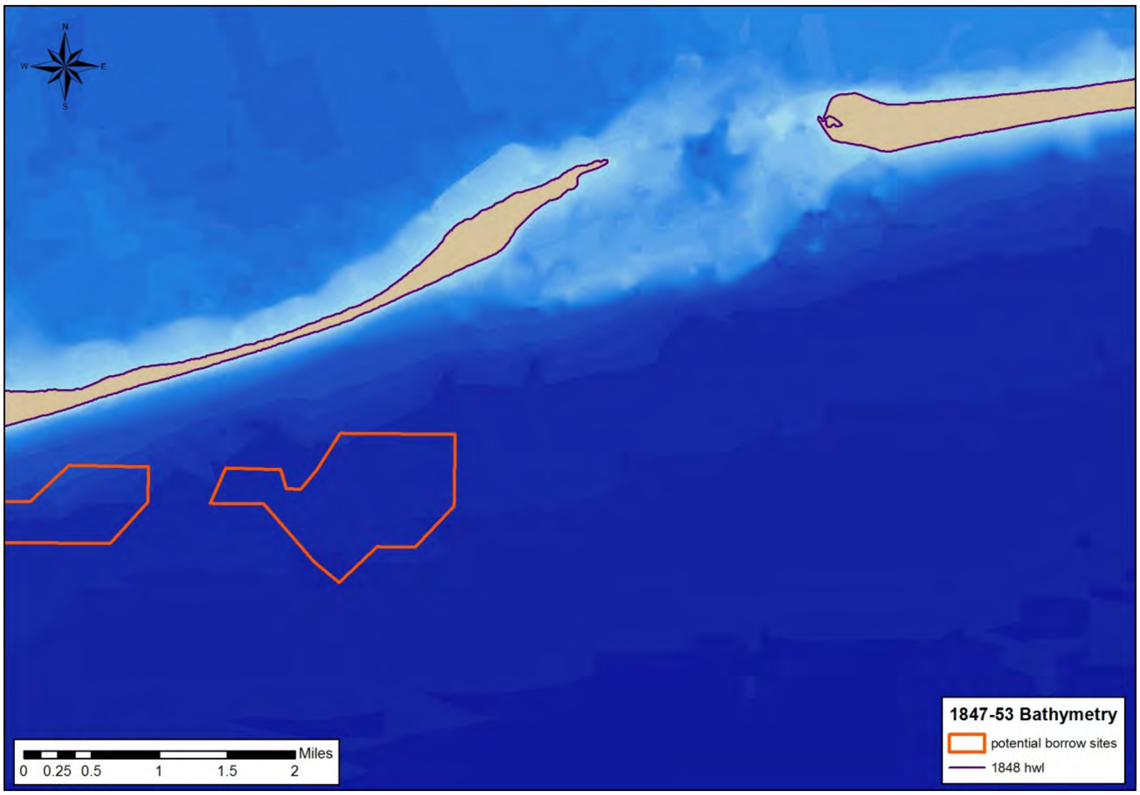

Figure 8. Bathymetric surface for Petit Bois Pass, 1847-53.

2.2.1.2 1917-20 Bathymetric Surface

Bathymetry data for the period 1917-20 were combined with 1916-17 shoreline data to create a continuous surface from the Sound seaward to about the 60-ft depth contour. Most general characteristics of the surface around the islands, pass, and on the shelf seafloor are similar to those identified from the 1847-53 surface. However, there are a few notable exceptions: 1) Dauphin and Petit Bois Islands were decimated by the July 1916 hurricane, creating a wide breach along 5 miles of central Dauphin Island and an eroded eastern end of Petit Bois Island; 2) the channel through Petit Bois Pass was better defined and was oriented to the southwest; and 3) Petit Bois Island exhibited significant erosion on its eastern end and Dauphin Island grew to the west, thereby forcing the inlet channel westward (Figure 9).

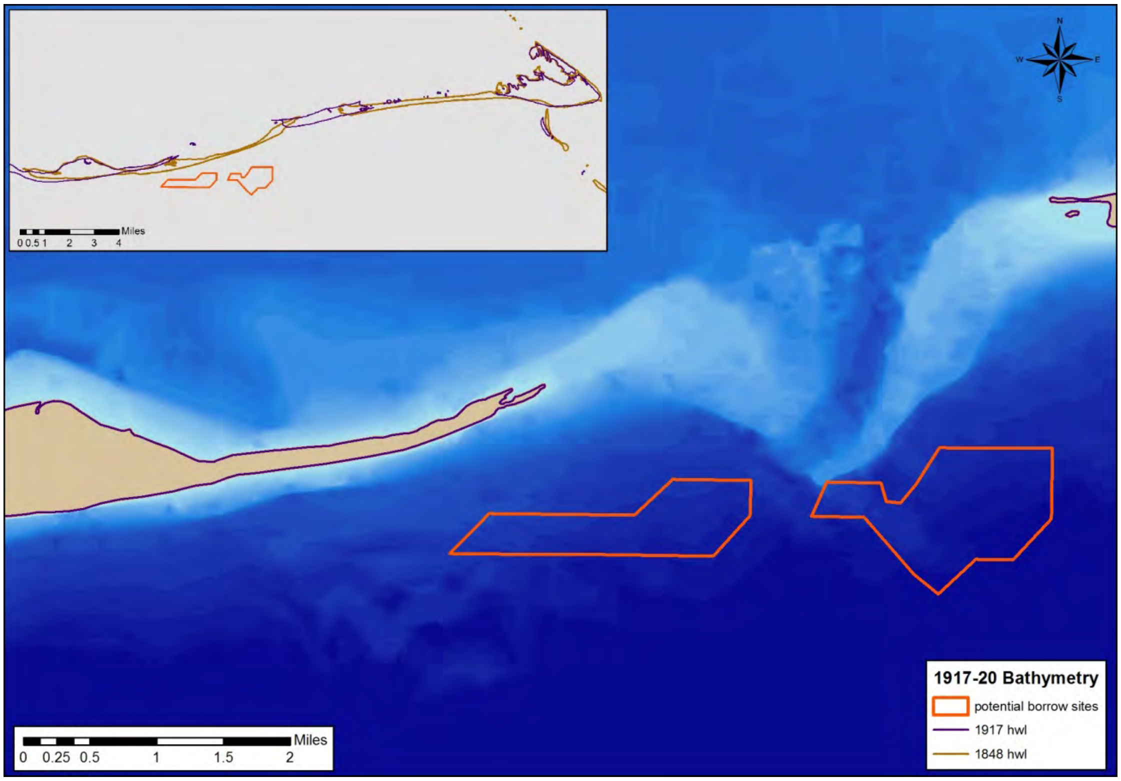

Figure 9. **B**athymetric surface for Petit Bois Pass, 1917-20. Inset illustrates shoreline position prior to and after the hurricane of 1916.

Although large sections of central Dauphin Island were dispersed by the 1916 hurricane, net westward island growth was illustrated between 1847-53 and 1917-20, consistent with all Mississippi Sound barrier islands for this period. Furthermore, natural channel migration to the west was forced by large quantities of littoral sand being transported from east to west throughout the system, filling old channel locations in response to net island growth. The ebb shoals at Petit Bois Pass were better defined than shoal deposits surveyed in the mid-1800s. Again, offshore contours appear relatively straight and parallel to shoreline orientation between the passes.

2.2.1.3 1961-62 Bathymetric Surface

Bathymetric surface characteristics for the period 1961-62 are similar to the 1917-20 surface with a few exceptions (Figure 10). First, geomorphic features are better defined because the number of data points is greater for the more recent time period. Second, deposition along the western end of Dauphin Island caused rapid growth of the beach and migration of the inlet channel to the west. Third, as Dauphin Island grows to the west, it appears that gradual infilling of the channel is creating a broad, shallow entrance that may enhance natural westward island growth and downdrift sand transport to Petit Bois Island and other Mississippi barrier islands.

One drawback of the 1961-62 seafloor surface is that much of the offshore was not surveyed during this time. Mississippi Sound and inlet environments were well surveyed but adjacent areas fronting the islands were absent. Because much of the most active portion of the littoral zone illustrates consistent geomorphology for prior time periods, it is expected that only minor changes in nearshore morphology would be recorded. Westward growth of Dauphin Island and erosion on the east margin of Petit Bois Island continued between 1917-20 and 1961-62 at rates of about 166 feet/year and 377 feet/year, respectively (see Byrnes et al., 2012).

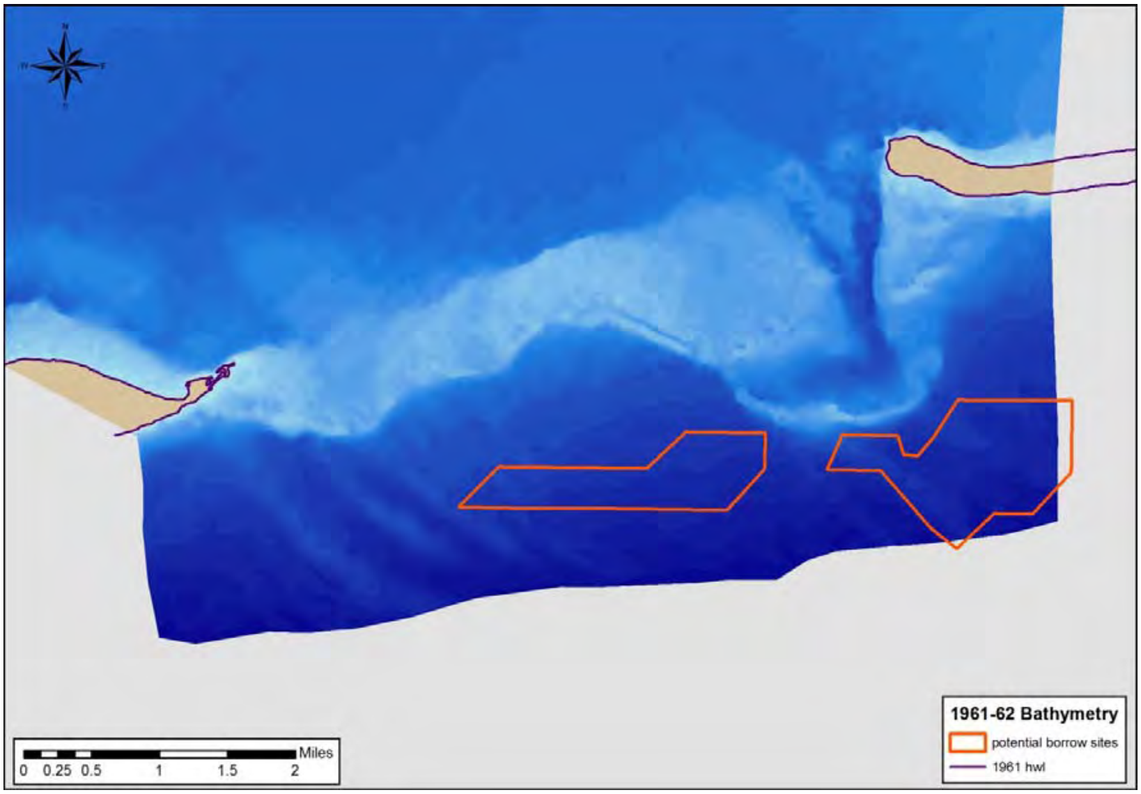

Figure 10. **B**athymetric surface for Petit Bois Pass, 1961-62.

2.2.1.4 1970/87 Bathymetric Surface

The general shape and position of the channel and shoals on the 1970/87 surface remained consistent relative to the 1961-62 time period (Figure 11). However, westward growth of Dauphin Island and erosion of the eastward end of Petit Bois Island did continue during this relatively short time period. Although the western tip of Dauphin Island was located directly north of the eastern side of the bifurcated channel at this time, channel position remained stable and continued to infill from westward moving sand moving along the island.

2.2.1.5 2006/11 Bathymetric Surface

A number of significant geomorphologic changes were recorded by the 2006/11 bathymetry surveys (Figure 12). The largest tropical cyclones were recorded between 1961-62 and 2006/11, so large changes in island and inlet shoal configuration would be expected. Most obvious changes were those associated with island breaching on Dauphin Island during Hurricane Katrina in August 2005. Westward island growth of Dauphin Island effectively closed the main channel at Petit Bois Pass. The entrance remains as wide as it was in 1961-62, but flow within the entrance must have diminished as the main channel became filled in response to dominant west-directed longshore sediment transport. Although the eastern end of Petit Bois Island continued to erode, the western end of the island has maintained its position relative to 1961-62 because it abuts the Pascagoula navigation channel at Horn Island Pass. Sediment transport processes during this period also have exposed a pipeline on the west side of Petit Bois Pass.

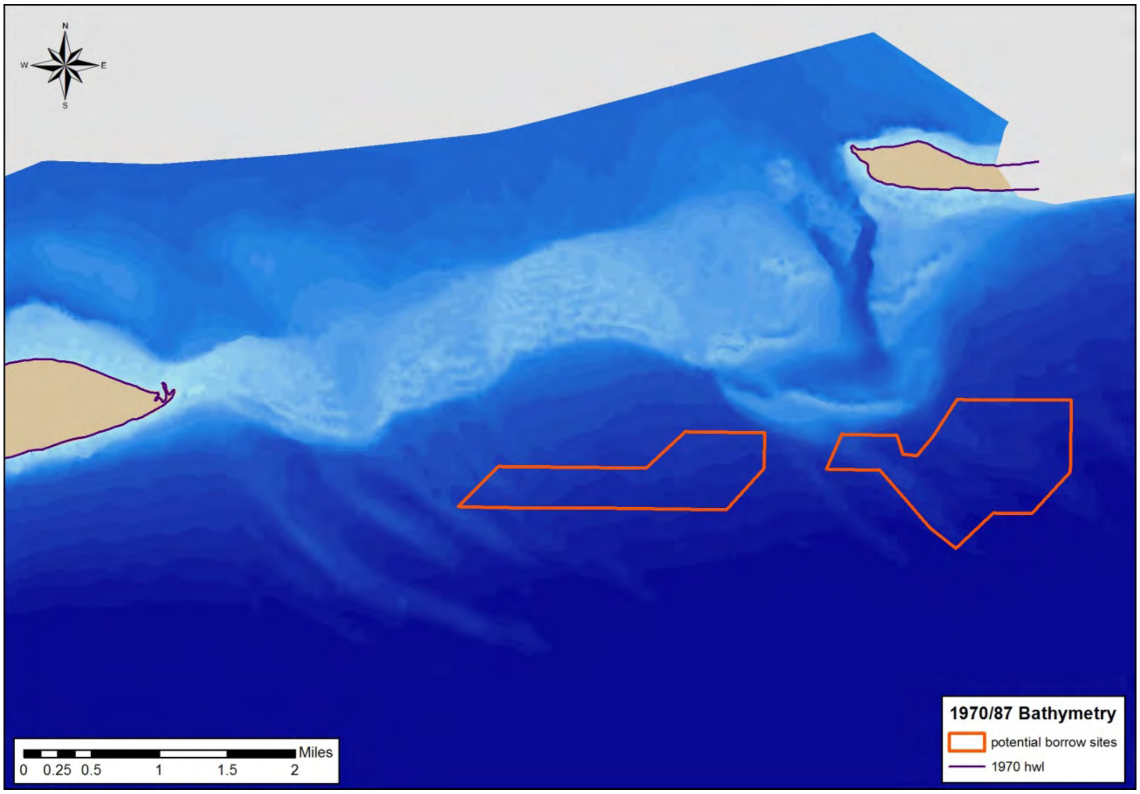

Figure 11. **B**athymetric surface for Petit Bois Pass, 1970/87.

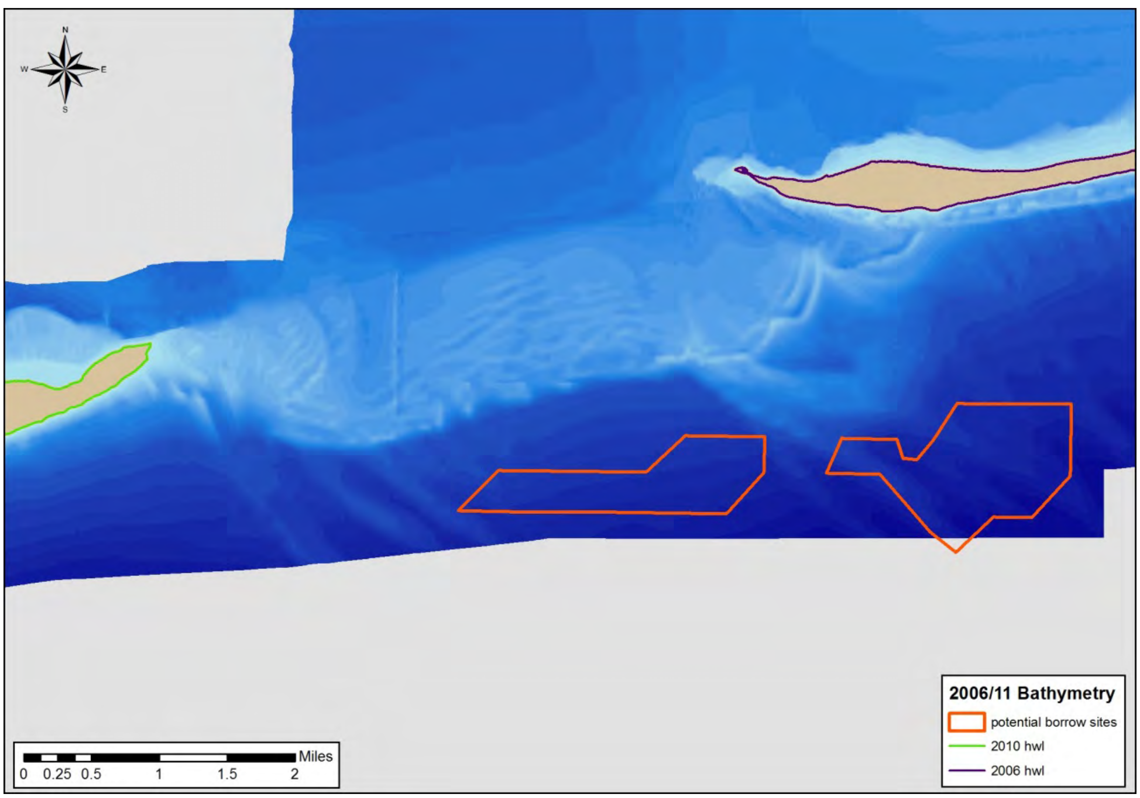

Figure 12. **B**athymetric surface for Petit Bois Pass, 2006/11.

2.2.2 Island and Channel Migration

Evolution of Petit Bois Pass has been controlled by net westward migration of Dauphin Island, primarily in response to tropical cyclones and normal incident coastal processes. Mariners, engineers, and scientists have recognized the natural westward shift of the island and channel since the earliest historical records. Physical parameters, such as entrance width between islands, channel depth, and shoal dynamics, control the exchange of sediment within the littoral zone between islands and the pass. Changes in inlet morphology document factors that may have significant impact on historical evolution of Dauphin and Petit Bois Islands. Inlet cross-sections were compiled to document changes in shoal and channel characteristics that influence the quantity of sediment bypassing to downdrift beaches.

Figure 13 illustrates transect locations for each cross-section year at Petit Bois Pass. Island configuration and changes required separate transect locations for documenting channel and shoal evolution. However, the westernmost location for each transect terminates at a similar longshore position, providing a means for comparing island and channel migration, changes in inlet width, and seafloor elevations between 1847 and 2006. In 1847, the eastern side of the pass was approximately 24,500 feet east of its present location, channel depth was about 17.5 feet, and inlet width was approximately 9,800 feet (Figure 14). Over the following 70 years, westward littoral transport from Dauphin Island moved large quantities of sand toward Petit Bois Pass, promoting island growth (sand spit development), inlet migration, and erosion along the eastern end of Petit Bois Island.

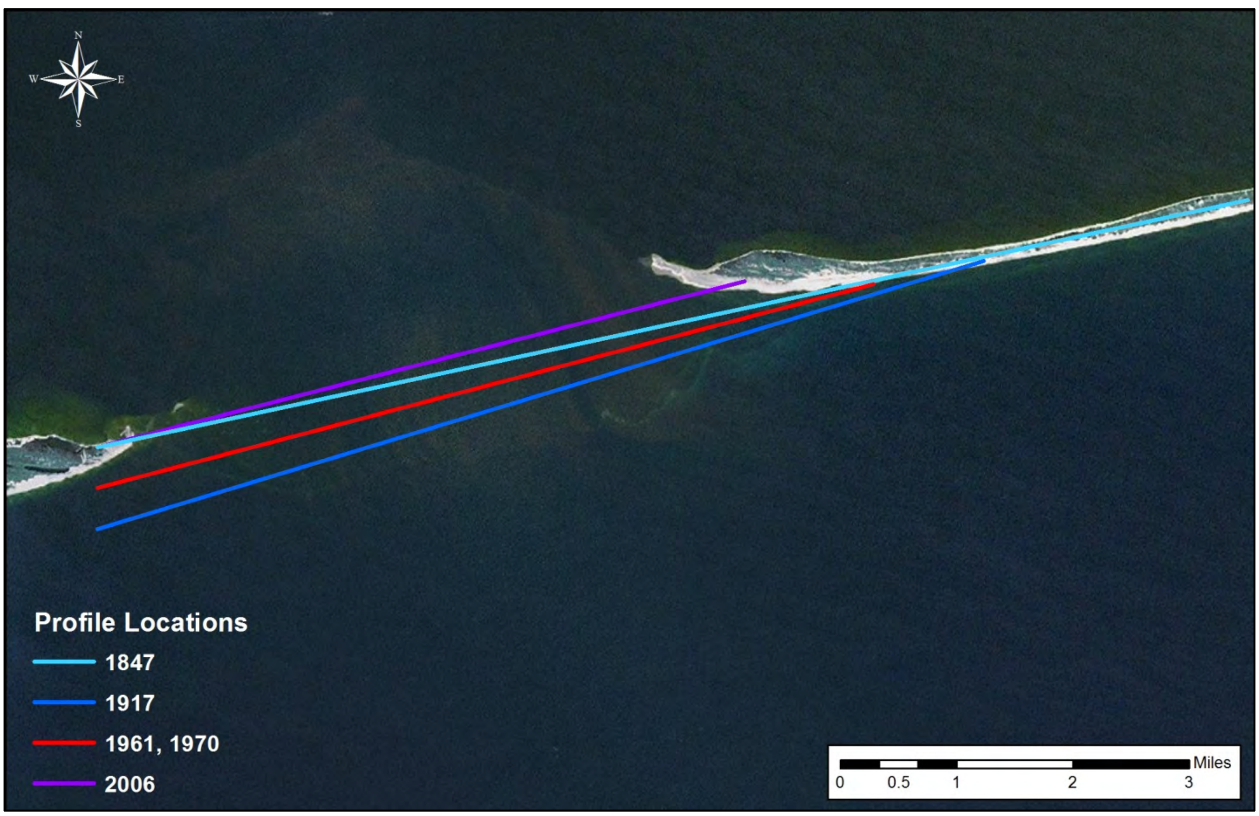

Figure 13. Transect locations for illustrating historical inlet cross-sections for Petit Bois Pass.

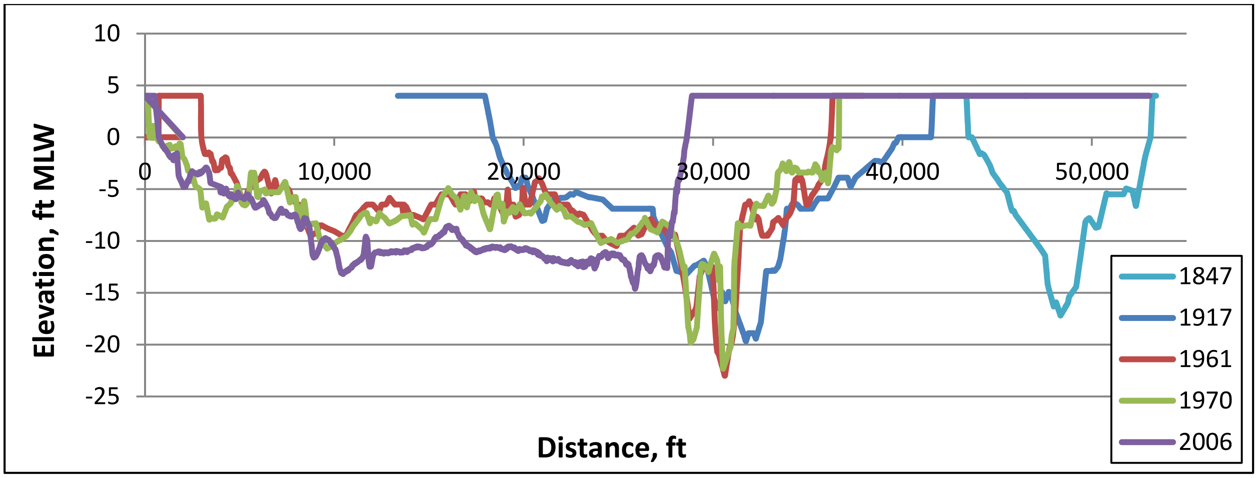

Figure 14. Historical inlet cross-sections for Petit Bois Pass illustrating changes in seafloor shape, 1847 to 2006.

By 1917, one year after the intense hurricane of 1916, the eastern end of Petit Bois Island had eroded and migrated approximately 42,000 feet west of its location in 1847, resulting in an inlet about 23,700 feet wide. Maximum channel depth along the cross-section increased to about 19 feet and channel location was approximately 16,400 feet west of its location in 1847. The trend of westward spit growth, channel migration, and erosion along the eastern end of Petit Bois Island continued through 1961 when the dominant inlet channel reached it greatest depth (22.9 feet) and inlet width was about 33,000 feet. By 2006, west-directed island growth on Dauphin Island had filled the entrance channel, decreasing inlet width by about 5,600 feet and creating a broad and relatively shallow entrance area. A well-defined channel for exchange of water and sediment between Mississippi Sound and the Gulf of Mexico was no longer present, perhaps signaling a change in inlet hydraulics that may promote more efficient bypassing of sand between Dauphin and Petit Bois Island in the future.

2.3 REGIONAL SEDIMENT TRANSPORT DYNAMICS

Comparison of bathymetric surfaces for the same geographic area but different time periods documents erosion and deposition patterns that reveal sediment transport pathways. An analytical comparison of bathymetry data yields a difference plot that isolates areas of erosion and deposition for documenting these patterns and quantifying trends. The natural movement of sand within the Mississippi coastal zone is controlled predominantly by east-to-west directed waves and currents, hydraulics associated with passes between the islands, and the availability of sand sources east of the study area. Changes in seafloor topography of the Petit Bois Pass region were documented for the periods 1847-53 to 1917-20, 1917-20 to 1961-62, 1961-62 to 1970/87, and 1970/87 to 2006/11.

The most significant changes between the 1847-53 and 1917-20 bathymetric surfaces were associated with erosion along Dauphin and eastern Petit Bois Islands (Figure 15). Deposition occurred along the western end of Dauphin Island as sand spit development. Shoal deposition and erosion occurred in the entrance where sand transport to and from the inlet was unbalanced as the channel and shoals evolved toward equilibrium with incident wave and current energy. Fluid flow and sediment transport at and adjacent to Petit Bois Pass results in relatively predictable seafloor changes. Littoral zone transport is dominated by west-directed waves and currents; however, minor and localized areas of transport reversal do exist at the very eastern end of Petit Bois Island.

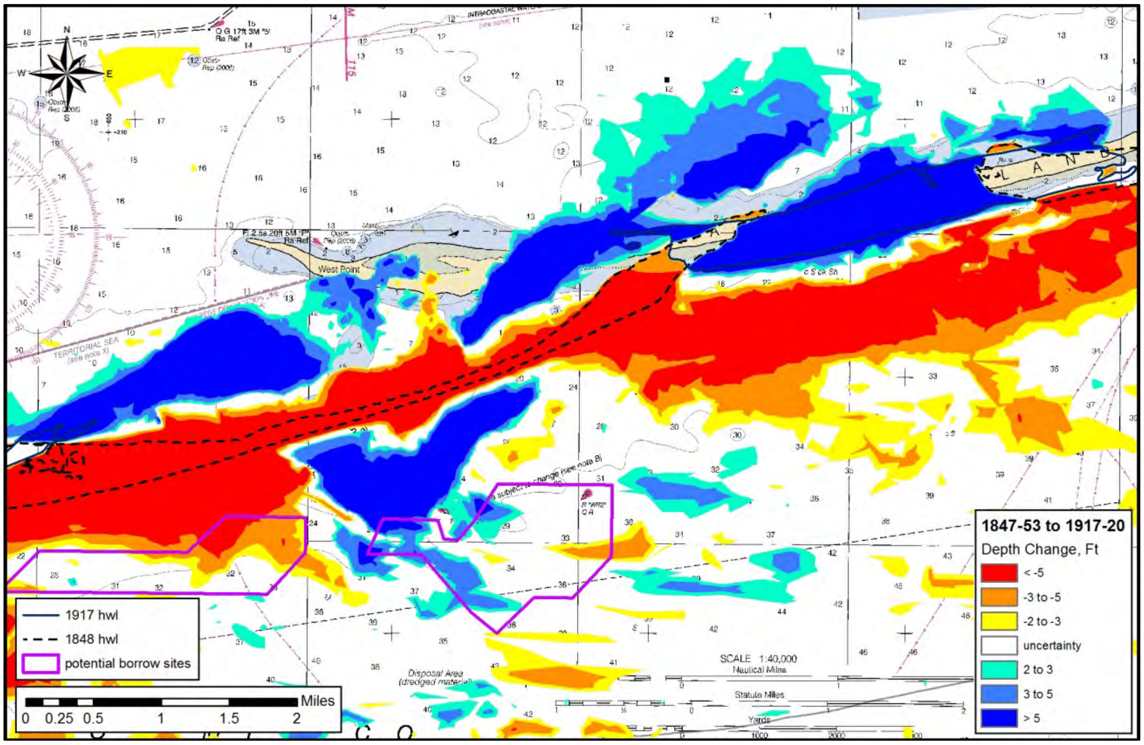

Figure 15. Bathymetric change between 1847-53 and 1917-20 for Petit Bois Pass.

Polygons of yellow to red (erosion) and green to blue (deposition) in the channel and on the shoals of the ebb-tidal delta illustrate the dynamic nature of these features as waves and currents transport and redistribute sediment from east to west throughout the system. Overall, Dauphin Island beaches supply sand for spit growth and inlet shoal formation, which in turn forces the inlet channel and entrance boundaries to migrate westward in a conveyor-like process. Most coastal systems experience significant reversals in sand flux that redistribute sediment more evenly along beaches and at entrances, but for the Petit Bois Pass system, net sand transport to the west is nearly equal to gross transport (addition of east- and west-directed transport). As such, long-term transport patterns are quite predictable. The continuous red zone along western Dauphin and eastern Petit Bois Islands reflects the primary impact of the 1916 hurricane that crossed this area (see Byrnes et al., 2010). Deposition landward and downdrift of this area is from storm overwash processes and longshore transport.

Between 1917-20 and 1961-62, similar patterns of erosion and deposition occurred throughout the study area (Figure 16). All parts of the littoral zone near the entrance were active during this period as the islands and inlet responded to storm and normal processes. The entrance survey recorded deposition along the western end of Dauphin Island and shoal deposition throughout the entrance. As the navigation channel continued migrating to the west in response to spit growth, erosion along the eastern end of Petit Bois Island supplied sand to downdrift beaches. By 1961-62, the channel was well-defined. As illustrated in the previous discussion on entrance cross-sections, spit growth on the western end of Dauphin Island, and associate channel and inlet shoal migration, were supplied by sand eroded from the eastern end of Dauphin Island. The potential borrow sites are located just south of active deposition on the ebb-tidal shoal, however, some deposition did occur offshore in these areas. Deposition and erosion from shoal or island migration occurred in the vicinity of both pipelines.

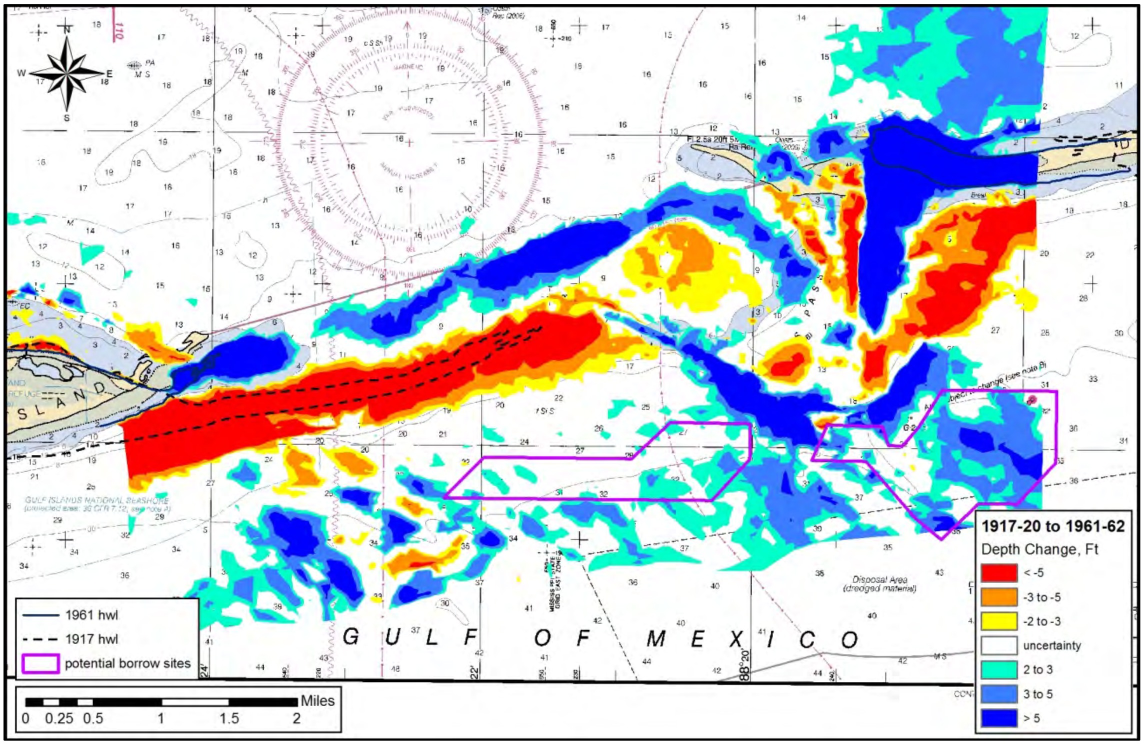

Figure 16. Bathymetric change between 1917-20 and 1961-62 for Petit Bois Pass.

There were a few significant changes recorded in the pass between 1961-62 and 1970/87 (Figure 17). During this relatively short time interval, the eastern side of the bifurcated channel (adjacent to western Dauphin Island) shoaled but did not continue migrating to the west. This occurred as a result of deposition and continued spit growth at the western end of Dauphin Island. Bathymetric surface changes also reveal sand accretion at the southern end of the entrance platform around the 12-ft depth contour. Some of these shoals formed at or near the pipeline locations. Erosion of the old ebb-tidal shoal and subsequent westward transport of sand contributed to shoal formation in the western half of Petit Bois Pass. Erosion also occurred at the eastern end of Petit Bois Island as the shoreline continued to recede to the west and north. Minor erosion was present in the Petit Bois East borrow site, but no measureable change were detected in the western borrow site.

The pattern of beach erosion and deposition illustrated between 1970/87 and 2006/11 is similar to that recorded for the previous period (Figure 18). However, the magnitude of change was greater, in part because the time interval was longer. Regardless, very little change was recorded within the potential borrow sites. Natural sand transport continued on and around the location of the pipelines, with persistent net erosion in the central portion of the entrance and deposition north and south of this erosion zone. Beach erosion again dominated eastern Petit Bois Island and shoal deposition in the pass and along the western end of Dauphin Island was pervasive. Shoal reworking within the entrance was marked by updrift erosion at old shoal locations and downdrift deposition within the entrance as sand is transported from western Dauphin Island to eastern Petit Bois Island along the outer margin of entrance shoals. The pattern of sand movement from western Dauphin Island toward eastern Petit Bois Island illustrates the dominant direction of net transport through the entrance from east to west.

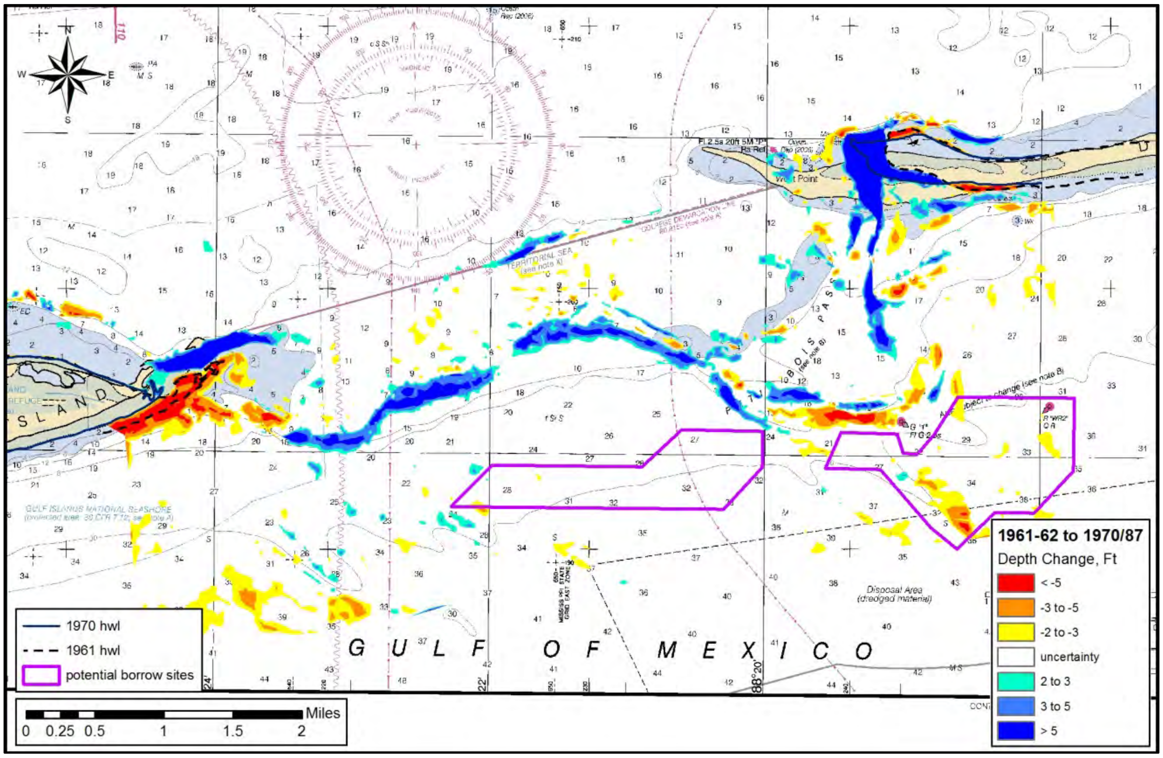

Figure 17. Bathymetric change between 1961-62 and 1970/87 for Petit Bois Pass.

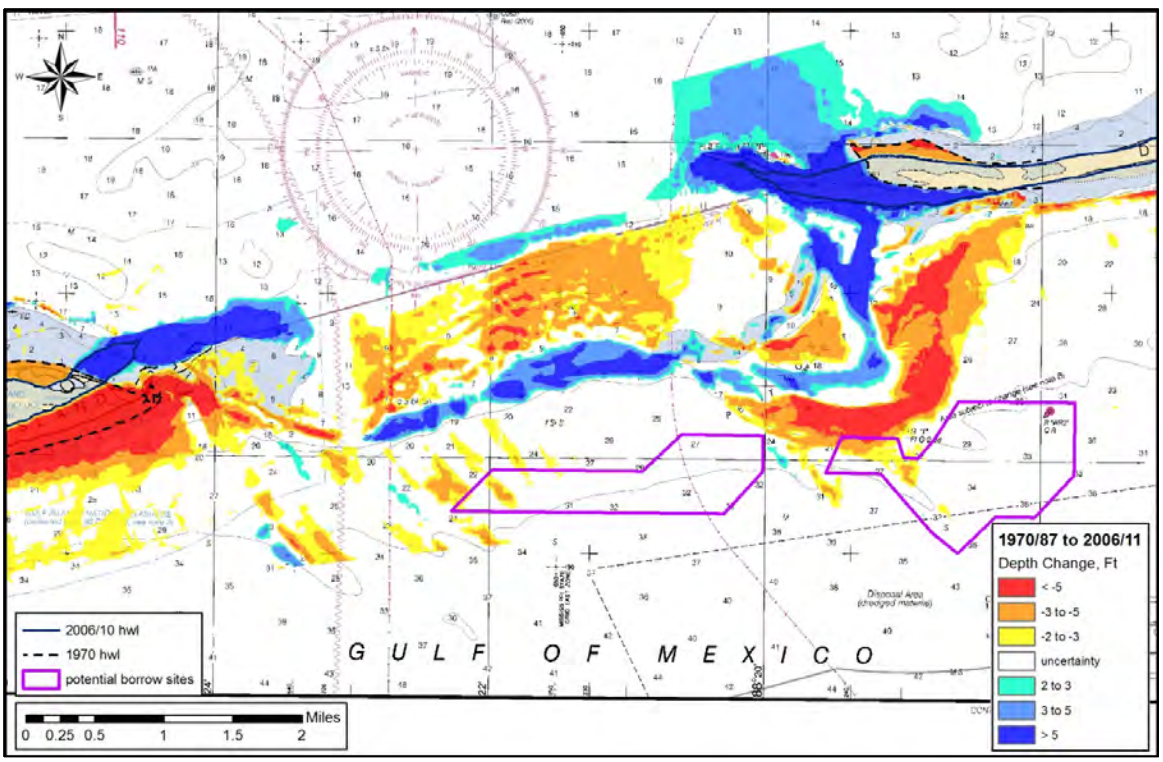

Figure 18. Bathymetric change between 1970/87 and 2006/11 for Petit Bois Pass.

3.0 MODEL DEVELOPMENT

The scope of this study involved the development of new model grids and the analysis of a variety of data sources for use as model bathymetry and boundary conditions. Additional sources of data were used to calibrate and corroborate model performance. In order to determine the magnitude of possible impacts to the pipeline caused by dredging of the Petit Bois borrow sites, an entire 12-month period was modeled using CMS. A single storm (Hurricane Katrina) was also modeled so that comparisons could be draw between morphology change that is expected for typical annual conditions and change resulting from extreme events.

3.1 WAVE MODELING

CMS-Wave was used to propagate waves from an offshore point in the Gulf of Mexico to the location of the proposed borrow sites near Petit Bois Pass. The source for offshore wave data is a hindcast developed by Oceanweather, Inc. (2012). This hindcast covers a 29-year period from January 1980 through to December 2008 for the entire Gulf of Mexico. Compared with other sources of wave data, the Ocean Weather product has the advantage of providing complete 2-dimensional wave spectra at hourly intervals for the longest continuous span of time. Other available sources of wave data in the study area include the Wave Information Study (WIS) database of the Army Corps and directional wave buoy datasets archived by the National Data Buoy Center (NDBC).

3.1.1 Wave Data

<u>WIS Waves.</u> The WIS hindcast covers the 20-year period between January 1980 and December 1999 at stations that are spaced 4.8 nautical miles (NM) apart along the entire shoreline of the US Gulf Coast. The hindcast product that is available for general public consumption does not include wave spectra. Parameterized wave conditions (i.e., wave height, mean direction and period) are provided at a three-hour interval. The closest WIS station to the Petit Bois borrow sites is 73150 (Figure 19), which lies 6.9 nautical miles offshore Petit Bois West (PBW).

<u>Buoy Data.</u> Measured directional wave data from buoy stations for periods long enough to be useful source information for development of input conditions are not available. National Data Buoy Center (NDBC) station 42018 has a short period (in February 1990) of directional wave data. This station was 12.5 NM due south of Katrina Cut on Dauphin Island and 13.6 NM from PBW (Figure 19).

<u>Oceanweather Hindcast.</u> Oceanweather Inc. (OWI) provides 29-year wave hindcast datasets at grid points spaced 7 km (3.8 NM) for the entire Gulf of Mexico. Complete 2-dimensional wave spectra are available from a subset of the 7 km grid at 14 km intervals. The closest OWI station to Petit Bois Pass that has available spectral data is grid point 9984, located 12.4 NM southeast of PBW and 13.8 NM due south of Dauphin Island (Figure 19). In addition to the long-term hindcast, OWI provides data for individual storm events, such as tropical storms and hurricanes. The data provided for each storm simulation includes wave parameters, wind speed, and ocean surface elevation for all 7 km grid points in the Gulf of Mexico at 15-minute time steps.

Figure 20 illustrates rose plots of wave height and period for the entire OWI record. The predominant wave direction is from the SSE, though waves are distributed nearly evenly between the SSE and SE sectors. The combined occurrence of waves between the east and south sectors is 61% of the whole record. Waves propagate from the SSE 16% of the time, which is the same percent occurrence for wave from the SE. Wave heights are most commonly less than 2 feet, which occurs 45% of the time. Waves larger than 10 feet occur less than 0.4% of the time, representing a cumulative occurrence of 940 hours during the entire 29-year record.

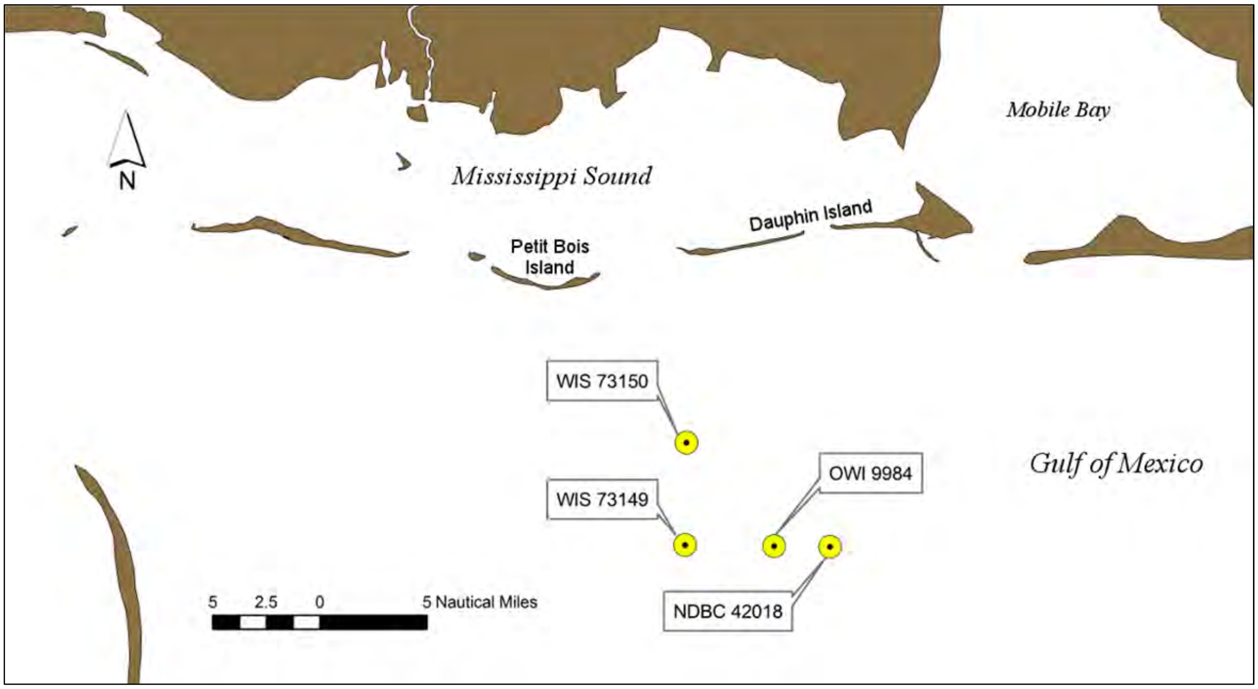

Figure 19. Locations of available wave data sets.

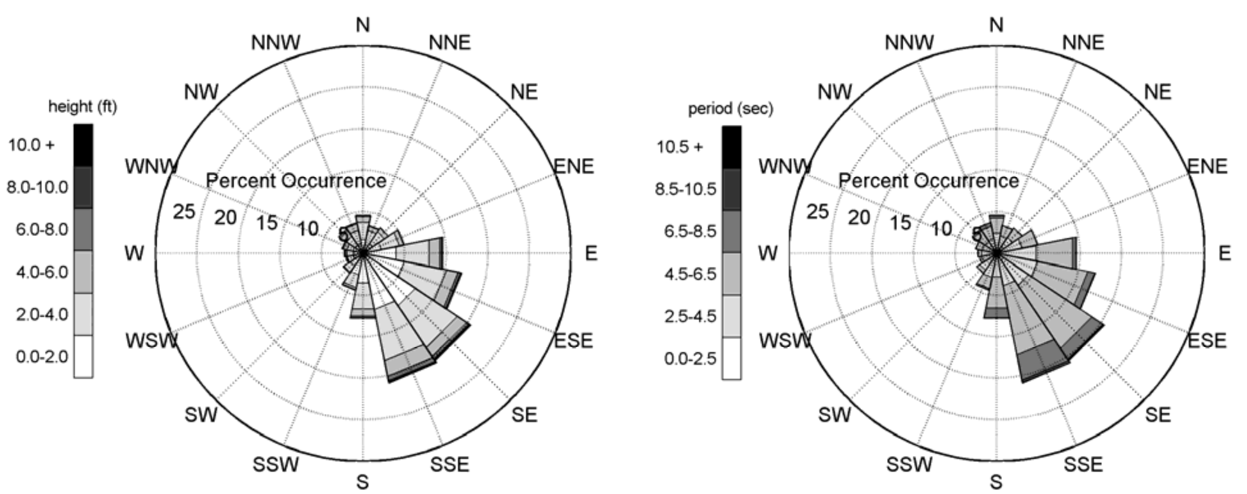

Figure 20. Wave height and period for Oceanweather, Inc hindcast grid point 9984 (14 NM south of Dauphin Island) for the 29-year period between January 1980 and December 2008. Direction indicates from where waves were traveling, relative to true north. Radial length of gray tone segments indicates percent occurrence for each range of wave heights and periods. Combined length of segments in each sector indicate percent occurrence of all waves from that direction.

The most common wave periods from all compass sectors are between 4.5 and 6.5 seconds, which occurs 45% of the time. Waves with periods longer than 10.5 seconds occur less than 0.3% of the time, representing a cumulative occurrence of 640 hours out of the 29-year span of time covered by the hindcast.

3.1.2 CMS-Wave Model

CMS-Wave was implemented in this study using two grids: A coarse grid that propagates wave from the offshore location of the wave data source and a fine nested grid that lies completely within the domain of the coarse grid.

Bathymetric data used to develop these grids was assembled from four sources. The majority of the area covered by the coarse wave model grid uses bathymetry data extracted from an ADCIRC grid of the Gulf of Mexico developed by the USACE. It includes high-resolution representations of navigation channels and passes between Mississippi Sound and the Gulf. Bathymetry data from Petit Bois Pass and at the proposed borrow sites comes from high resolution ship-track surveys that were performed in 2006, 2009, and 2011 (Table 1).

Coarse Wave Grid. The coarse grid is composed of regular Cartesian elements with a 300 meter (984 feet) cell size. It was created to extend 16.5 NM (30.6 km) from the Oceanweather hindcast station (OWI 9984; Figure 21) north to the sound side of Petit Bois and Dauphin Islands. The grid extends east 62.6 NM (116.0 km) from Ship Island to beyond the eastern end of the Fort Morgan Peninsula. The northernmost 7.3 km of the Chandeleur Islands also is included within the limits of the grid. The wide east-west extent of the coarse grid is designed to minimize shadowing effects from the lateral boundaries (east and west sides) on the main study area at Petit Bois Pass. The total number of cells used in this grid is 39,474, with 387 cells along the east-west axis (J) and 102 cell along the north-south axis (I). Greatest depths in this grid occur along the offshore boundary, with a maximum of 96.5 feet (29.4 m).

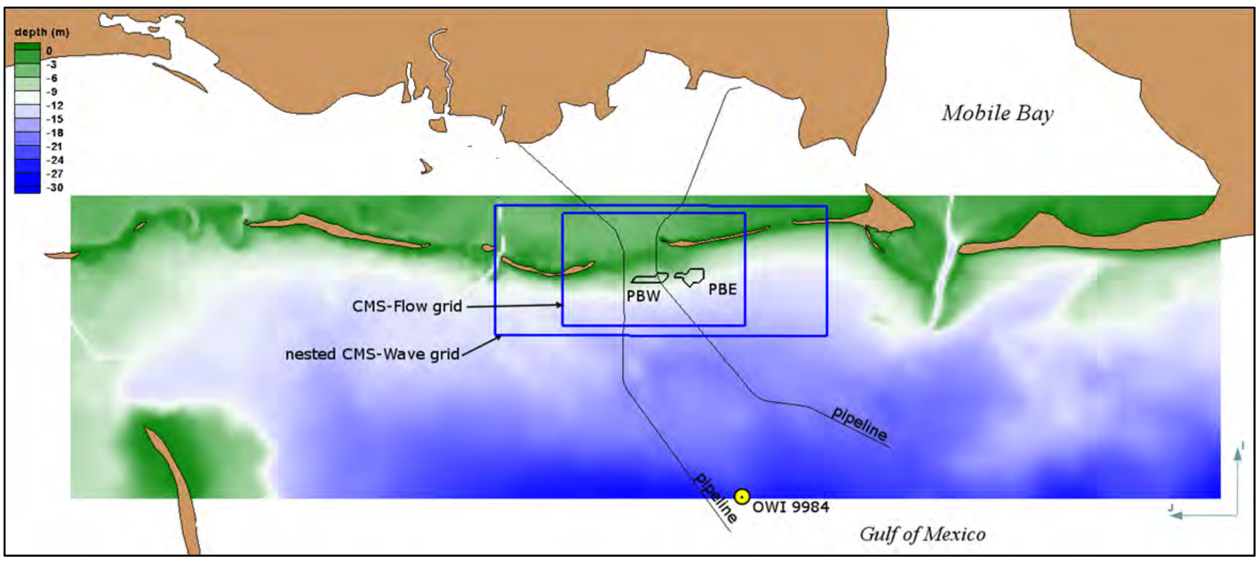

Figure 21. Map showing extent of CMS-Wave coarse grid with color-shaded bathymetric contours. The extents of the nested CMS-Wave grid of Petit Bois Pass and the CMS-Flow grid are indicated by blue rectangles. Paths of the two pipelines that traverse Petit Bois Pass are illustrated.

Fine Wave Grid. The fine nested grid is composed of irregular Cartesian elements that vary in size between 656 feet (200 m) and 102 feet (31 m). The areas of finest mesh resolution are over the borrow sites and along the shoreline (Figure 22). The short axis of the grid has 117 cells while the long east-west axis of the grid is divided into 279 cells, which describe 32,643 cells for this mesh. The average depth of the seaward open boundary of the grid is 55.1 feet (16.8 m) mean tide level (MTL), and the greatest depth along this edge is 60.7 feet (18.5 m). Wave spectra for the seaward open boundary are extracted from cells within the domain of the coarse grid that spatially correspond to the cells along the open boundary of the nested fine grid. The coarse grid cells that are used for open boundary spectral output can be automatically specified in SMS. The user must simply specify which grid is the nested grid (or “child” grid, using the native parlance of SMS).

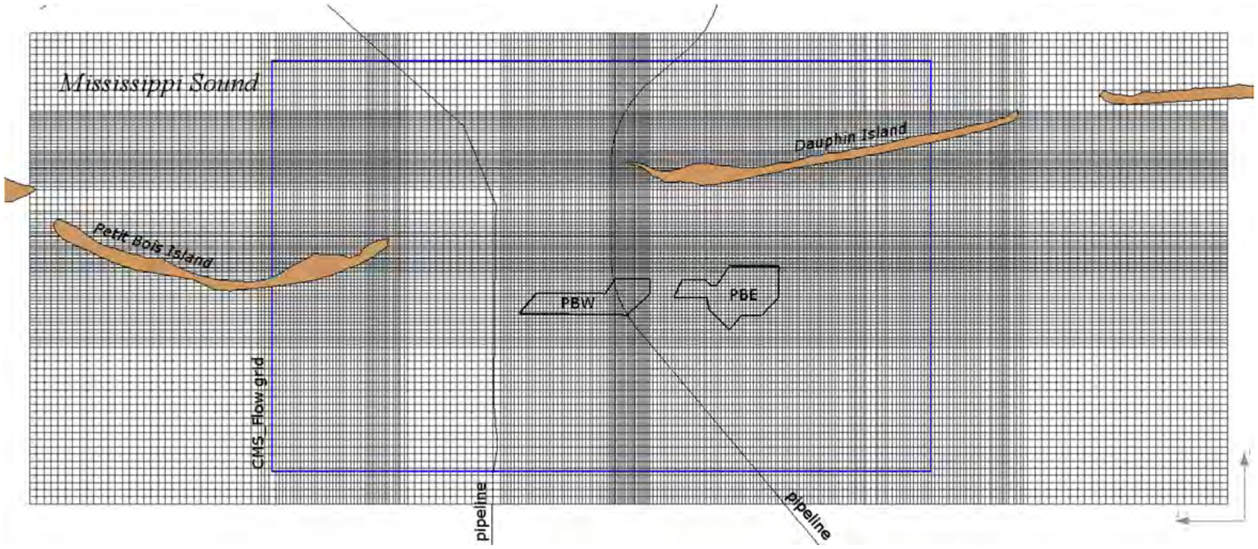

Figure 22. CMS-Wave fine nested grid mesh for Petit Bois Pass. The CMS-Flow mesh boundary is indicated using a blue box.

3.1.3 Annual Wave Input Conditions

Wave input spectra that were run with the coarse grid were developed using the OWI hindcast. These data have two main advantages over others that exist in the vicinity of Petit Bois Pass: the length of the record and the availability of full 2-dimentional wave spectra. It was necessary to reformat spectral output provided by OWI for use with CMS. Spectral energy binning used in the original data is 15-degree directional resolution (24 total bins around full 360 degree circle) and a variable frequency resolution between 0.039 and 0.322 Hz. CMS requires a directional binning of 5 degrees. The reformatting process used a cubic spline fit of each individual frequency in each separate spectrum to interpolate the original 15-degree bins to 5-degree directional bins.

One objective of this analysis is to run pre- and post-dredging conditions at the Petit Bois borrow sites for a complete year. The single year chosen to model from the complete 29-year OWI hindcast was selected based on how well it represented average conditions from the complete record. This was accomplished by comparing the wave energy distribution of all waves approaching Petit Bois Pass (the compass sector between 90 and 270 degrees) for the entire length of record to each separate year. Mean wave energy was calculated for each of nine 22.5 degree direction bins (East through West) for all 29 years in the OWI hindcast. These separate annual distributions of wave energy were compared to the distribution calculated for the same direction bins using the entire 29 year of data. A plot of wave energy by compass sector for all years and the annual average is presented in Figure 23. For the SSE sector (the predominant wave direction), annual wave energy varies between one-half to two-times the average energy of complete hindcast. The year that best represents wave conditions of the whole record is 1984, which has the distribution with the minimum RMS error (2% of total average wave energy of E through W sectors) and best R^2 correlation (0.94). The distribution of energy for the year 1984 is also shown in Figure 23. At the peak SSE sector, the average annual wave energy content is essentially equal to the peak in the 1984 distribution.

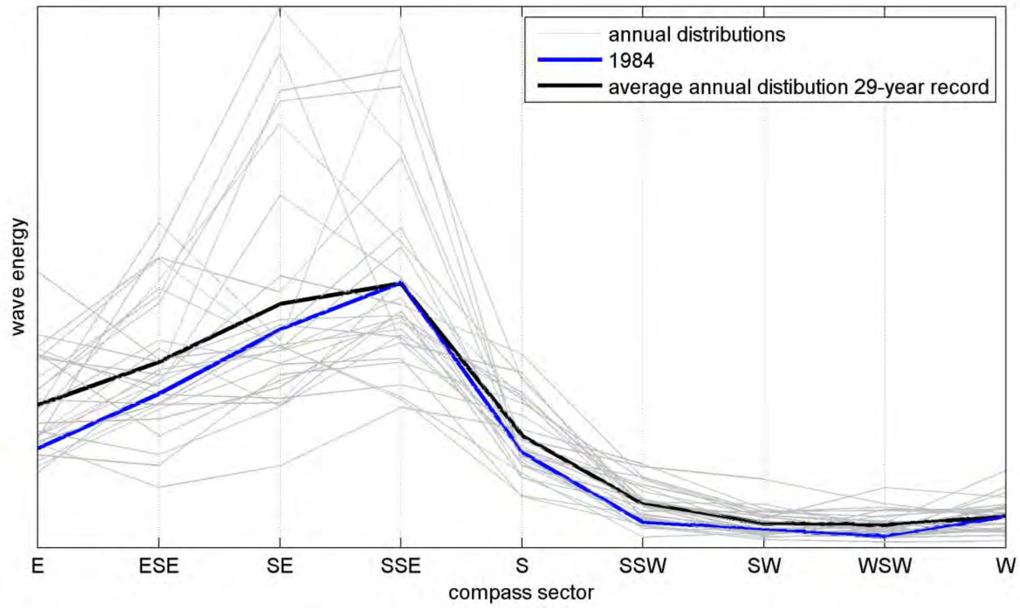

Figure 23. Distribution of total wave energy by compass sector from the OWI 29-year hindcast. Annual sums of wave energy (grey lines) are compared to the average for the entire record by sector (black line). The year with the best comparison to the entire record (1984) is indicated using a blue line.

3.1.4 Storm Wave Input Conditions

In addition to the year-long period of waves that were run at Petit Bois Pass, a separate storm simulation was executed to gauge how differently the morphology of the borrow sites would be affected by a major storm event compared with more typical conditions. A simple method was developed to select which storm event to use for the 29 years covered by the OWI hindcast, based on the magnitude of bottom orbital velocities that would be generated at the borrow sites by waves. By this method, waves are shoaled from the offshore location of the OWI hindcast station to a depth of 34.4 feet (10.5 m), which approximates the mean depth of water at the borrow sites. Water surface elevations from the OWI hindcast were added to the mean depth to account for tidal and storm surge variations. Orbital velocities at the borrow sites were then computed assuming linear waves.

Selection of Modeled Storm. The method used to shoal waves to the borrow sites used the simplifying assumptions of straight and parallel bottom contours and no dependence on wave direction. Wave height at the borrow sites is computed as $H_2 = H_1 K_s$ where H_1 is the wave height at the OWI station and K_s is the shoaling coefficient (Dean and Dalrymple, 1991). K_s is determined using the relationship $K_s = \sqrt{C_{g1}/C_{g2}}$,where C_{g1} and C_{g2} are the group celerity at the hindcast station and borrow site, respectively. Group celerity C_g is calculated as $C_g = nC$. In this equation C is the wave celerity (propagation speed), and n in a coefficient determined by

$$n = 0.5[1 + 2kh/\sinh 2kh]$$

where k is the wave number and h is the total water depth. The wave number k is solved for iteratively using the dispersion relationship

$$\sigma^2 = gk\tanh kh$$

where σ is the angular frequency of the wave ($\sigma = 2\pi T$) and g is the gravitational constant. After shoaling waves to the borrow site depth, their height is reduced if necessary to account for wave breaking. If a wave is greater than 0.78 times the water depth, then it is reduced to equal that amount. The maximum orbital velocity is finally calculated using the equation

$$u = \frac{H}{2}\sigma\frac{\cosh k(h+z)}{\sinh kh}\sin kx \sin \sigma t$$

which simplifies to

$$u_{max} = \frac{H}{2}\sigma\frac{1}{\sinh kh}$$

at the seabed (when $z = -h$).

Because the largest waves in the 29-year record approaching the borrow sites are depth limited, the largest annual events in the record produce velocities that occur within the narrow range of 8.2 and 13.1 ft/sec (2.5 and 4.0 m/s). The top four annual events produce bottom velocities that occur in an even tighter range, between 12.1 and 13.1 ft/sec (3.7 and 4.0 m/s). These occurred during Hurricane Opal (October, 1995), Hurricane Georges (September, 1998), Hurricane Ivan (September, 2004) and Hurricane Katrina (September 2005), listed in order of increasing calculated bottom velocity.

An extremal analysis of the calculated maximum bottom orbital velocities was performed to provide further insight into how waves during extreme storm events affect sediment mobility at the borrow sites. Based on this analysis of extreme bottom velocities, Hurricane Katrina has a return period of between 33 and 52 years, using Weibull (k=1.0) and Fisher–Tippett I probability distribution plotting functions, respectively (USACE, 2002). The four top storms have return periods of between 7 and 52 years based on bottom velocities. This indicates that events that generate bottom velocities that are equal to or greater than 12 ft/sec occur on average once every 7 years.

Because large bottom velocities occur relatively frequently, it was decided that Hurricane Katrina would be a useful storm to simulate using CMS. Though this storm produced the greatest bottom velocities in this quick analysis, the magnitude of velocities is not much larger than more commonly occurring events. With regard to maximum wave orbital velocities at the borrow sites, Katrina well represents the typical maximum event for this site, even though it is the most extreme, by most measures, in the record.

<u>Katrina Waves.</u> Oceanweather Inc. provides storm hindcast data similar to their long-term hindcast product. Instead of providing data at only one grid point at one-hour intervals, the storm hindcast provides data over a grid of nodes with a 7 km spacing at a 15 minute interval for the duration of the storm. The storm hindcast of Katrina encompasses the period between August 23 and 31, 2005.

Figures 24 through 26 show how water level, wave height, and wind speed varied during the storm at a hindcast grid point located 5 NM SE of Petit Bois Island. Maximum water levels offshore the Pass were approximately 9 feet above mean sea level at peak storm intensity in this region. Maximum wave heights during the hurricane were 35 feet (Figure 25). These largest waves had a period of 14 seconds. With the surge, the water depth at the borrow sites is only a few feet greater than the maximum wave height, which is an initial indication that wave conditions at peak storm intensity were depth limited at the borrow sites. Wind speeds reach a maximum of 69 knots offshore Petit Bois Pass (Figure 25). At the time of peak wind speed, the wind was blowing to the NNW.

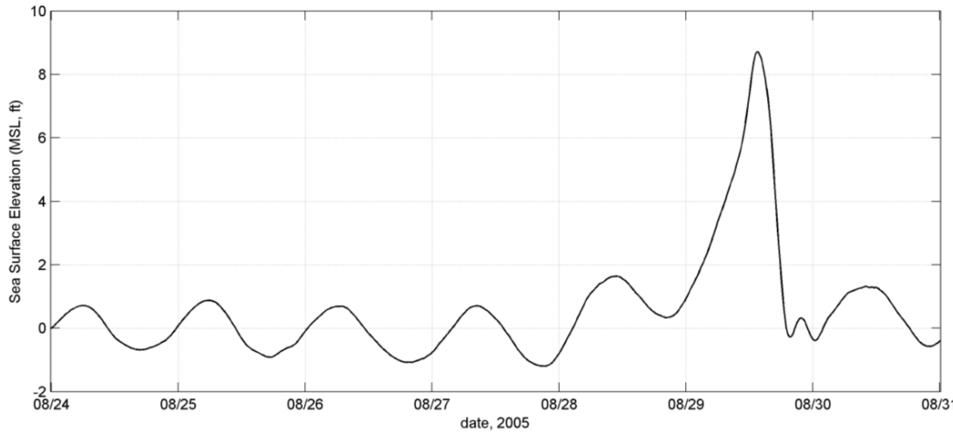

Figure 24. Water surface elevation offshore Petit Bois Pass during Hurricane Katrina from the Oceanweather storm hindcast.

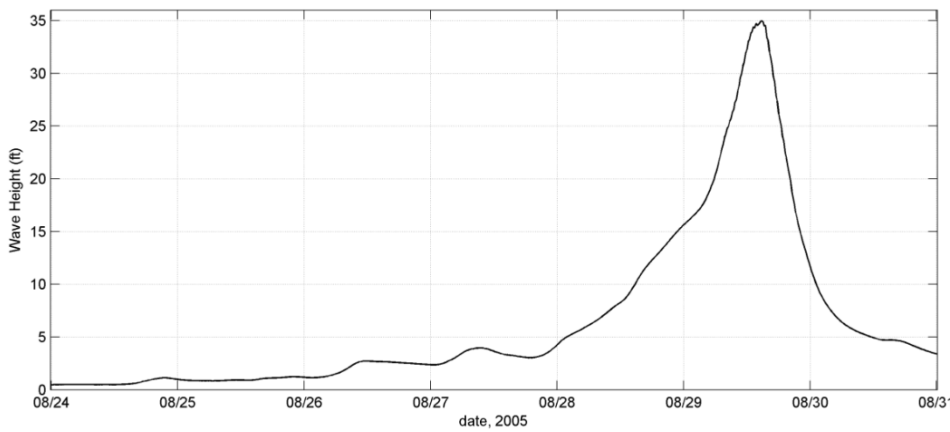

Figure 25. Significant wave height offshore Petit Bois Pass during Hurricane Katrina from the Oceanweather storm hindcast.

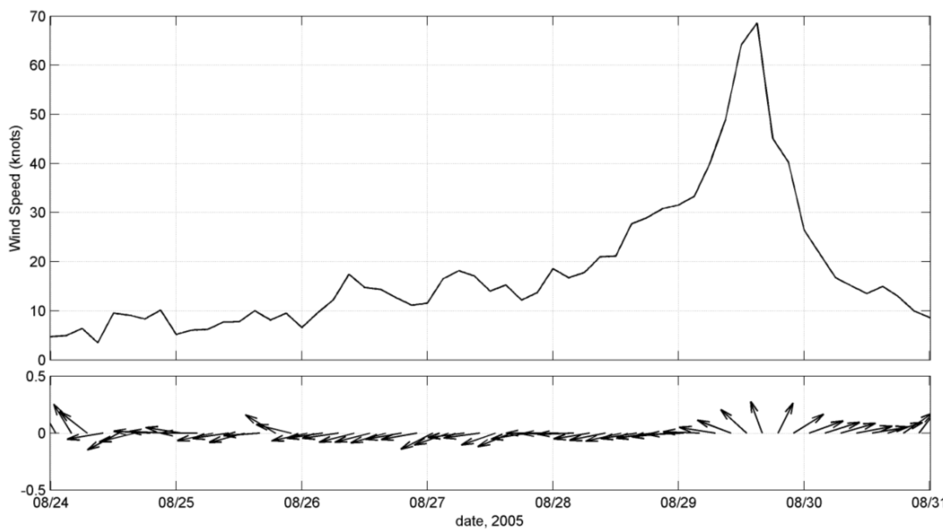

Figure 26. Plot of wind speed and direction during Hurricane Katrina from the Oceanweather storm hindcast. Vectors indicate compass direction to where the wind was blowing.

3.2 HYDRODYNAMIC MODELING

CMS-Flow was used in this study to simulate hydrodynamics and sediment transport in the vicinity of the borrow sites, including Petit Bois Pass. Tidal flows through the Pass influence the movement of sediment and morphology change across the planform of the Pass and at the ends of Petit Bois and Dauphin Islands. The extent of the CMS-Flow grid was designed with a focus on the borrow sites and to include the Pass and a portion of the islands that mark the boundary of Mississippi Sound and the Gulf of Mexico (Figure 21).

Because the study area is located more than 8 NM from the mainland along the barrier islands of Mississippi Sound, it is necessary to create a model mesh that has open boundaries on both the Sound and Gulf sides of the grid. The hydrodynamic boundary conditions for both grid open boundaries were extracted from a simulation of tides for the entire Gulf of Mexico computed using ADCIRC.

3.2.1 ADCIRC Simulation of Tides

The ADCIRC simulation of tides used to develop hydrodynamic boundary conditions for the CMS-Flow grid utilized a grid of the entire Gulf of Mexico (GOM) that was employed in a previous study of sediment transport pathways at Mobile Pass (Byrnes *et al*., 2010). The grid domain has open boundaries at the Straits of Florida (between Key West, Florida and Havana, Cuba) and across the Yucatan Channel (between Cabo San Antonio, Cuba and Cancun, Mexico). The grid is composed of 61,043 nodes that describe 115,401 total elements. Figure 27 shows the grid mesh with contours overlaid on a global terrain map. Depths in the grid range from a maximum of 12,372 feet (3,770 meters) to approximately 30 feet above sea level.

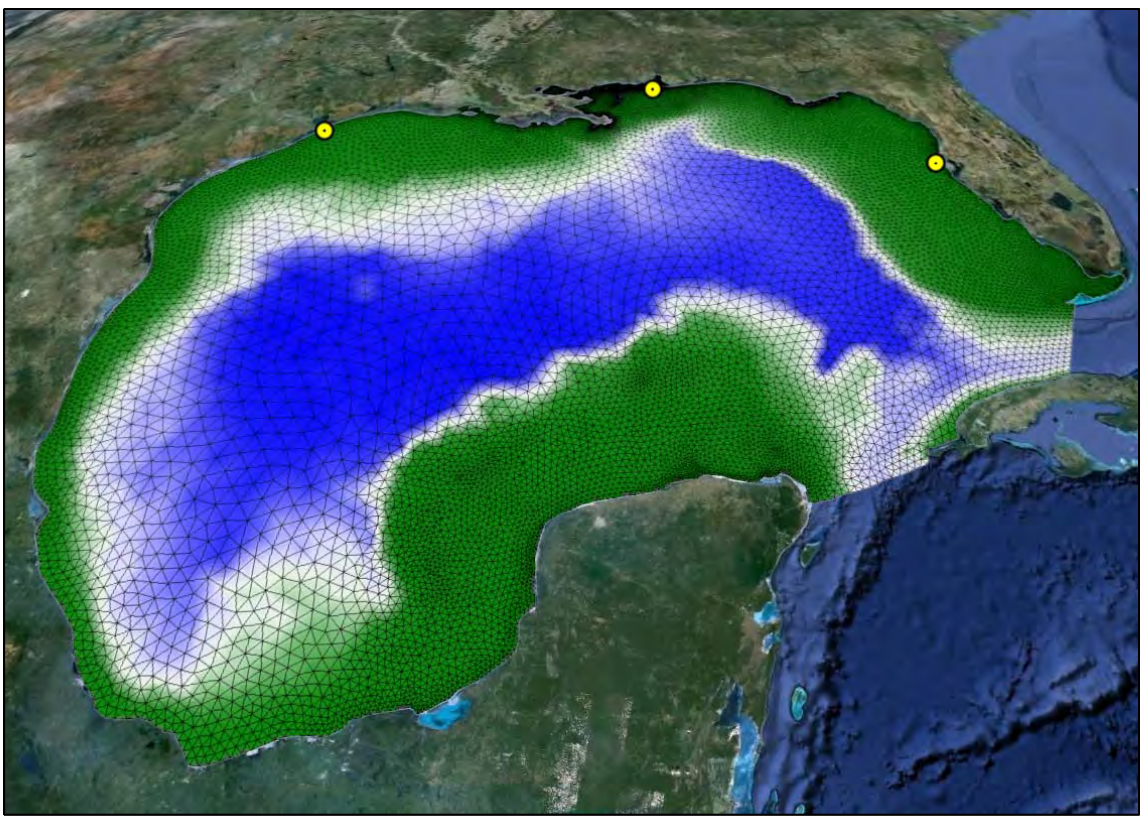

Figure 27. ADCIRC mesh of the Gulf of Mexico, showing grid elements and color contours overlaid on the Google Earth terrain map of the globe. NOAA tide stations used to calibrate the model are indicated by yellow markers (Galveston, TX; Dauphin Is., AL; Clearwater Beach, FL from west to east).

A close-up of the GoM mesh between the Mississippi River Delta and Mobile Bay is shown in Figure 28. The finest grid resolution occurs in this area of the mesh, where the smallest element side lengths are about 131 feet (40 meters) in the main navigation channels (e.g., to Mobile, AL and Pascagoula, MS). The grid was modified to include latest available ship-track bathymetry for Petit Bois Pass (2006 through 2011) and most recent shoreline for Petit Bois and Dauphin Islands (2010). Mesh resolution in the Pass was also refined.

The GoM model was calibrated using a month-long simulation. The modeled month was November 2007. This month was selected based on the comparison of calculated variance of astronomical tides for each separate month of 2007 to the variance of the astronomical tide calculated for the whole year. This test indicates that tidal energy in November best approximates average conditions for the entire year. The year 2007 was selected because it is recent enough that NOAA tide gauge data are available from stations across the Gulf that can be used to calibrate the model and because this year was relatively quiet with regard to storm activity in the area around Petit Bois Pass.

Model Parameterization. The GoM model was configured to simulate the entire month of November (2007) using the complete set of harmonic constituents (e.g., M2, K1, S2 and N2) available from the latest ADCIRC tidal constituent database (Mukai, *et al*., 2002). Tidal potential forcing was applied to the model domain. At the two open boundaries, time varying water surface elevations at each separate grid node along each open boundary were determined using the harmonic database.

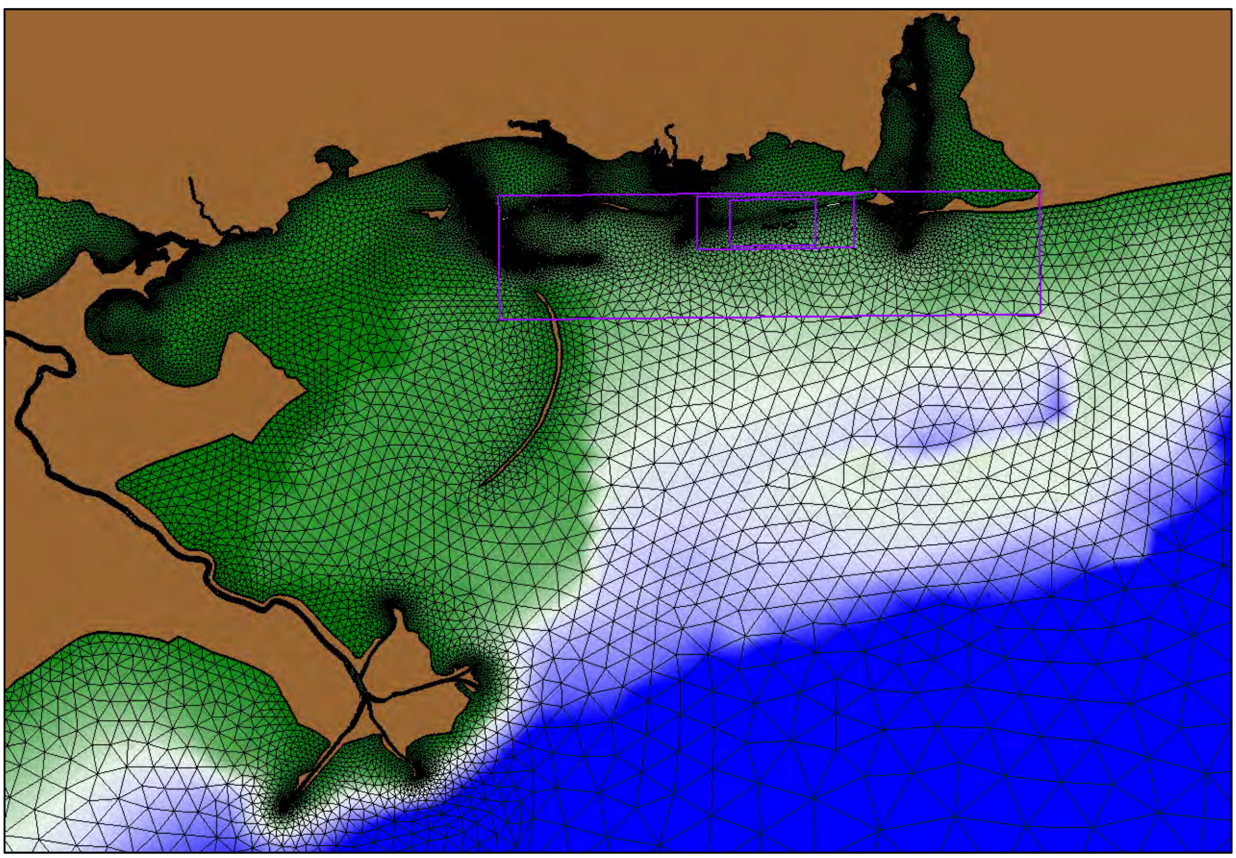

Figure 28. Close up of GoM ADCIRC grid with purple colored outlines denoting the CMS-Wave and Flow grid extents.

The GoM simulation implemented all optional terms available in the model formulation including finite amplitude, advective, and time derivative terms. Wetting and drying of elements and variable Coriolis forcing also were included. A lateral viscosity of 2.0 m^2/sec and a constant quadratic friction coefficient of 0.0025 were applied to the entire model domain. The model was run using a time step of 2.0 seconds, which was necessary because of numerical stability requirements resulting from fine mesh resolution used in deep navigation channels included in the GoM grid. A 15-day model spin up period was added to the beginning of the modeled month to ensure sufficient time for tides to fully develop across the grid. Finally, an output interval of 10 minutes was specified for modeled water surface elevation and velocity components.

Model Calibration. The GoM model was calibrated using predicted tides from three active NOAA tide stations: 1) Dauphin Island, AL at the entrance to Mobile Bay; 2) Galveston Island, TX; and 3) Clearwater Beach, FL. Predicted tides from NOAA were used because measured tide data include non-tidal fluctuations in water level caused by atmospheric forcing or warm-water eddies shed from the Loop Current, which are not included in the GoM model. For the Dauphin Island NOAA tide station, non-tidal variance (a measure of energy content) of water level fluctuations amounts to 49% of the total variance of the measured tide for the whole of 2007. For the modeled month of November 2007, the non-tidal variance is 28% of the measured tide.

Comparisons of model output and predicted NOAA tide (astronomical tide) are provided in Figures 29 through 31 for three NOAA stations used for the GoM model calibration. A comparison is also provided in Table 3 of the main tidal constituents computed for model output and predicted NOAA tides for November 2007. Tidal constituents with the largest amplitudes at all three locations are the K_1 and O_1, which are both diurnal constituents. The K_1 is the principle solar diurnal constituent while O_1 is a lunar diurnal constituent. Together, they describe the effect of the declination (similar to latitude) of the moon in its orbit around the earth (NOAA, 2001).

Model output at the three stations compares well with NOAA astronomical tide. At the Dauphin Island station the calculated R_2 between the two data sets is 0.93 and the RMS error is 0.2 feet. Calculated error between tide constituents computed for the model and NOAA data is smaller than 0.05 feet at Dauphin Island. The error of the K1 constituent (the largest constituent for NOAA data) is less than 7% of its amplitude. Tidal calibration is also good at the Galveston and Clearwater Beach stations, with R^2 values of 0.910 and 0.91 and RMS errors of 0.3 and 0.2 feet, respectively.

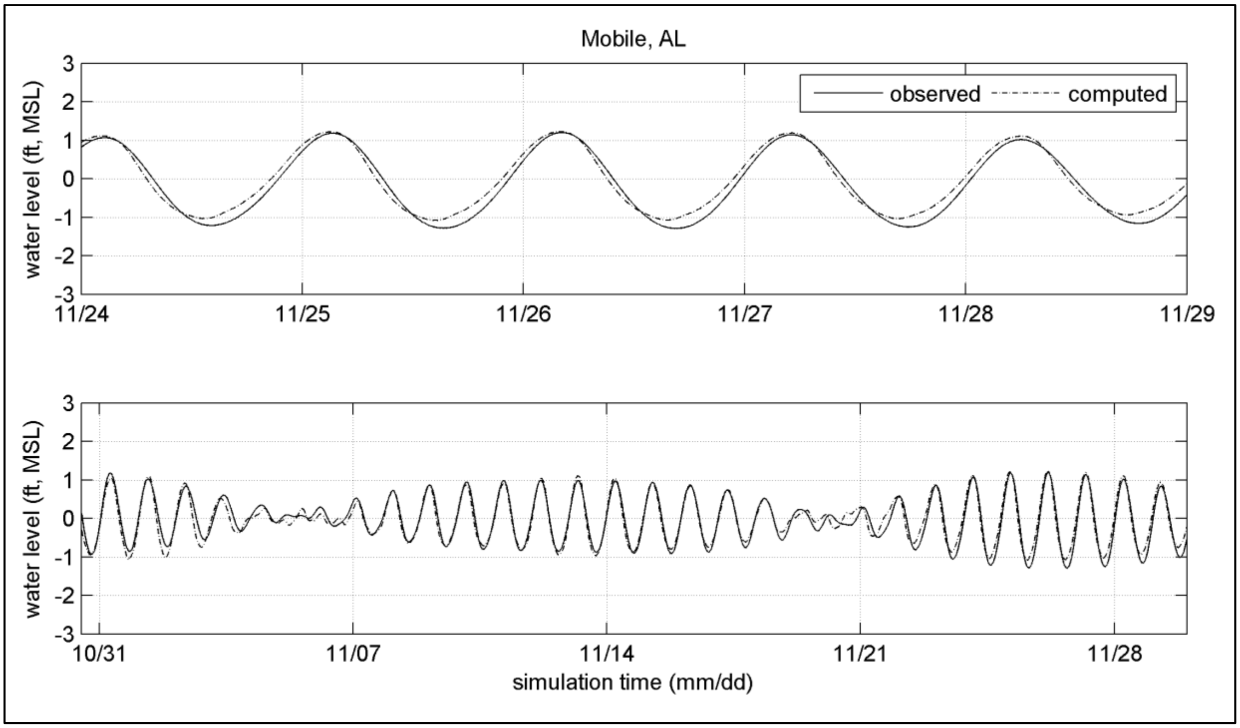

Figure 29. Comparison of modeled and NOAA predicted tide at Dauphin Island, AL. R^2 correlation is 0.93 and RMS error is 0.2 feet. The top plot is a subset of the complete month shown in the bottom plot.

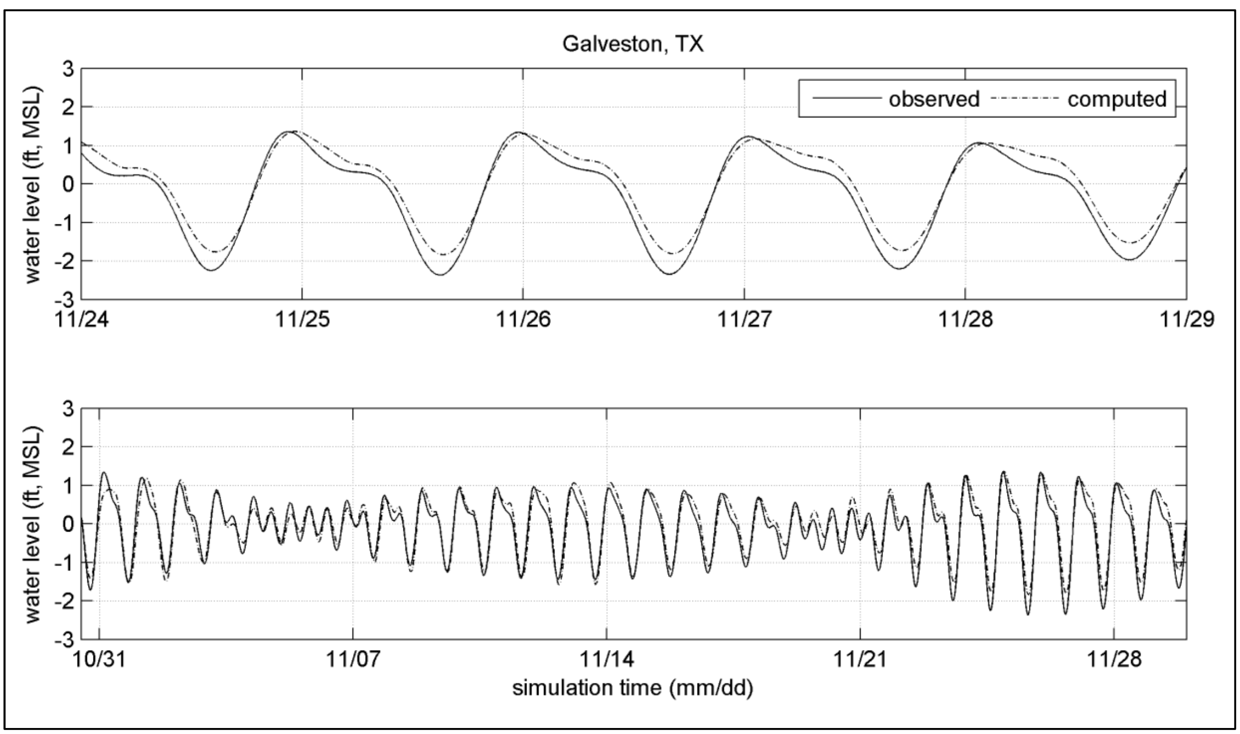

Figure 30. Comparison of modeled and NOAA predicted tide at Dauphin Island, AL. R^2 correlation is 0.91 and RMS error is 0.3 feet. The top plot is a subset of the complete month shown in the bottom plot.

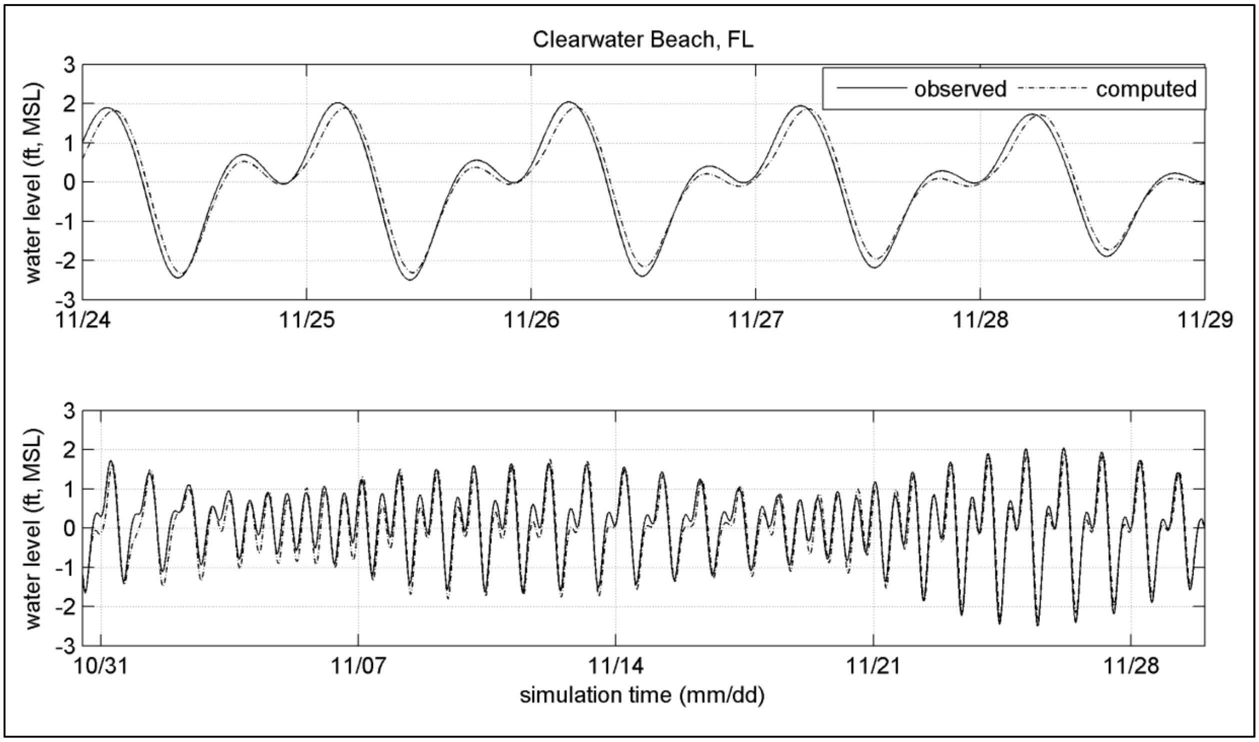

Figure 31. Comparison of modeled and NOAA predicted tide at Clearwater Beach, FL. R2 correlation is 0.90 and RMS error is 0.2 feet. The top plot is a subset of the complete month shown in the bottom plot.

Table 3. Tidal constituents for astronomical tide and calibrated ADCIRC model output, with model error amplitudes, during modeled November 2007 calibration time period.

Location	Constituent Amplitude (ft)				Phase (deg)	
Model Calibration Run						
	K_1	M_2	S_2	O_1	ϕK_2	ϕO_1
Dauphin Island, AL	0.53	0.09	0.05	0.55	-94.2	-94.4
Galveston Is., TX	0.67	0.44	0.11	0.62	-106.9	-107.9
Clearwater Beach, FL	0.59	0.79	0.32	0.58	-118.5	-114.9
Measured Tide During Calibration Period						
Location	Constituent Amplitude (ft)				Phase (deg)	
	K_1	M_2	S_2	O_1	ϕK_2	ϕO_1
Dauphin Island, AL	0.57	0.04	0.05	0.53	-87.0	-85.9
Galveston Is., TX	0.65	0.34	0.13	0.65	-98.1	-98.5
Clearwater Beach, FL	0.62	0.77	0.30	0.59	-131.5	-124.8
Error						
Location	Error Amplitude (ft)				Phase error (min)	
	K_1	M_2	S_2	O_1	ϕK_2	ϕO_1
Dauphin Island, AL	0.04	-0.05	0.00	-0.02	28.7	36.4
Galveston Is., TX	-0.03	-0.09	0.02	0.02	-34.8	-40.5
Clearwater Beach, FL	0.03	-0.02	-0.02	0.01	-52.0	-42.0

ADCP Verification. An additional check of the tidal velocities is possible using data collected using an Acoustic Doppler Current Profiler (ADCP) survey of Petit Bois Pass that was performed by the USACE on March 25, 2011. The survey vessel transited the Pass 11 times over the duration of the six-hour survey. The tide was flooding into Mississippi Sound for all but the last transect crossings record that day. Due to quality issues with the ADCP data (e.g., large unmeasured segments of the water column compared with total water depth), the survey results cannot be directly compared to GoM model output. However, an average of the velocity measurements across the 3.1 NM transect can be compared quantitatively to a similar average velocity across Petit Bois Pass in the GoM model. From the usable ADCP data, during maximum flood, average velocity was calculated to be 1.5 ft/sec. Maximum model flood velocities were 1.1 ft/sec during a flooding tide with a similar range as the tide measured during the survey and averaged across Petit Bois Pass. Though it is not a precise comparison, this check shows that the ADCP measurements and model output qualitatively compare well.

3.2.2 CMS-Flow

Output from the ADCIRC GoM simulation was used to drive the open boundaries of the CMS-Flow grid developed to model annual wave and tidally driven sediment transport at the borrow sites and the general area of Petit Bois Pass. The CMS-Flow mesh is illustrated in Figure 32. This telescoping grid has a total of 37,475 cells, with a cell size that varies between 102 and 1627 feet (31 and 496 meters). The finest grid resolution was used primarily in the area around borrow sites. The greatest depths in the grid occur along the southern open boundary (approximately 17 meters) near the point where the Gulfstream pipeline exits the grid domain to the south.

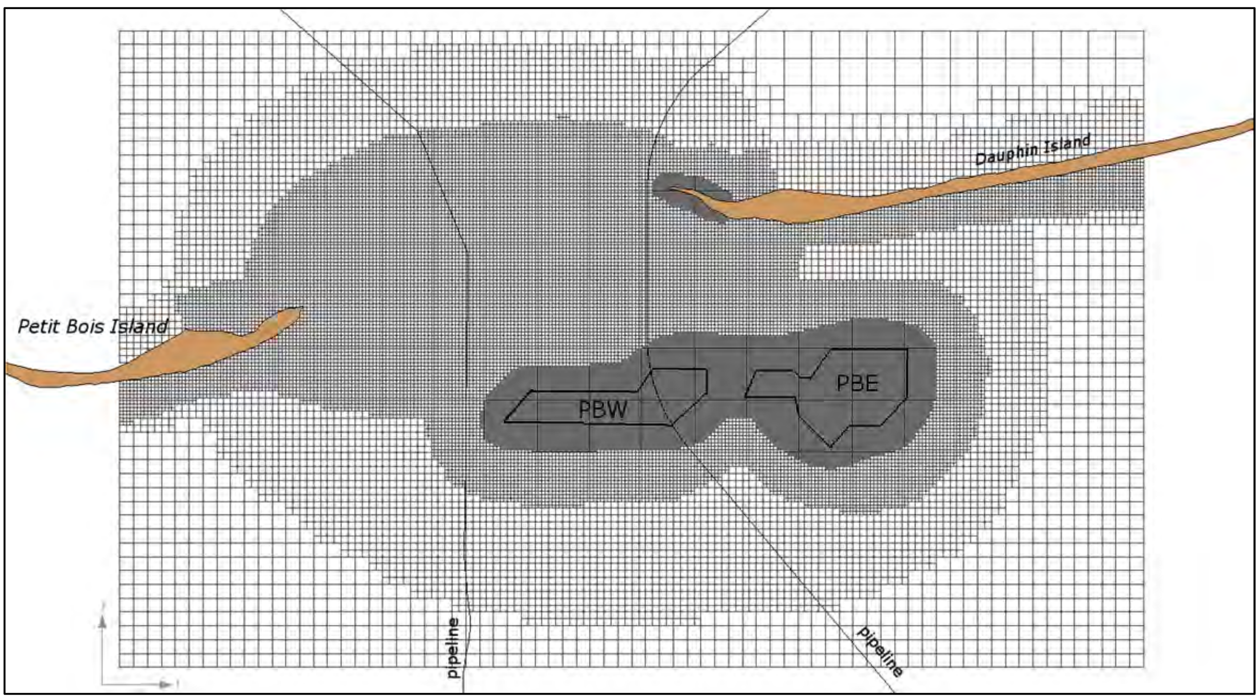

Figure 32. CMS-Flow telescoping mesh of Petit Bois Pass.

The most recent available ship track bathymetry was use to development this grid, including a 2011 survey of the borrow sites. The 2010 high-water shoreline derived from high-resolution aerial imagery for Dauphin and Petit Bois Island also was incorporated in the grid.

The Flow model was run using a 10-minute time step for an entire year (1984) and for the modeled storm. This time step is the same specified as the output interval for the GoM ADCIRC model. The implicit formulation of the model was used. This formulation was made available in the latest versions of CMS and allows the user to specify time steps of the order one to ten minutes. The explicit formulation is generally much less numerically robust when used with time steps that are large. A uniform Manning's friction factor of 0.003 was applied to the model domain.

For the Hurricane Katrina simulation, storm water levels were applied to both open boundaries. The storm simulation was run for 122 hours, beginning at 0000h UTC August 26, 2005. The same time step and model parameters used for the annual simulation were used for the storm simulation.

3.3 MORPHOLOGICAL MODELING

Sediment transport and morphology change were modeled using CMS-Flow. The same telescoping mesh used for hydrodynamic was used for morphology change simulations. The same 10-minute model time step used with the hydrodynamic computations was used for morphology change computations. The Lund-CIRP transport capacity formula was selected as the basis for sediment transport computations. A sediment density of 2650 kg/m^3 was specified. A median grain size of 0.32 mm was applied to the whole model domain based on available sediment core data at the borrow sites from a recent USACE geotechnical investigation of the area.

For the annual model run, the CMS steering module was set up to run CMS-Wave every two hours of simulation time. For the Hurricane Katrina simulation, CMS-Wave ran every hour of simulation time.

Initially, the full morphological model, including waves and tidal currents, was run using NDBC spectral wave data from February 1990 to compare measured trends in bathymetric change with model results. This check is intended to provide a qualitative comparison based on observed trends. Because measured change is calculated using a much longer time period than the year-long simulation, it is difficult to make a direct comparison. Trends in computed bathymetric change for the month long simulation as shown in Figure 33 compare well with change patterns derived from most recent measured data (see Figure 18).

For modeled and measured results, the planform of Petit Bois Pass erodes along a broad (greater than one mile) swath in the center of the pass, while material is deposited in a thinner band along Gulf and Sound sides of the Pass. A large area of erosion seen in the measured data (Figure 18) just to the north of PBE is not present in the model results. This is because this area was a remnant of Petit Bois Island that existed when the Pass existed farther to the east (circa 1850). This remnant was not present in the bathymetric data (2006/2010) used to develop the CMS-Flow model grid, so material could not be eroded in this area of the model like it had from the longer time period covered in the historical change analysis (see Section 2.0).

A test was conducted to ensure that the resolution of the CMS-Flow mesh was fine enough that the cell size was not biasing the results computed by the model. A simulation of Hurricane Katrina was run using two separate Flow grids, one with a preferred 30 meter minimum cell size within the area surrounding the borrow sites, and another with four times the resolution (a 15 meter minimum cell size). Total bottom change at the end of both simulations was compared along a transect line that follows the path of the Gulfstream pipeline across PBW (Figure 34). This output along the pipeline is shown in Figure 35. This comparison shows that there is no great advantage to using the 15 meter minimum cell size, as the results show the same magnitudes of change. The average difference in computed change along the pipeline transect is 0.002 feet, another indication that the difference between the two grids is negligible. Because of this result, it was decided that the grid with the 30 meter minimum cell size was the optimal choice considering accuracy and computational efficiency (i.e., less time required to run the simulation with no trade-off in accuracy).

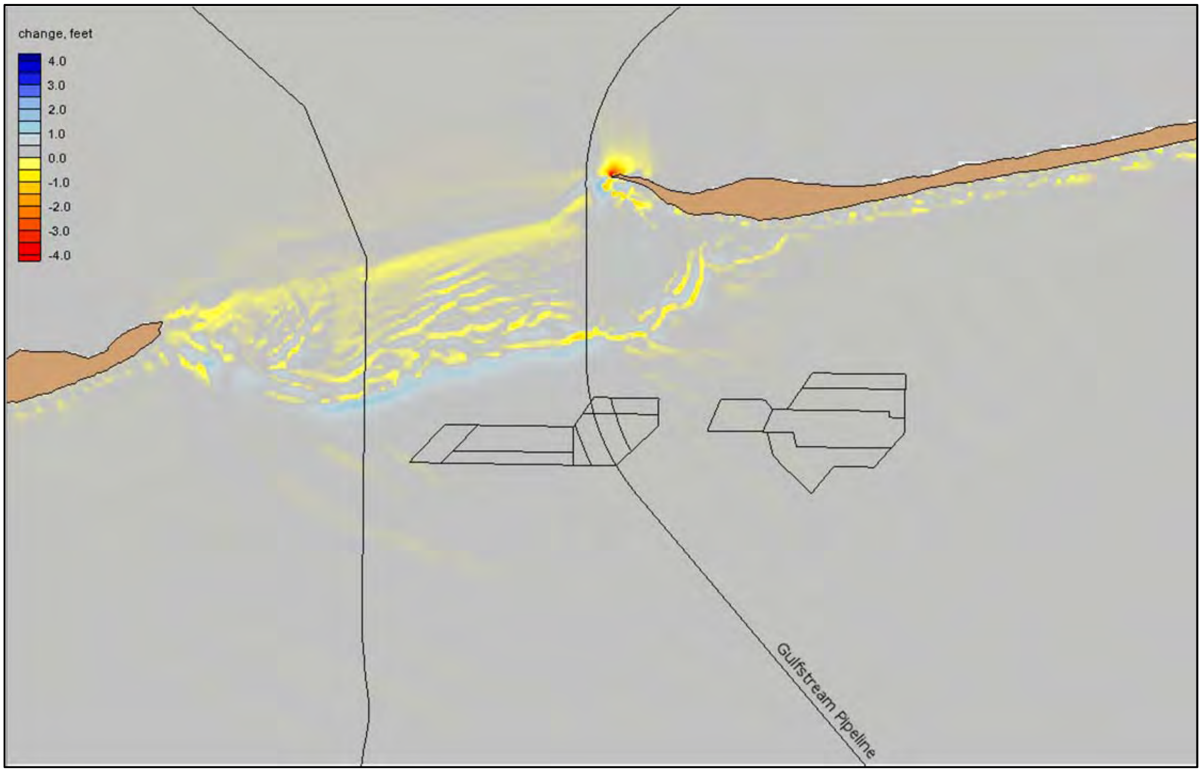

Figure 33. Morphological change computed for the month-long CMS simulation of February 1990.

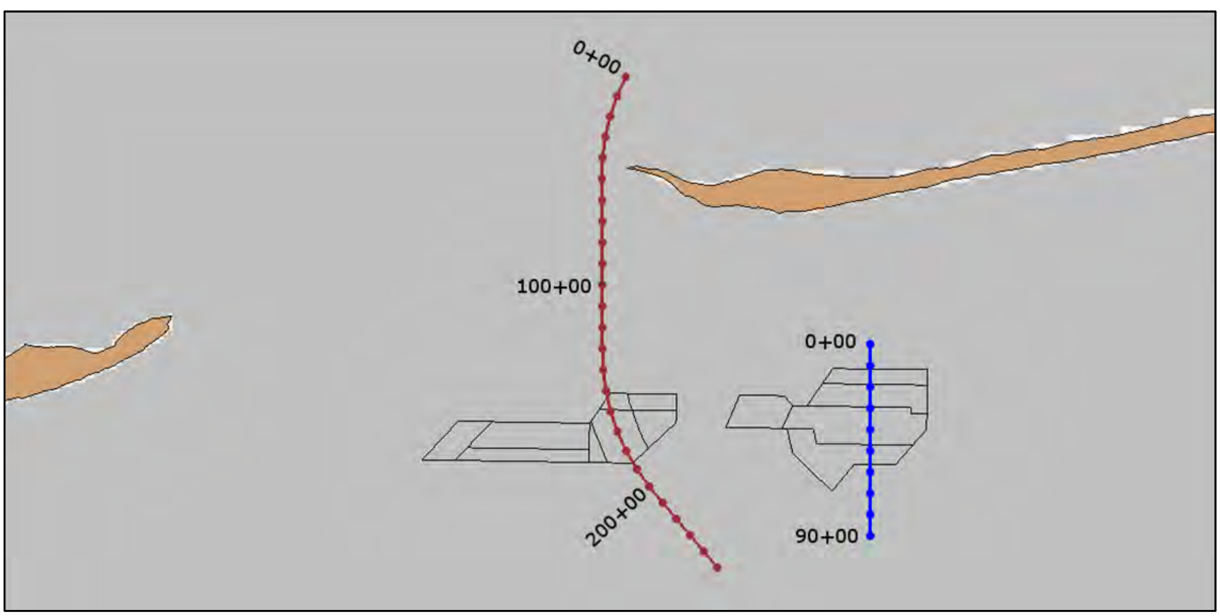

Figure 34. Transects used to plot morphology data across borrow sites. The blue transect that cross PBW follows the lay of the Gulfstream pipeline. Markers along lines are spaced every 1000 feet. Stationing is also provided in feet.

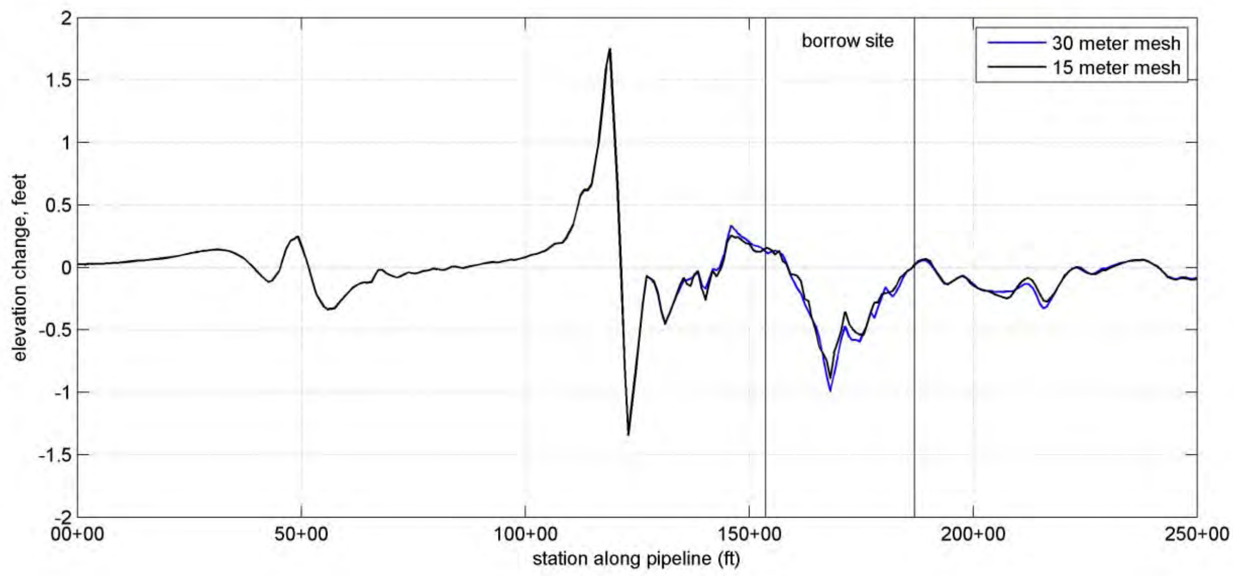

Figure 35. Comparison of simulations of Hurricane Katrina, run with two CMS-Flow meshes; a mesh with a 30 m minimum cell size (blue line) and a 15 m minimum cell size (black line). Output is provided along a segment of the Gulfstream pipeline shown in Figure 34.

4.0 MODELING RESULTS

Once CMS-Wave and CMS-Flow model development for the Petit Bois Pass borrow sites was completed, separate simulations of annual and storm-induced morphological change were performed. The same annual and storm conditions were used for existing conditions and the preferred borrow site excavation scenario to evaluate potential impacts to sediment transport processes.

4.1 WAVE MODELING

Because water depths within the boundaries of the proposed borrow sites range from 24 to 40 feet MSL, waves propagating through the Petit Bois Pass area must be relatively large (greater than 15 feet or so, depending on water surface elevation) for there to be significant changes in wave height at the borrow sites between existing and the post-dredging bathymetry.

Wave heights at the peak of Hurricane Katrina attained a maximum of about 26 feet offshore Petit Bois Pass (Figure 36). Under these conditions, waves begin to break when water depth is approximately 52 feet, farther seaward than the limits of the borrow sites. As waves continue to break across the borrow sites, heights decrease to less than 16 feet at the northern perimeter of PBW. When waves reach the offshore boundary of the ebb-tidal shoals at Petit Bois Pass, height is reduced further to less than 9 feet over a relatively short distance through the pass.

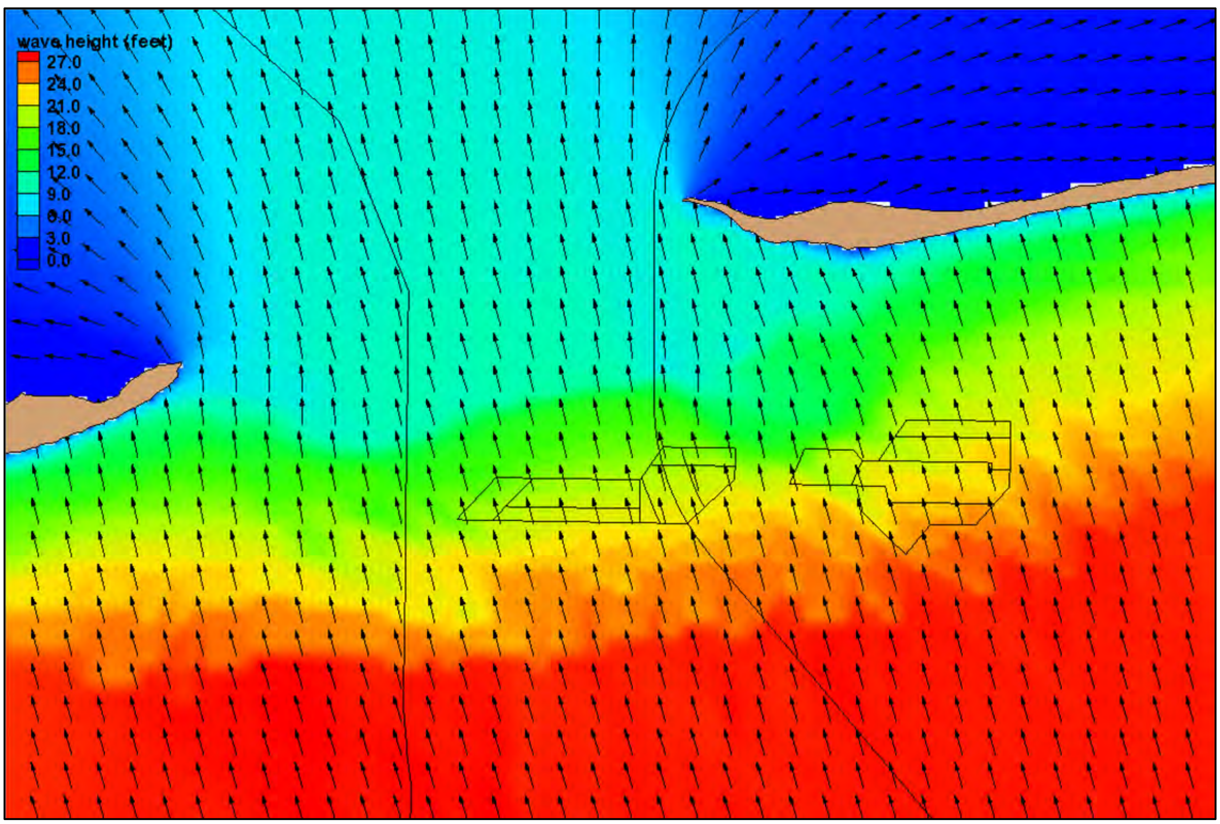

Figure 36. Contour plot of wave height with vectors indicating wave direction for maximum wave height conditions during Hurricane Katrina for existing conditions (pre-dredging) at the Petit Bois Pass.

Model output for the same wave condition after simulating borrow site excavation is presented in Figure 37. Wave heights document a similar pattern as illustrated in Figure 36 for existing conditions. Minor differences include larger wave heights within the boundary of PBE under the post-dredging scenario. At the northern edge of PBE, wave heights are 2 feet greater for the borrow site excavation simulation. Differences at PBW were present but smaller than those at PBE.

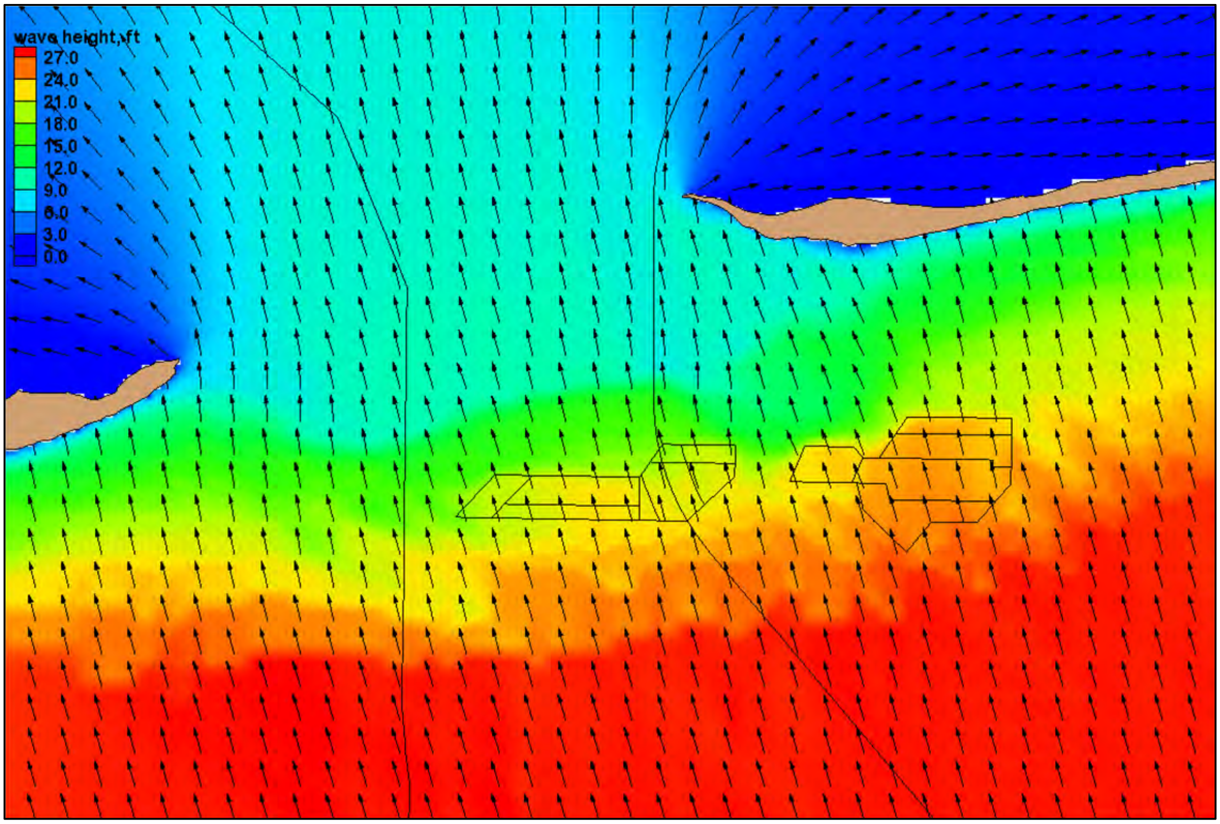

Figure 37. Contour plot of wave height with vectors that indicate wave direction for maximum wave height condition during Hurricane Katrina, for proposed dredged conditions (post-dredge) at the Petit Bois Borrow sites.

A plot of wave heights during the Hurricane Katrina simulation is shown in Figure 38 for PBW and in Figure 39 for PBE. The location of model output shown in Figure 38 is the point where the Gulfstream pipeline intersects the northern edge of the borrow site. This plot shows that wave heights are essentially unchanged at this location. Waves break along the 1000 ft excavation buffer zone just as they do for existing conditions, reducing height by 3 feet as they cross the borrow site perimeter.

At PBE, there is a visible change in wave heights at the northern border of the site. Wave heights are 2 feet larger in the post-dredging simulation. Under existing conditions, wave heights continue to break as they cross the borrow site area. For the post-dredging simulation, waves are larger because they propagate into deeper water across the excavated borrow site.

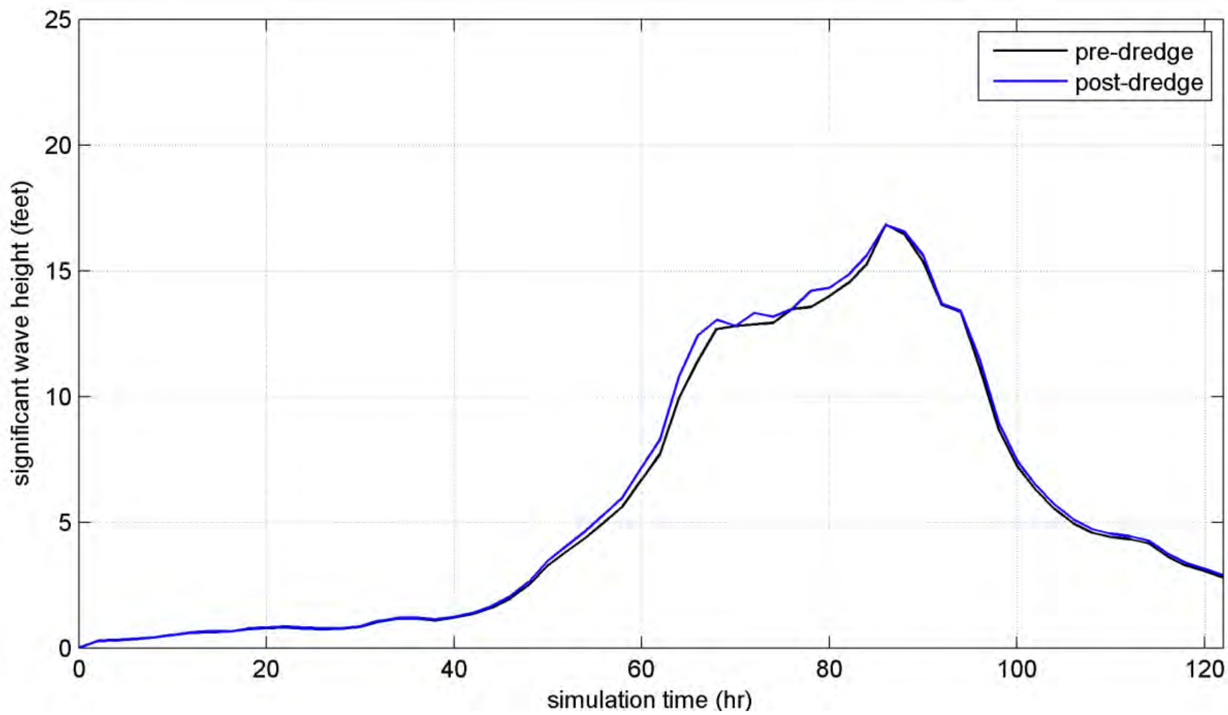

Figure 38. Plot of model wave height at the point where the Gulfstream pipeline intersects the northern boundary of PBW for existing and post-dredging conditions at the borrow site.

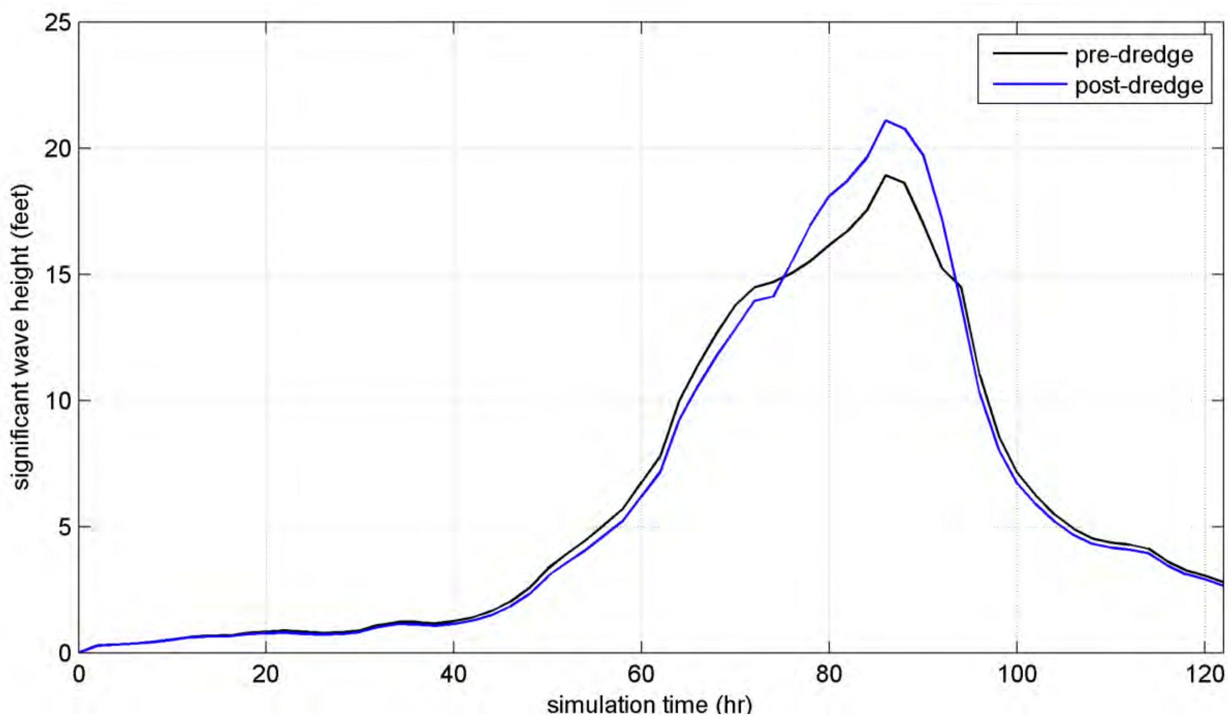

Figure 39. Plot of model wave height at the northern margin of PBE for existing and post-dredging conditions at the borrow site.

4.2 MORPHOLOGICAL MODELING

Waves are the primary force for sediment transport within the boundaries of the proposed borrow sites. In the absence of strong tidal currents, there tends to be little net transport at the depths where these sites are located. The situation changes when a borrow site is excavated. Net sediment transport occurs as sediment moves into the borrow area perimeter along the margin and settles into the excavated surface. In the shallower area of Petit Bois Pass, sediment movement is more strongly influenced by tidal currents.

4.2.1 Existing Conditions

Annual Simulation. Cumulative bathymetric change from the year-long (January through December, 1984) simulation for existing conditions is presented in Figure 40. Morphology change trends computed for this simulation are similar to the single month simulation presented in Section 3.3. Erosion occurs along the main portion of Petit Bois Pass, and eroded sediment is carried by currents to both the Gulf and Sound side of the Pass. Within the boundaries of the proposed borrow sites, very little bathymetric change occurs. Within the perimeter of PBE, a band of erosion along the SW extent of the site is present. The maximum change in seafloor elevation is -0.3 feet, and the change occurs along an existing ridge. Within the outline of PBW, maximum elevation change is about -0.4 feet at the SW corner of the site, also along an existing ridge. Within the proposed 1000-foot pipeline buffer in PBW, seafloor change is less than or equal to 0.1 feet. Elevation changes along the pipeline are generally of an order of magnitude less than the maximum change seen anywhere else within the boundaries of the borrow sites (less than 0.04 feet).

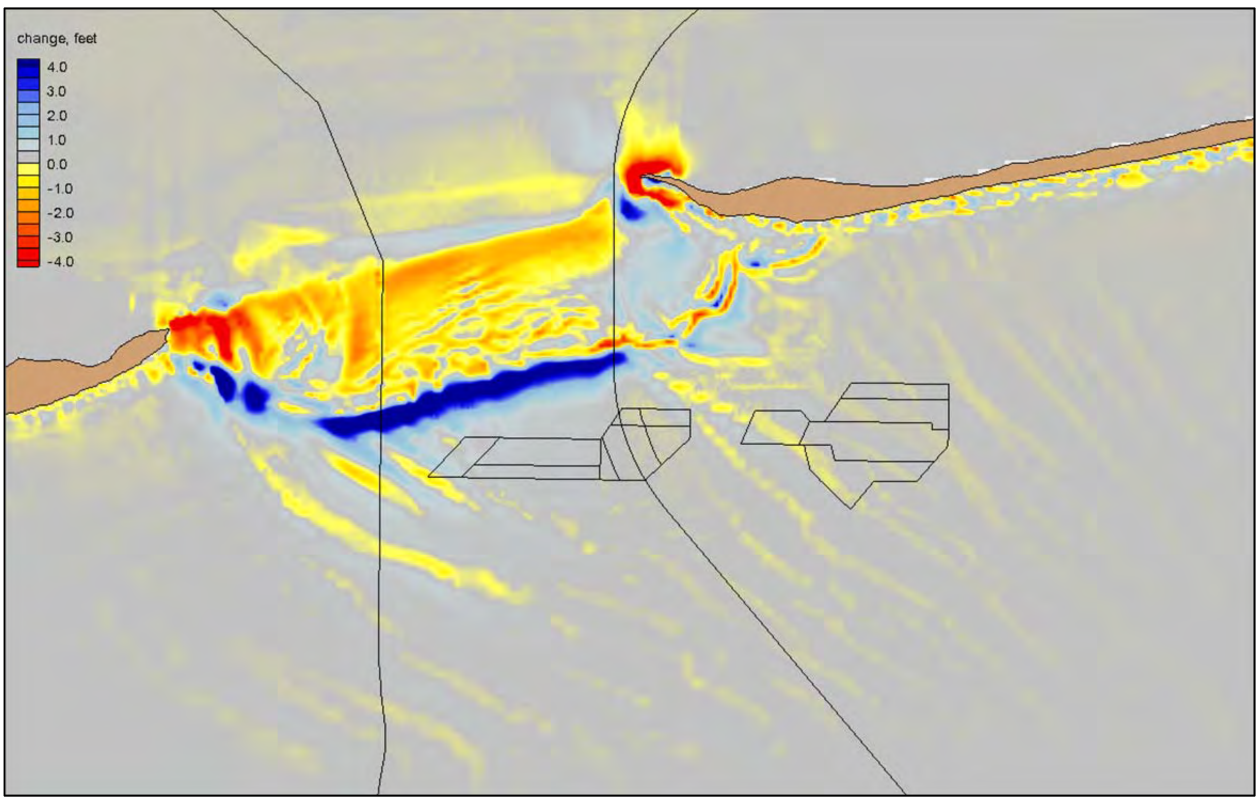

Figure 40. Contour map of bathymetric change for existing conditions at the Petit Bois borrow sites, from the year-long simulation. Borrow site boundaries and pipelines also are shown.

Storm Simulation. Morphological change from the CMS simulation of Hurricane Katrina is presented in Figure 41. Under these storm conditions, more change occurs in deeper water, including areas around the borrow sites. A key difference between this storm simulation and the year-long run is how sand moves within the main area of Petit Bois Pass. Rather than causing sediment to be pushed from the higher elevations of the Pass to down slope areas (in the case of the annual results), in the storm simulation, sediment is actually pushed up-slope from the southern boundary of the Pass to the top of the ridge crest that exists along the seaward edge of the ebb shoal. Sediment added to the shoal crest increases its elevation by approximately one foot.

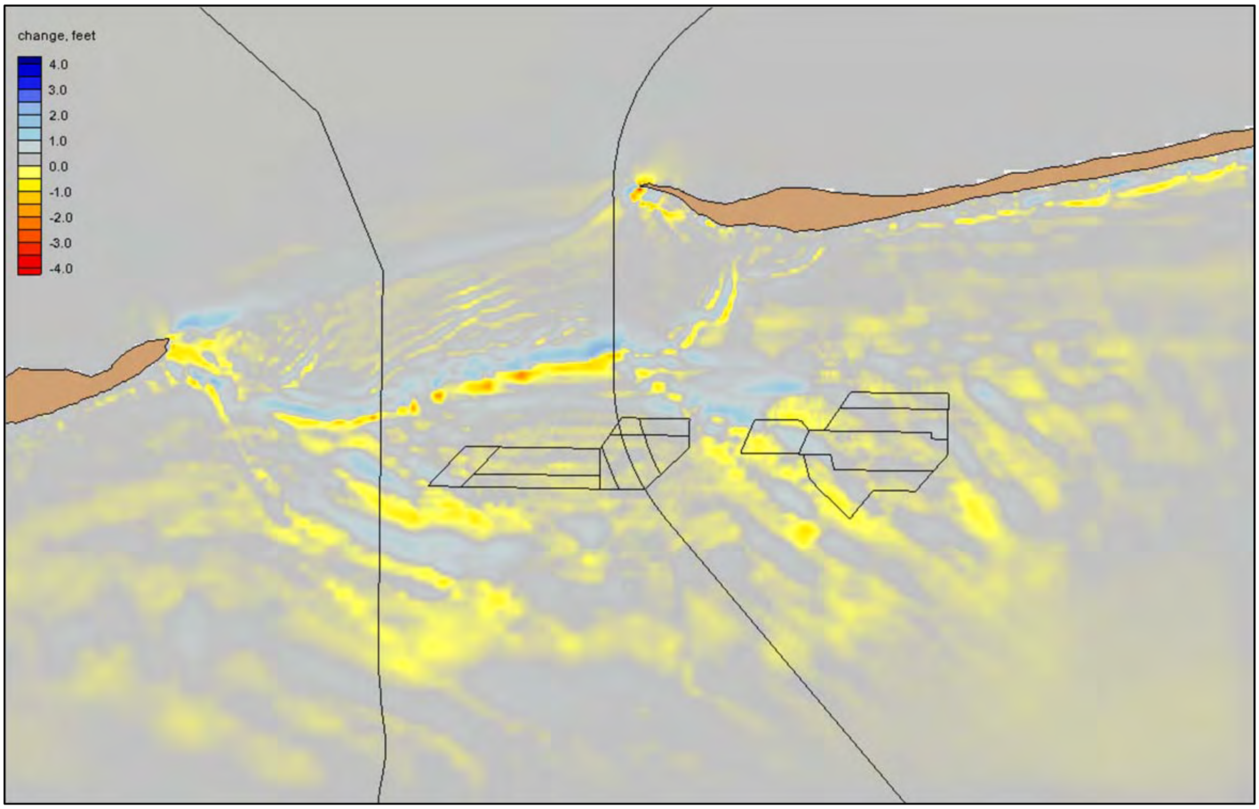

Figure 41. Contour map of bathymetric change for existing conditions at the Petit Bois borrow sites for the simulation of Hurricane Katrina. Borrow site boundaries and pipelines also are shown.

4.2.2 Dredged Borrow Sites

Annual Simulation. Morphology change computed for the 12-month simulation with borrow sites dredged (excluding the 1000 ft pipeline buffer) is illustrated in Figure 42. Patterns of change are similar to existing conditions results for most of the modeled domain. The differences between pre- and post-dredging simulations are documented in Figure 43, which represents the difference between the surfaces shown in Figures 40 and 42. This difference map shows that the perimeter of the dredged areas (including the pipeline buffer) eroded over the course of the simulated year and that sediment deposits in the excavated areas. Maximum additional erosion along the pipeline caused by dredging at the borrow sites is about 0.1 feet. This difference is dwarfed by changes that occur in the simulation of existing conditions along the pipeline pathway through the Pass (up to 3 to 4 feet of erosion).

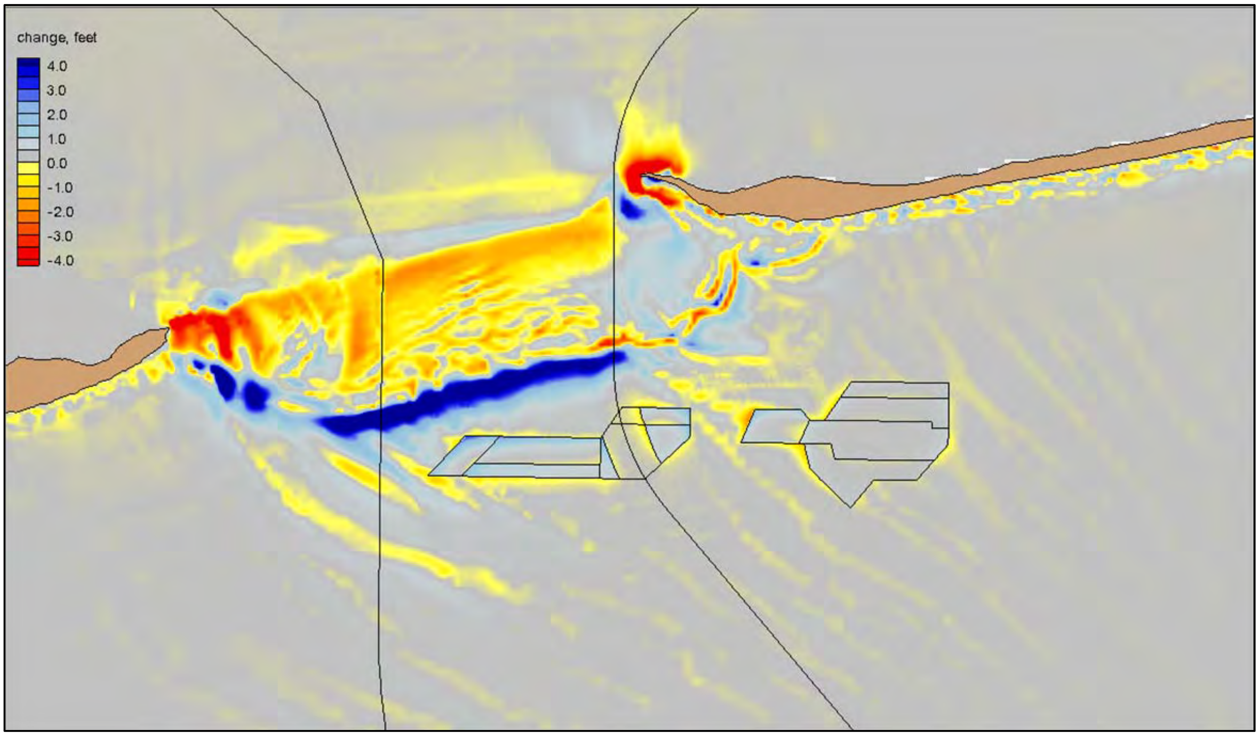

Figure 42. Contour map of bathymetric change for post-dredging conditions at the Petit Bois borrow sites from the year-long simulation. Borrow site boundaries and pipelines also are shown.

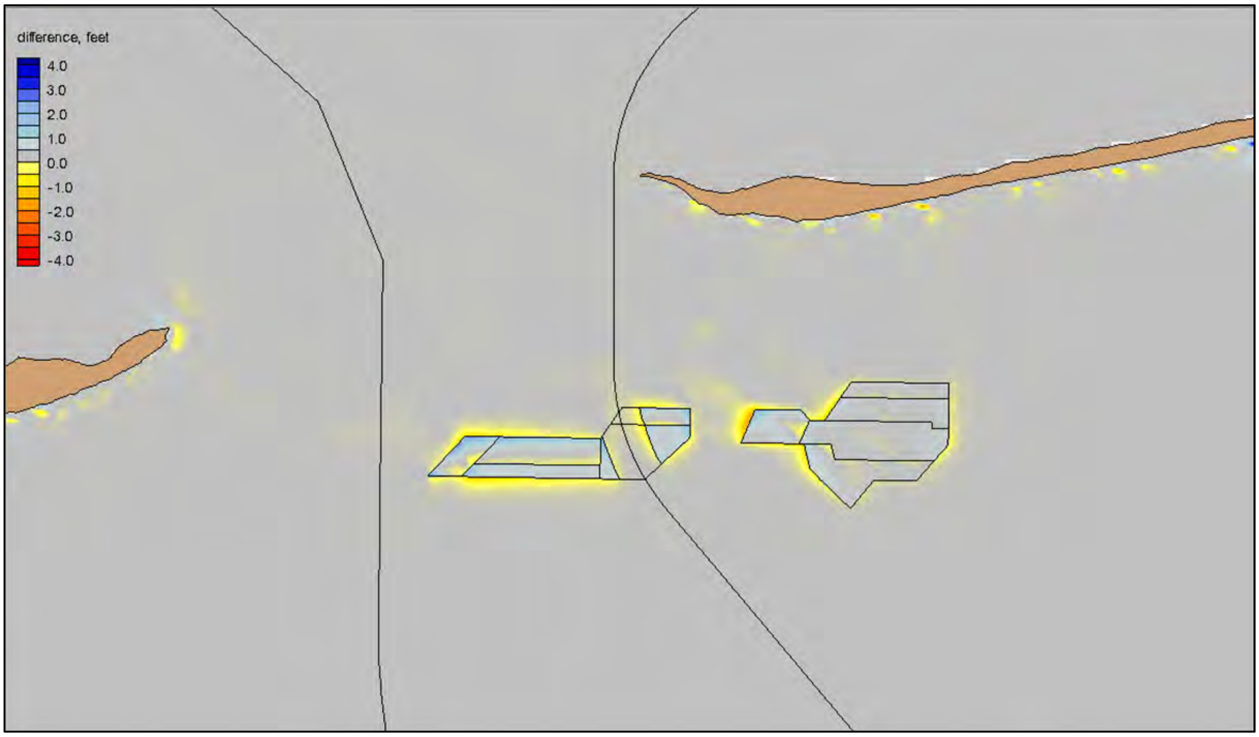

Figure 43. Difference map for existing and post-dredging morphology change from simulations of annual conditions.

Storm Simulation. For the Hurricane Katrina simulation with excavated borrow sites, seafloor morphology change is illustrated in Figure 44. Under storm conditions, there is more erosion of the buffer area, and significant erosion along the pipeline. Maximum magnitude of seafloor erosion above the pipeline pathway is 1 foot. Seafloor change directly resulting from the borrow sites is illustrated in Figure 45, which shows the difference between simulations of existing conditions (Figure 41) and excavated conditions (Figure 44). The maximum difference is an area of 5 feet of erosion that occurs at the western end of PBE. Overall, the change documented in this storm simulation is greater and more widespread than illustrated in the annual simulation.

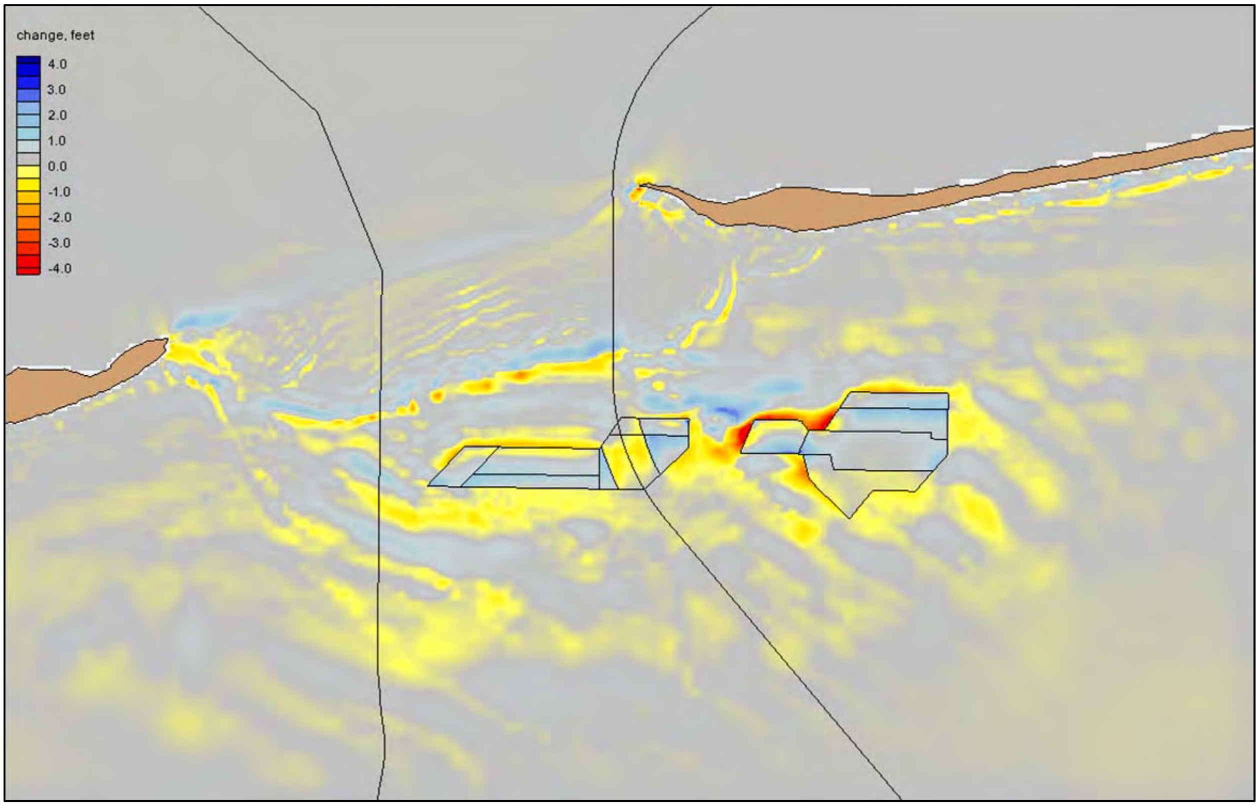

Figure 44. Contour map of bathymetric change for post-dredging conditions at the Petit Bois borrow sites from the simulation of Hurricane Katrina. Borrow site boundaries and pipelines also are shown.

Cumulative Storm Impacts. Because the storm simulation showed that erosion of the pipeline buffer is controlled more by storm waves than typical annual conditions, two additional runs of Katrina were made to simulate cumulative impacts from major storms. These additional runs were made to determine whether impacts to the seafloor along the pipeline progress linearly or reach some sort of equilibrium.

Output from these three storm simulations was taken along transect lines that were placed across both borrow sites (Figure 34). The transect line that crosses PBW follows the path of the Gulfstream pipeline starting from a point on the Sound side of the Pass to a point 6,300 feet SE of the southern perimeter of the borrow site. Bottom elevation along the route of the pipeline is shown in Figure 46. The segment of the transect that lies within the boundary of PBW is indicated on this figure.

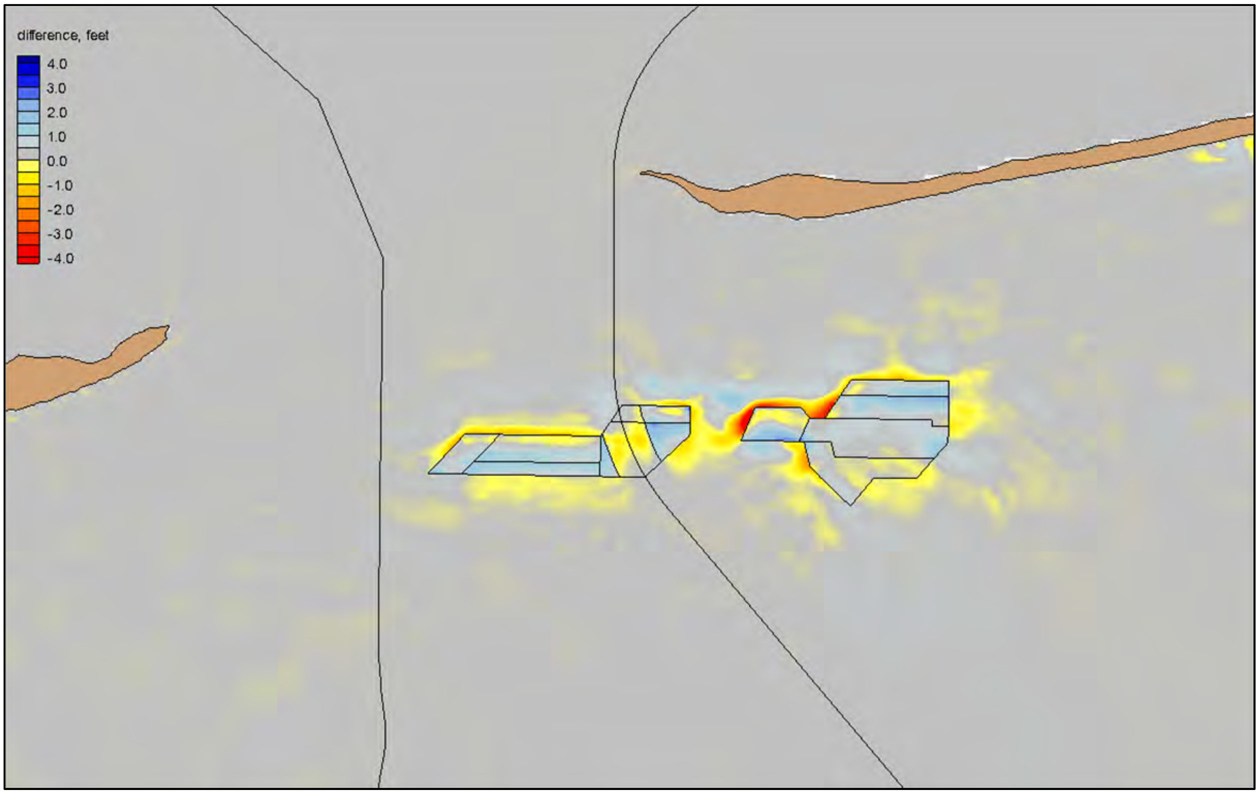

Figure 45. Difference map for existing and post-dredging morphology change from simulations of annual conditions.

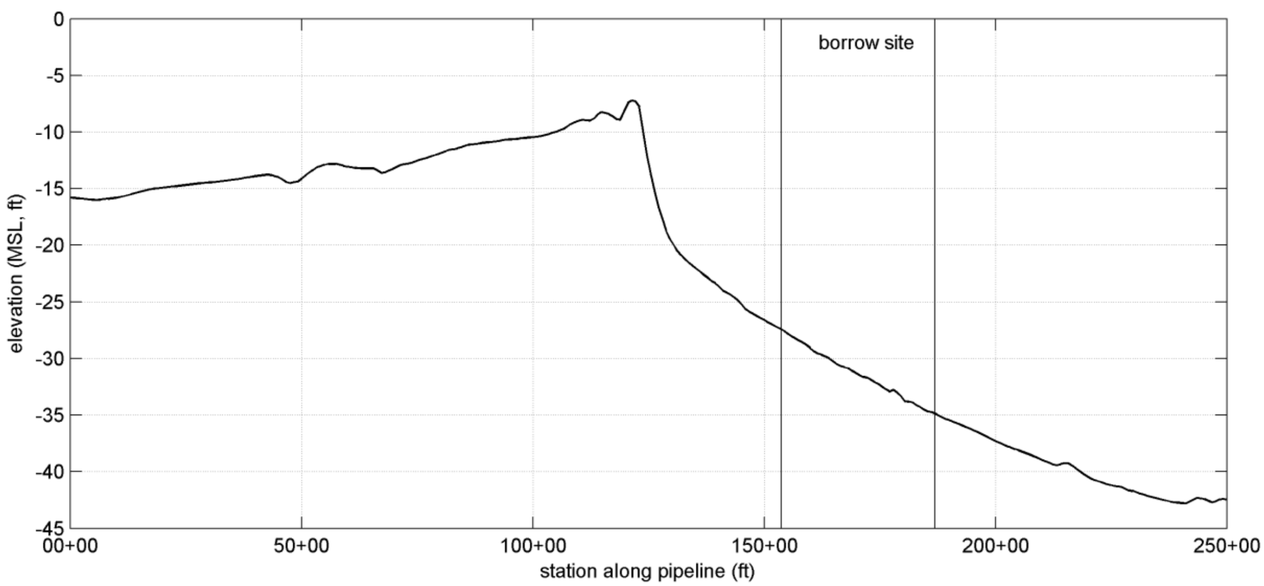

Figure 46. Bottom elevation along the Gulfstream pipeline transect (Figure 34), including the north and south limits of the PBW boundary.

Depth changes after each of the three Hurricane Katrina simulations are shown in Figure 47 along the Gulfstream pipeline transect. Results indicate that the pipeline buffer within PBW erodes by approximately one foot with each storm. This suggests that successive storms would erode the buffer by equal amounts and that the cumulative impacts from storms would evolve linearly beginning with initial dredging of the borrow site.

The evolving cross section of PBE is shown in Figure 48 for the same three simulations of Hurricane Katrina. Bottom profiles are taken along the PBE transect shown in Figure 34. Results illustrate that each storm erodes the undisturbed bottom that is proximate to the dredged pit. The eroded sediment spills into the borrow site excavation area.

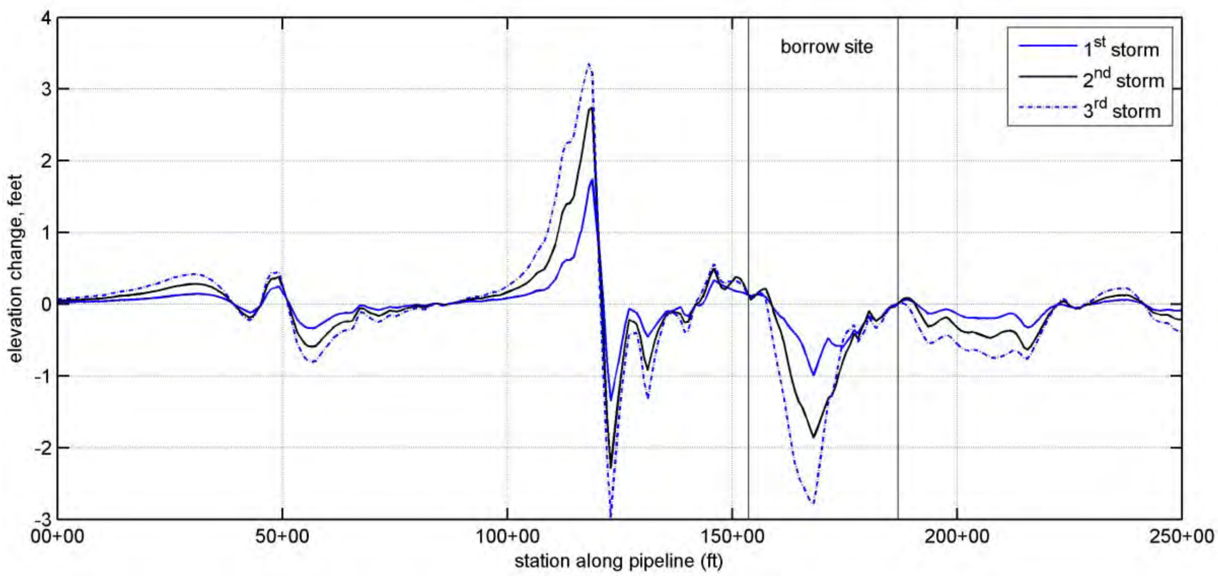

Figure 47. Cumulative morphology change along the Gulfstream pipeline transect (Figure 34) resulting from three Hurricane Katrina scale storms.

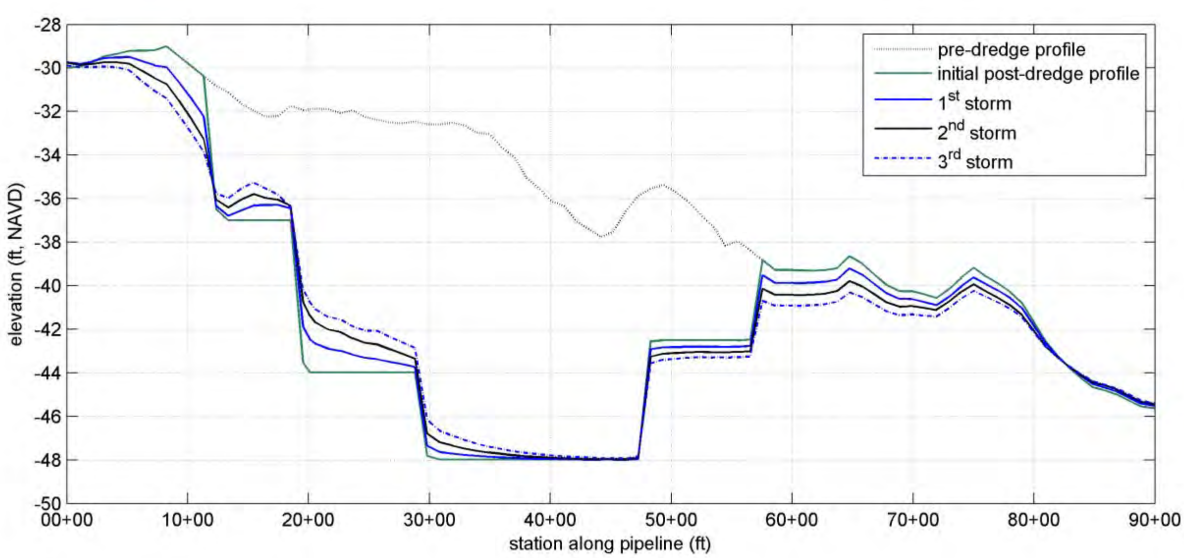

Figure 48. Bottom elevation along the PBE transect (Figure 34). Existing and post-dredging elevations are shown with bottom elevations after three consecutive runs of Hurricane Katrina.

4.2.3 Modified Pipeline Buffer

Because the 1000 ft buffer does not mitigate seafloor erosion over the pipeline during extreme storms, a further modification to PBW was made with the aim of reducing potential impacts. For this scenario, excavation of areas PBW1 and PBW2 (two sub-areas the pipeline crosses; Figure 34) was eliminated. This reduces the sand volume available from PBW by 2.3 MCY.

The results of the storm simulation with the modified design of PBW indicate that the maximum erosion along the Gulfstream pipeline caused by dredging the borrow site is reduced to less than 0.2 feet (Figure 49). The average change between stations 125+00 and 250+00 (a segment that includes the borrow site) is -0.01 feet, effectively zero. For the original dredging plan with the 1000 ft buffer, the average change along this segment is -0.15 feet. Area wide morphological change difference between the existing and modified post-dredging simulations is shown in Figure 50. Compared with Figure 44, the buffer area is less erosional with the modified borrow site excavation plan.

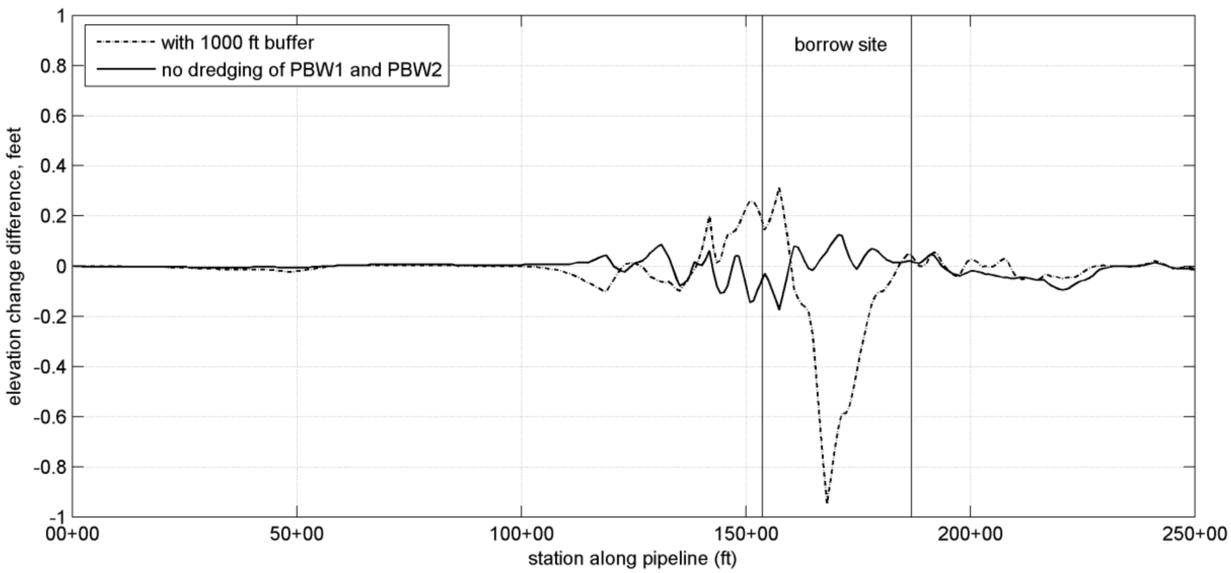

Figure 49. Comparison of bottom change difference (relative to existing conditions) between original PBW design with a 1000 ft pipeline buffer and the modified design with no dredging in PBW1 and PBW2 sub-sections.

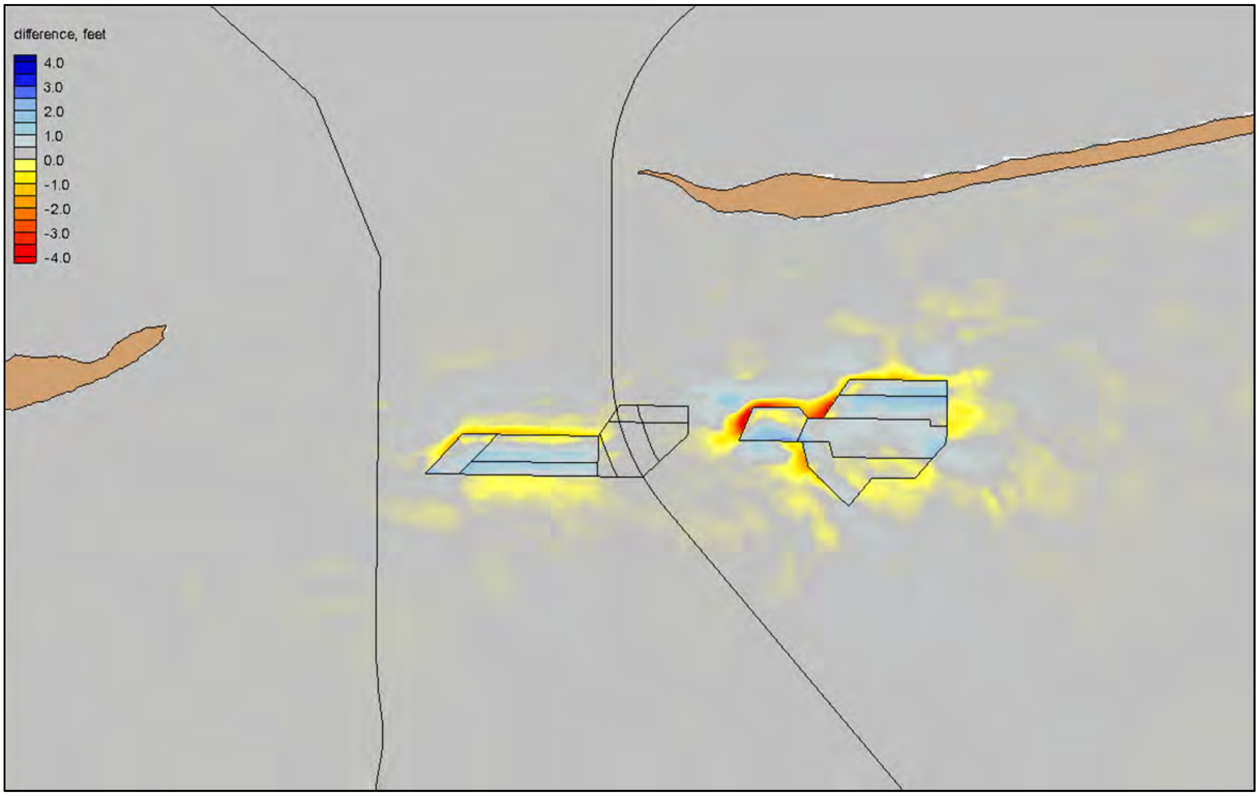

Figure 50. Difference between existing and modified post-dredging (no dredging of PBW1 and PBW2) morphology change from simulations of storm conditions.

5.0 CONCLUSIONS AND RECOMMENDATIONS

The results of this analysis show that the proposed Petit Bois Pass borrow sites are within the zone of active sediment movement, even though it has been demonstrated that the range of depths at the sites are deeper than the typical depth of closure for this area of the Gulf Coast. The sediment transport model shows that in an average year, sand from shallower depths of Petit Bois Pass are moved by tidal currents to deeper areas at Mississippi Sound and Gulf sides of the Pass. During storm events, the path of transport at the Pass is reversed, and sand from the Gulf facing shoals of the Pass is moved from deeper water on to and around the ebb shoal. Sediment movement at the borrow sites is much less active than within the Pass for both average annual conditions and extreme storms.

The storm modeled in this study was Hurricane Katrina, which produced the largest offshore waves for the entire 29-year hindcast records. Waves from Katrina also produced the largest wave-induced bottom currents at the borrow sites. However, because the largest storm waves are breaking in the depths encountered at the sites, currents generated by Katrina waves are not much larger than those generated by more frequently occurring storms. As a result, bottom currents with magnitudes similar to Katrina can be expected to occur with a return period of about seven years.

Morphology change trends in the model simulation for an average year are corroborated by the results of the bathymetric change analysis from historical survey data sets. Measured data indicate that shallower depths in the Pass are eroding, resulting in shoaling of depths along the outer margins of the ebb shoal.

A comparison of morphology change for the simulation of average annual and storm conditions indicates that sediment movement at the borrow site is more influenced by storms than by typical long-term waves conditions. This is a logical result, considering the borrow sites are located in water depths that are greater than the depth of closure in this region, but within the range of depths where sediment can be mobile during higher-energy events.

Because large storm waves that have the capacity to mobilize sediment at the borrow sites can occur statistically every seven years, it was considered important to investigate cumulative impacts of storms on borrow site excavations and the 1000 ft buffer zone along the Gulfstream pipeline. Model results indicate when the Petit Bois West borrow site is dredged following the originally proposed excavation area (excluding the 1000 ft pipeline buffer zone), seafloor erosion from each storm simulation was of equal magnitude. For a single Hurricane Katrina storm event, maximum seafloor erosion of approximately 1 foot occurs along the pipeline. Each subsequent storm causes an additional 1 foot of erosion.

Because model results for the proposed excavation plan of PBW indicate there is a credible risk of long-term erosion impacts to the seafloor covering the pipeline, the original excavation plan was modified so that no sand would be removed from PBW sub-areas PBW1 and PBW2 that lie outside the 1000 ft pipeline buffer. Morphological model results of Hurricane Katrina simulations with this reduced excavation illustrates that maximum seafloor erosion along the pathway of the pipeline within the boundary of the borrow site is reduced by an order of magnitude.

Based on these borrow site analysis results, it is recommended that the dredging plan for PBW be altered so that there is no dredging of sub areas PBW1 and PBW2. Though the amount of sand available from PBW is reduced by 2.3 MCY (53%) when these sub areas are excluded from the plan, the modification greatly reduces seafloor erosion risks to the pipeline during extreme storm events.

It is possible that the amount of sand available from PBW could be optimized by increasing the width of the pipeline buffer to the point where erosion impacts along the pipeline corridor are reduced to a similar level that occurs when no sand is dredged from PBW1 and PBW2.

6.0 REFERENCES

Baker, J.L. and M.R. Byrnes, 2004. Appendix F: Shoreline and Bathymetry Data. In: Kraus, N.C. and H.T. Arden (editors), North Jetty Performance and Entrance Channel Maintenance, Grays Harbor, Washington. Technical Report ERDC/CHL TR-03-12, US Army Engineer Research and Development Center, Vicksburg, MS.

Birkemeier, W.A., 1985. "Field Data on Seaward Limit of Profile Change," Journal of Waterway Port, Coastal and Ocean Engineering, ASCE, 111,3, pp. 598-602.

Byrnes, M.R., J.D. Rosati, S.F. Griffee, and J.L. Berlinghoff, 2013. Historical sediment transport pathways and quantities for determining an operational sediment budget: Mississippi Sound barrier islands. *In:* Brock, J.C., Barras, J.A., and Williams, S.J. (eds.), *Understanding and Predicting Change in the Coastal Ecosystem of the Northern Gulf of Mexico,* Journal of Coastal Research, Special Issue, No. 63, pp. 166-183.

Byrnes, M.R., J.D. Rosati, S.F. Griffee, and J.L. Berlinghoff, 2012. Littoral Sediment Budget for the Mississippi Sound Barrier Islands. Technical Report ERDC/CHL TR-12-9, U.S. Army Engineering Research and Development Center, Vicksburg, MS, 184 p.

Byrnes, M.R., S.F. Griffee, and M.S. Osler, 2010. Channel Dredging and Geomorphic Response at and Adjacent to Mobile Pass, Alabama. Technical Report ERDC/CHL TR-10-8, U.S. Army Engineer Research and Development Center, Vicksburg, MS, 309 pp.

CIRP (Coastal Inlets Research Program), 2012. Coastal Modeling System, v4r14. Software Executable, Engineer Research and Development Center, Vicksburg, MS.

Dean, R.G., and R.A. Dalrymple, 1991. *Water Wave Mechanics for Engineers and Scientists*. World Scientific, Singapore.

Dean, R.G., and R.A. Dalrymple, 2002. *Coastal Processes With Engineering Applications.* Cambridge University Press.

Foxgrover, A.C., S.A. Higgins, M.K. Ingraca, B.E. Jaffe, and R.E. Smith, 2004. Deposition, Erosion, and Bathymetric Changes in South San Francisco Bay: 1858-1983. USGS Open-File Report 2004-1192, U.S. Geological Survey, Reston, VA.

Hallermeier, R.J., 1978. "Uses for a Calculated Limit Depth to Beach Erosion," Proc. 16th International Conference on Coastal Engineering, ASCE, pp. 1493-1512.

Harris, D.L., 1981. Tides and Tidal Datums in the United States. Special Report No. 7, U.S. Army Coastal Engineering Research Center, Fort Belvoir, VA, 382 p.

Hess, K.W., 2003. Tidal datums and tidal coordination. In: Byrnes, M.R., M. Crowell, and C. Fowler (editors), Shoreline Mapping and Change Analysis: Technical Considerations and Management Implications. *Journal of Coastal Research*, Special Issue 38, pp. 33-43.

Hicks, S.D., 1981. Tidal datums and their uses – A summary. *Shore and Beach*, 53(1): 27-32.

Larson, M. and N.C. Kraus, 1995. Prediction of cross-shore sediment transport at different temporal and spatial scales. In: J.H. List and J.H.J. Terwindt (editors), Large-Scale Coastal Behavior. *Marine Geology*, 126: 111-127.

Luettich, R. and Westerink, J., 2004. Formulation and Numerical Implementation of the 2D/3D ADCIRC Finite element Model. Institute of Marine Sciences, Morehead City, NC.

Marmer, H.A., 1951. Tidal Datum Planes. Special Publication No. 135, NOAA National Ocean Service, U.S. Coast and Geodetic Survey, U.S. Government Printing Office, Washington, D.C., 142 p.

Meyer, T.H., D.R. Roman, and D.B. Zilkoski, 2004. What does height really mean? Part I: Introduction. *Surveying and Land Information Science*, 64(4): 223-233.

Mukai, A.Y., Westerink, J.J., Luettich, R.A. and Mark D., 2002. Eastcoast 2001, A Tidal Constituent Database for Western North Atlantic, Gulf of Mexico, and Caribbean Sea. Technical Report, ERDC/CHL TR-02-24. USACE Coastal and Hydraulics Laboratory, Vicksburg, MS.

Nairn, R., S. Langendyk, and J. Michel. 2004. Preliminary Infrastructure Stability Study, Offshore Louisiana. OCS Study MMS 2004-019, U.S. Department of the Interior, Minerals Management Service, Herndon, VA, 30 p.

NOAA, 2001. Tidal Datums and Their Applications. NOAA Special Publication NOS CO-OPS 1, U.S. Department of Commerce, National Oceanic and Atmospheric Administration, Silver Spring, MD, 112 p.

NOAA, 2003. Computational Techniques for Tidal Datums Handbook. NOAA Special Publication NOS CO-OPS 2, U.S. Department of Commerce, National Oceanic and Atmospheric Administration, Silver Spring, MD, 98 p.

Oceanweather, Inc., 2012. GOMOS08: Gulf of Mexico Oceanographic Study 2008 Project Description. Cos Cob, CT. pp. 141.

Petrie, G., 1991. Modelling, interpolation and contouring procedures. In: Petrie, G. and Kennie, T.J.M. (editors), Terrain Modelling in Surveying and Civil Engineering, McGraw-Hill, Inc., New York, NY, p. 112-127.

Sanchez, A., Lihwa, L., Demirbilek, Z., Beck, T., Brown, M., Li, H., Rosati, J., Wu, W., Reed, C., 2012. Coastal Modeling System, Draft User Manual. Coastal and Hydraulics Laboratory, U.S. Army Engineer Research and Development Center 3909 Halls Ferry Road, Vicksburg, MS, pp. 315.

Tracy, B.A. 2002. Directional characteristics of the 1990-1999 Wave Information Studies Gulf of Mexico hindcast. 7th International Workshop on Wave Hindcasting and Forecasting, Banff, Alberta, Canada.

USACE, 2002. Coastal Engineering Manual (CEM). USACE Coastal and Hydraulics Laboratory, Vicksburg, MS.

ADDENDUM

US Army
CORPS OF ENGINEERS
Mobile District

DATE: December 3, 2013

SUBJECT: Petit Bois Pass Borrow Areas: Modified Geometry Modeling Results

Background:

The Petit Bois Pass borrow area is composed of two sites, Petit Bois East (PBE) and Petit Bois West (PBW). These sites are proposed sand sources for the MsCIP Comprehensive Barrier Island Restoration Plan (Figure 1). The borrow areas have undergone several modifications due to the vicinity of two pipelines. Of the two pipelines the Gulfstream Pipeline is most likely to be affected since it traverses the original PBW borrow area. The original plan employed a 1000 ft buffer to the pipeline to abate adverse impacts. A study completed by Applied Coastal Research and Engineering investigated the impacts of the borrow areas to the pipelines using CMS-Wave and CMS-Flow which were coupled and run through the SMS interface. The 1000 ft buffer originally applied to the pipeline was found to be insufficient resulting in a maximum increase of 1.0 foot of erosion along the Gulfstream pipeline during storm events. A new geometry which eliminated all the borrow area in PBW to the east of the pipeline was recommended after simulations found the bottom elevation along the Gulfstream pipeline experienced less than 0.2 ft of change. Additional geotechnical investigations were performed in 2012 along the margins of BPW, west of the pipelines as well as PBE in an effort to optimize the volume obtained from these sites. The modified borrow area geometry resulting from the geotechnical investigations was simulated to investigate erosion impacts along the pipeline corridor relative to erosion that would occur when no sand is dredged from the sites. The results of the modified borrow area simulations are the focus of this addendum to Applied Coastal Research and Engineering's final report "Simulating the Potential Impact of Borrow Site Excavation on Sediment Transport Along the Gulfstream Pipeline, Petit Bois Pass, Alabama."

Modified Borrow Area Geometry:

A modified geometry was developed to offset a 56 percent volume reduction from the PBW site after elimination of two subcuts immediately to the east of the Gulfstream Pipeline, shown in Figure 1 as well as the original geometry for reference. As shown, the area of PBW was reduced by removing a large section of the borrow area from the West side adjacent to the pipeline. Furthermore, the overall geometry of the borrow area was modified to a more "squared-off" shape and shifted to the West. The modified borrow area now covers 379 acres and is approximately 1380 ft from the Gulfstream pipeline at the nearest point, which is measured from the northeast corner of the borrow site bearing N76°8'19"E. The depth profile of the borrow site has not changed.

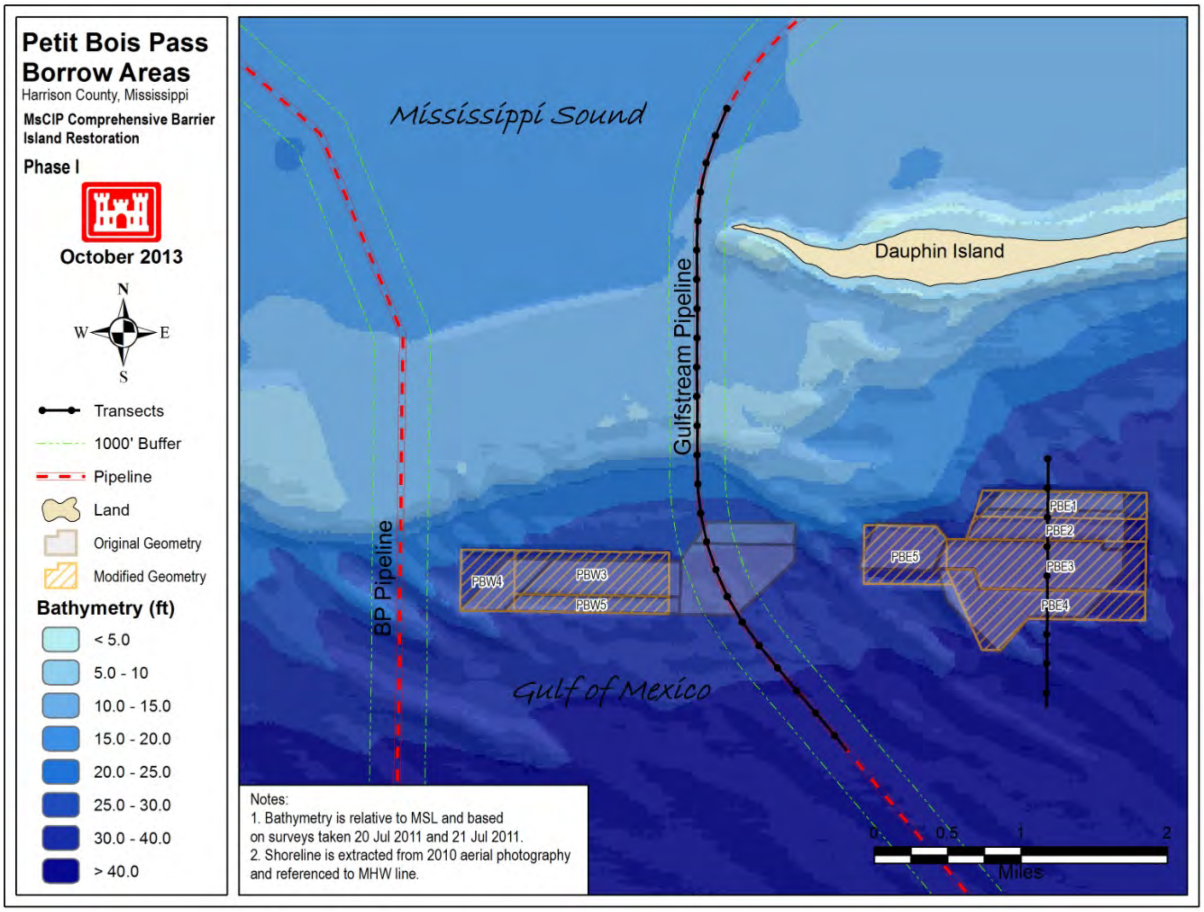

Figure 1: Petit Bois Pass borrow area geometry modification in response to Gulfstream pipeline owner's concerns.

Modeling Methodology:

Due to the depth of the borrow area and results from the Applied Coastal Research and Engineering report, the only model applied to the modified geometry was the storm conditions (Hurricane Katrina). Hurricane Katrina simulation results compared to the annual conditions showed a greater impact to the pipeline from storm waves in the vicinity of the borrow area. The model grid and input parameters were unchanged from that Applied Coastal Research and Engineering utilized. The model parameters are summarized in Table 1.

Table 1: Selected CMS-Flow model parameters used for the storm conditions simulation (Hurricane Katrina).

Model Parameter	Value
Time Step	10-minutes
Grid Type	Telescoping
Grid Cell Size	31 - 496 meters
Simulation Time	122 Hours
Simulation Start Date	0000h UTC August 26th, 2005
Median Grain Size	0.32 mm
Sediment Density	2650 kg/m^3
CMS-Wave Run Interval	1.0 Hour
Manning's friction factor	0.003

Modeling Results/Discussion:

Modeling results based on dredging the modified borrow area geometry show little to no bathymetric change within the buffer of the Gulfstream Pipeline adjacent to PBW borrow area, for the simulated storm conditions (Figure 2). Bathymetric change occurring as a direct result of the dredged conditions within the buffer zone (less than 0.25 feet) is shown in Figure 3.

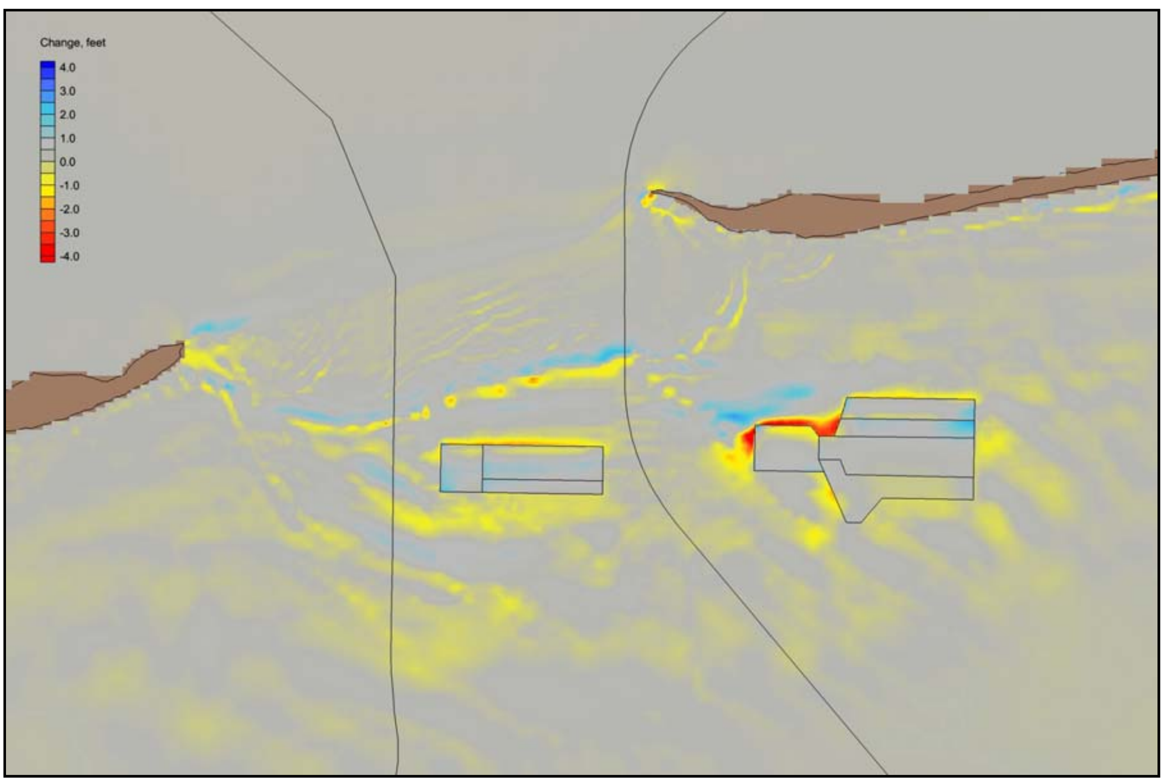

Figure 2: Morphological change for post-dredging conditions at the Petit Bois borrow sites from the simulation of Hurricane Katrina.

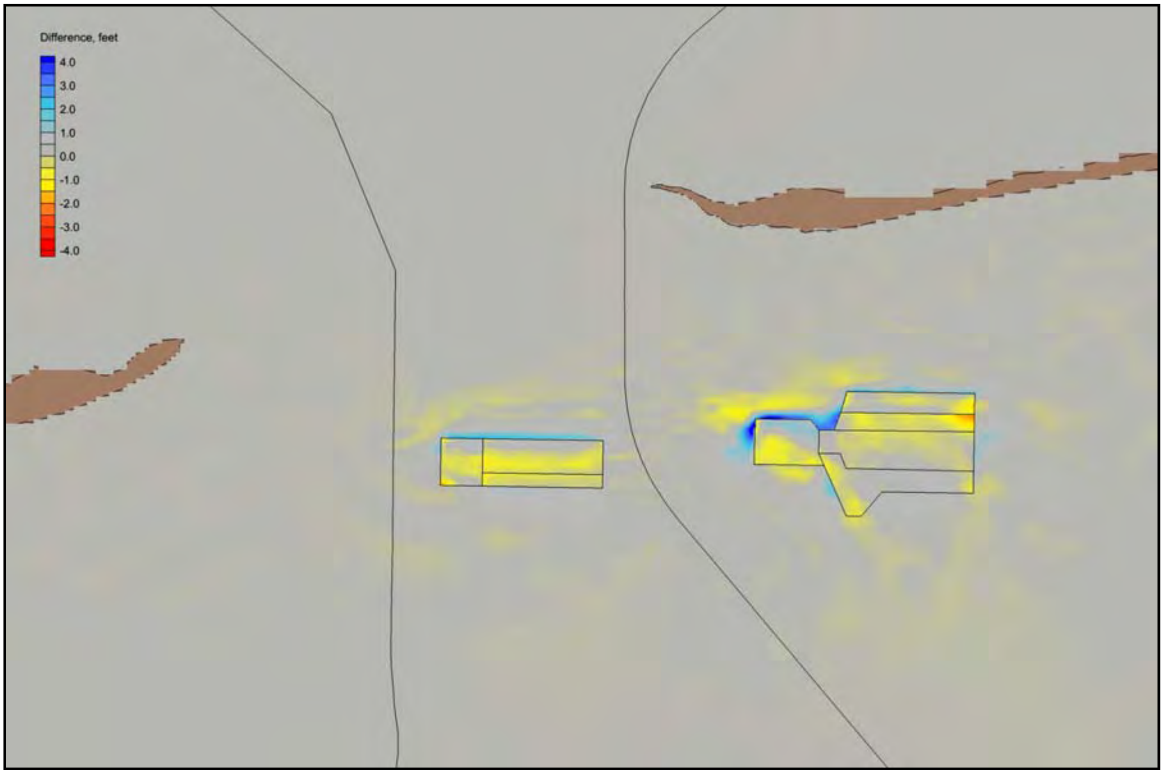

Figure 3: Difference of existing conditions morphology change and modified geometry morphology change for the Hurricane Katrina simulation.

Comparison of Borrow Area Geometries:

The three borrow areas produce different morphological results, but the results may not be statistically different. The following analysis focuses on the Hurricane Katrina simulation and the entire length of the Gulfstream pipeline transect shown in Figure 1, which represents approximately 25,000 ft of the pipeline beginning North of Dauphin Island and extending southward. The model results for morphological change represent the change in depth during the 122 hours of simulated time for Hurricane Katrina. The morphological change values range from -1.38 to 1.89 ft for all cases. The morphological change is a directional value, but the statistical analysis is based on the magnitude of these values (e.g., the absolute value). A summary of the simple statistics for each case is provided in Table 2.

Table 2: Simple statistics for the absolute value of morphological change for each case resulting from Hurricane Katrina simulation along the entire Gulfstream pipeline transect.

	Pre-Dredge	**Original with 1000 ft Buffer**	**Original with eastern cuts of PBW eliminated**	**Modified**
Average	0.15	0.19	0.16	0.16
Maximum	1.84	1.74	1.89	1.89
Std. Deviation	0.23	0.25	0.23	0.23
Variance	0.05	0.06	0.05	0.05

*Note that these are absolute change and relative change resulting from the borrow area

Statistical comparison of the four cases is tested first using a single factor ANOVA to determine if the observed variances are statistically different. The single factor ANOVA tests if the four cases are the same by calculating the F-ratio. The F-ratio is representative of the variation among the groups. An F-ratio of 1.0 proves the hypothesis is true; whereas, a large F-ratio is indicative of a wrong hypothesis or large degree of separation in the values. The F-ratio obtained from the ANOVA test is 4.45 which is greater than one and proves there is a difference within the four cases; however, the ANOVA does not identify which case is different from the other.

The ANOVA results prove there is a statistical difference in the four cases but to determine which case is different than the other an F-test is performed. The F-test is used to test the variances between two samples by hypothesizing two samples of data have an equal variance distribution. The F-test reports the F-ratio which is defined the same as for the ANOVA test to confirm or deny the hypothesis based on a confidence interval. For the F-tests in this analysis a confidence interval of 95% is used. The results of the F-test are provided in Table 3.

Table 3: Summary of F-tests for the four cases using a confidence interval of 95%.

Cases Compared		**F-ratio**
Pre-Dredge	Original with 1000 ft buffer	0.84
Pre-Dredge	Original with eastern cuts of PBW eliminated	0.96
Pre-Dredge	Modified	0.97
Original with eastern cuts of PBW eliminated	Modified	1.00

From the F-tests it is clear the “Original” with a 1000 ft buffer case is least similar to the “Pre-Dredge” conditions. The summary also shows the “Original” with eastern cuts of PBW eliminated and “Modified” cases are identical; however, the “Modified” case does show slightly less variation with the “Pre-Dredge” than the “Original” with eastern cuts of PBW eliminated case but the statistical difference between the "Original" with eastern cuts of PBW eliminated and "Modified" cases proves the variance is not statistically different and likely due to rounding.

The results of the statistical analysis prove there is no difference in the morphological change for the "Pre-Dredge", "Original" with eastern cuts of PBW eliminated, and "Modified" cases. Using a more simplistic observational comparison to augment the statistical analysis, the "Pre-Dredge" and "Modified" cases are near equal in trends as well as magnitude (Figure 4), with a maximum absolute difference of 0.05 ft. Additionally, the statistical comparison of the "Original" with eastern cuts of PBW eliminated and "Modified" cases being identical is apparent, with no measurable or identifiable differences. The summary of the F-test identifying the "Original" with a 1000 ft buffer case as the least similar is also shown in Figure 4.

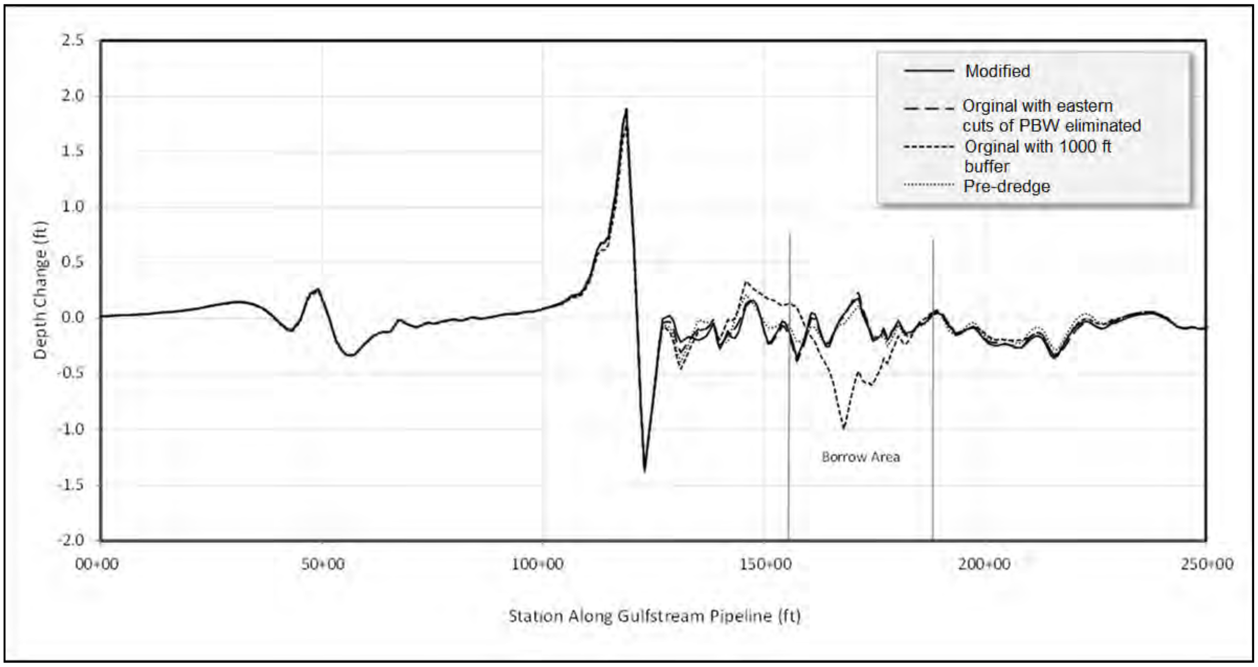

Figure 4: Comparison of change in depth along the Gulfstream pipeline as a result of the Hurricane Katrina model run for all geometries.

Conclusion:

The modified borrow area geometry proposed in this addendum is not expected to adversely impact the Gulfstream pipeline more than would be expected with the "pre-dredge" existing condition. Bathymetry change results of the storm simulation show an average difference of 0.01 ft and a maximum absolute difference of 0.05 feet along a 25,000 ft length of the Gulfstream pipeline shown in Figure 1. The calculated difference was found to not be statistically different and confirmed through observational comparisons using the graph in Figure 4. Furthermore, the statistical analysis and depth change comparison graph in Figure 4 suggest the borrow area geometry with the eastern cuts of PBW eliminated is identical to the modified borrow area geometry and also shown to be not statistically different than the "pre-dredge" condition.

Based on the analysis completed in this addendum and results from the Applied Coastal Research, it is recommended the PBW borrow area be modified. The geometry proposed by

Applied Coastal Research and Engineering produces identical results; however, the geometry proposed herein will provide a larger volume within a more simplistic geometry.